NuPhys2023: Prospects in Neutrino Physics

18-20 Dec 2023

CEνNS review and BSM implications

Matteo Cadeddu
matteo.cadeddu@ca.infn.it

In collaboration with
M. Atzori Corona, N. Cargioli, F. Dordei, C. Giunti, Y. F. Li, C. A. Ternes and Y. Y. Zhang

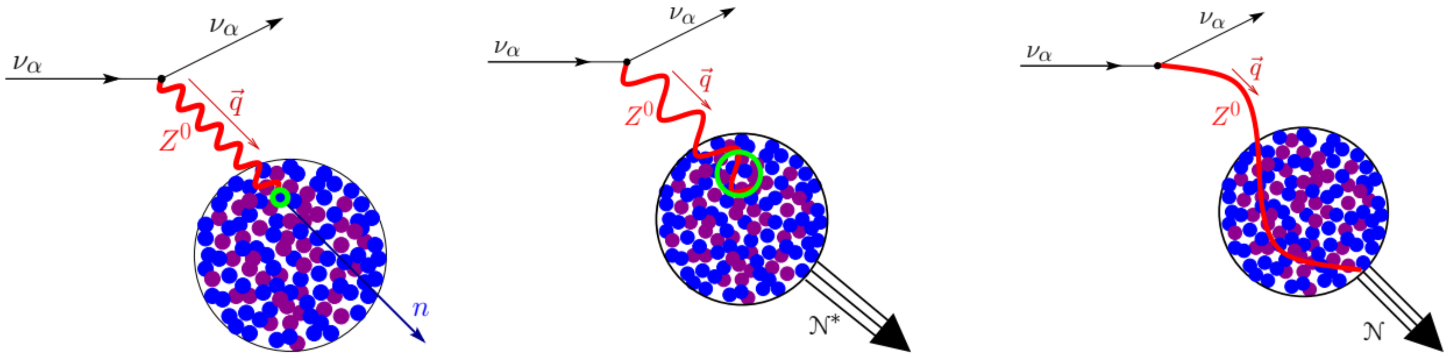

For a recent review see Europhysics Letters, Volume 143, Number 3, 2023 (EPL 143 34001), arXiv:2307.08842v2

Coherent elastic neutrino nucleus scattering (aka CEνNS)

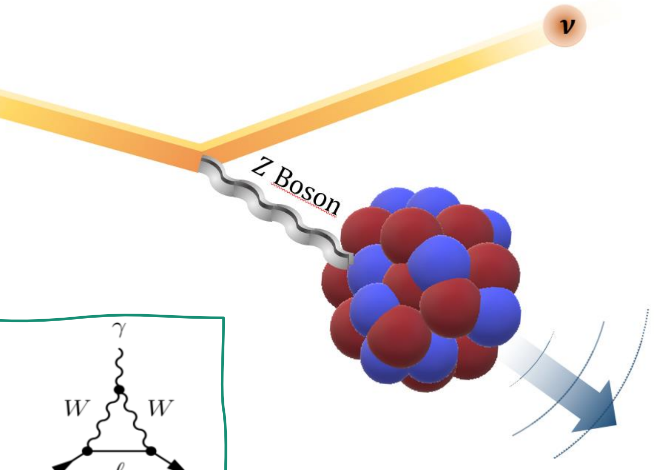

+ A pure weak neutral current process

$$\boxed{\frac{d\sigma_{\nu_\ell\text{-}\mathcal{N}}}{dT_{\text{nr}}}(E, T_{\text{nr}}) = \frac{G_F^2 M}{\pi}\left(1 - \frac{M T_{\text{nr}}}{2E^2}\right)(Q^V_{\ell,\text{SM}})^2}$$

+ Weak charge of the nucleus

$$Q^V_{\ell,\text{SM}} = \Big[\underbrace{g_V^p(\nu_\ell)\, Z F_Z\left(|\vec{q}|^2\right)}_{\text{protons}} + \underbrace{g_V^n N F_N\left(|\vec{q}|^2\right)}_{\text{neutrons}}\Big]$$

In general, in a weak neutral current process which involves nuclei, one deals with **nuclear form factors** that are different for protons and neutrons and cannot be disentangled from the neutrino-nucleon couplings!

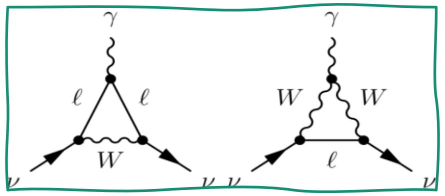

+ Neutrino-nucleon tree-level couplings

$$g_V^p = \frac{1}{2} - 2\sin^2(\vartheta_W) \cong 0.02274$$

$$g_V^n = -\frac{1}{2} = -0.5$$

J. Erler and S. Su. *Prog. Part. Nucl. Phys.* 71 (2013). arXiv:1303.5522 & PDG2022

+ Radiative corrections are expressed in terms of WW, ZZ boxes and the neutrino charge radius diagram → Flavour dependence

$$g_V^p(\nu_e) = 0.0382,\ g_V^p(\nu_\mu) = 0.0300 \text{ and } g_V^n = -0.5117$$

Nuclear physics, but since $g_V^n \approx -0.51 \gg g_V^p(\nu_\ell) \approx 0.03$ neutrons contribute the most

$$\boxed{\frac{d\sigma}{dE_r} \propto N^2}$$

WHAT CAN WE LEARN FROM CEνNS?

M. Cadeddu et al., JHEP 01 (2021) 116, arXiv:2008.05022

O. G. Miranda et al., JHEP 05 (2020) 130, arXiv:2003.12050

M. Atzori Corona et al., JHEP 05 109 (2022), arXiv:2202.11002

C. Giunti, *PRD* 101 (2020) 3, 035039, arXiv:1909.00466

D. K. Papoulias and T. S. Kosmas, PRD 97, 033003 arxiv:1711.09773

D. A. Sierra et al., PRD 98, 075018 (2018) arXiv:1806.07424

L. J. Flores et al., JHEP 06 (2020) 045, 2002.12342

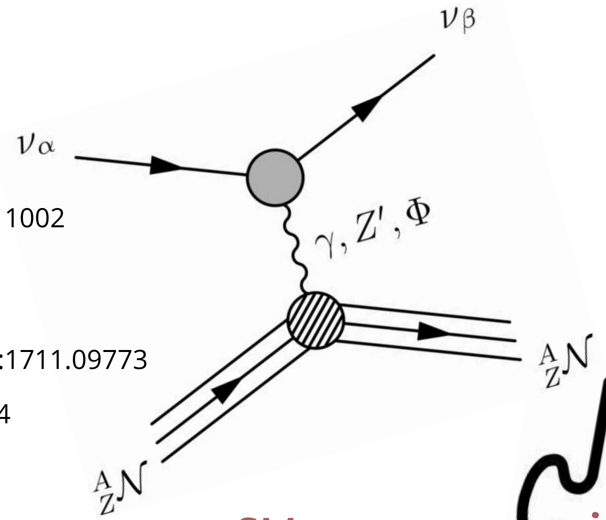

O. G. Miranda et al., JHEP 05 (2020) 130, arXiv:2003.12050

B. Dutta et al., Phys. Rev. Lett. 123, 061801 (2019)

O. G. Miranda et al., JHEP 07 (2019) 103, arXiv: 1905.03750

D. Aristizabal Sierra et al., Phys. Rev. D 98, 075018 (2018)

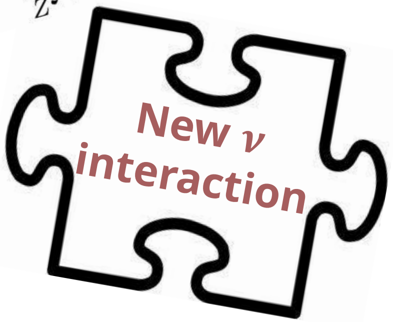

Neutrino energy

Mass of the nucleus

SM vector proton coupling

SM vector neutron coupling

$$\frac{d\sigma^{CE\nu NS}(E_\nu, E_r)}{dE_r} \cong \frac{G_F^2\, m_N}{\pi}\left(1-\frac{m_N E_r}{2E_\nu^2}\right)\left[g_V^p\left(\sin^2(\vartheta_W)\right) Z\, F_Z\left(|\vec{q}|^2\right) + g_V^n\, N\, F_N\left(|\vec{q}|^2\right)\right]^2 + \dots$$

Proton Form Factor

Weinberg angle

Neutron Form Factor

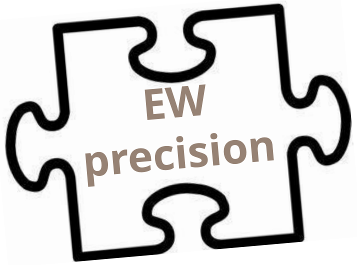

D. Papoulias et al., PLB 800 (2020) 135133, arXiv:1903.03722

Coloma et al., JHEP 08 (2020) 08, 030, arXiv:2006.08624

D. A. Sierra et al., JHEP 1906:141 (2019) arXiv: 1902.07398

B. Canas et al., PRD 101, 035012 (2020), arXiv:1911.09831

K. Patton, J. Engel, G. C. McLaughlin, and N. Schunck, Phys. Rev. C 86, 024612 (2012).

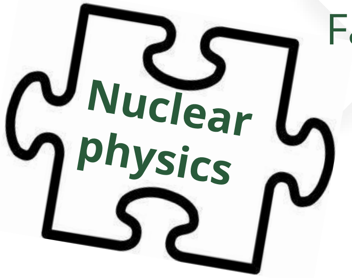

CEνNS players

$$\pi^+ \to \mu^+ + \nu_\mu$$ Prompt component

$$\mu^+ \to e^+ + \bar{\nu}_\mu + \nu_e$$ Delayed component

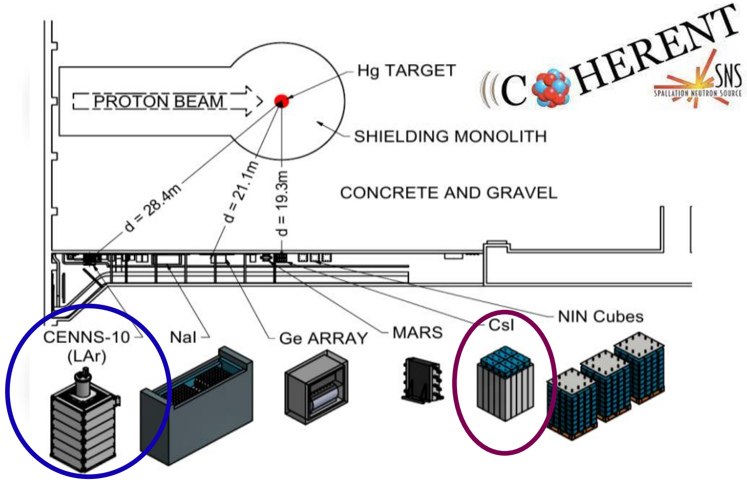

COHERENT CsI

D. Akimov et al. **Science** 357.6356 (2017)

+ Updated in Akimov et al., PRL 129, 081801 (2022)

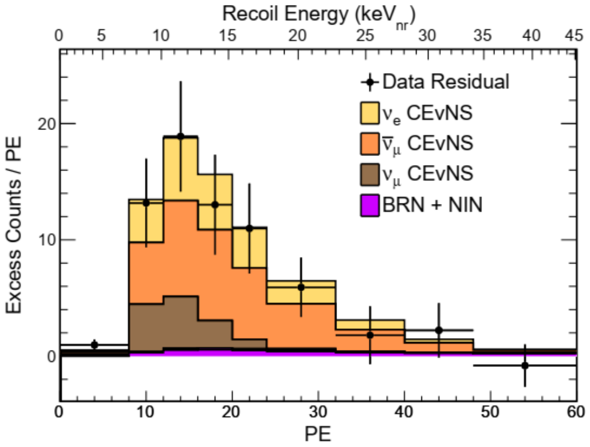

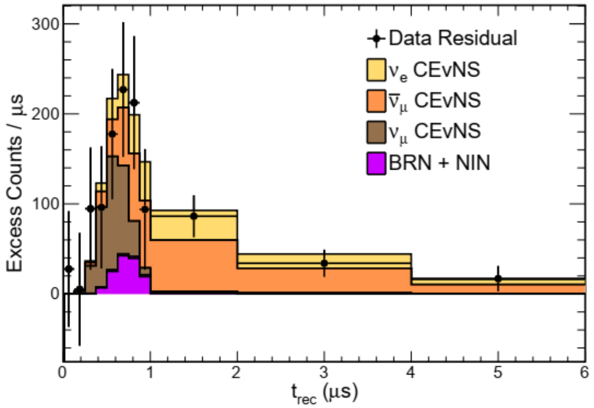

	Prior Prediction	Best-Fit Total
Steady-state background	1286 ± 27	1273 ± 24
BRN	18.4 ± 4.6	17.3 ± 4.5
NIN	5.6 ± 2.0	5.5 ± 2.0
CEvNS	–	306 ± 20

Table I. A summary of prior prediction and best-fit event rates and statistical uncertainties for CEvNS and each background type. The standard-model expectation for CEvNS is $341 \pm 11 \pm 42$.

COHERENT Ar

Akimov et al., COHERENT Coll. PRL 126, 01002 (2021)

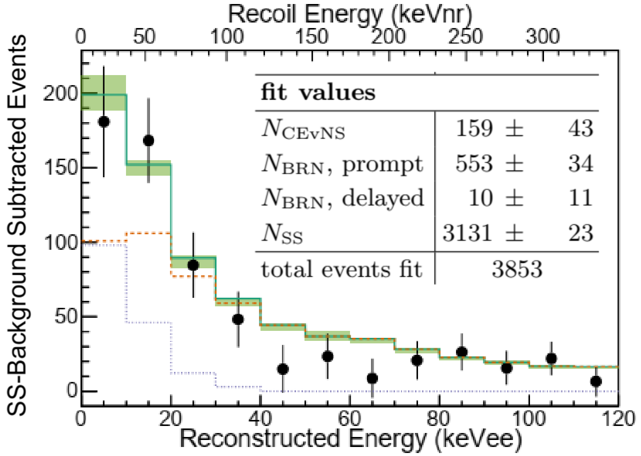

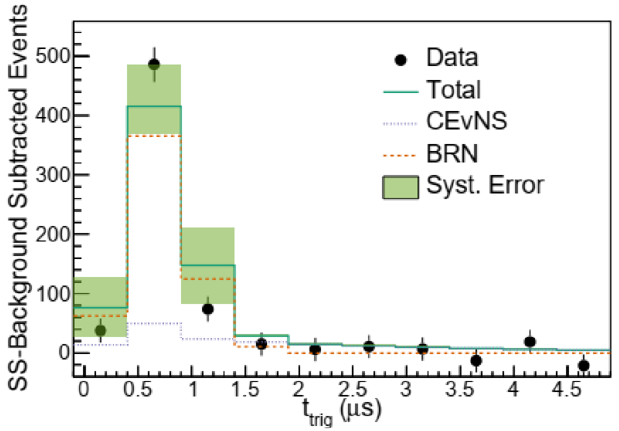

2022 New player:

NCC- 1701 (Dresden-II)

+ 3 kg ultra-low noise germanium detector.

A strong preference for the presence of CEνNS is found.

Colaresi et al. PRL129, 211802 (2022)

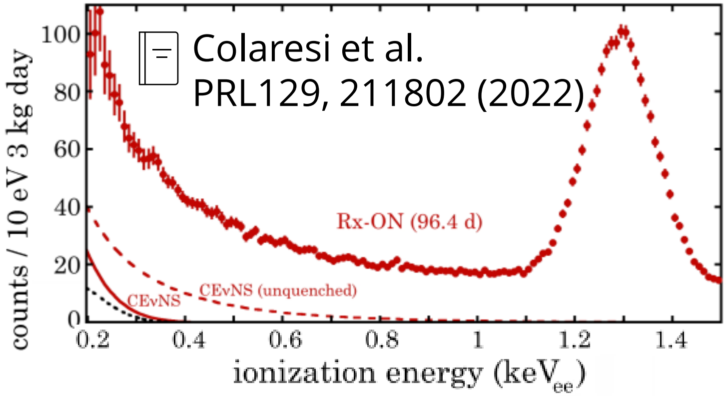

Suppression of the full coherence in CsI COHERENT data

$$\frac{d\sigma_{\nu_\ell\text{-}\mathcal{N}}}{dT_{\mathrm{nr}}}(E, T_{\mathrm{nr}}) = \frac{G_{\mathrm{F}}^2 M}{\pi}\left(1 - \frac{M T_{\mathrm{nr}}}{2E^2}\right)\left[g_V^p(\nu_\ell)\, Z F_Z(|\vec{q}|^2) + g_V^n N F_N(|\vec{q}|^2)\right]^2$$

Neutron form factor to be fitted

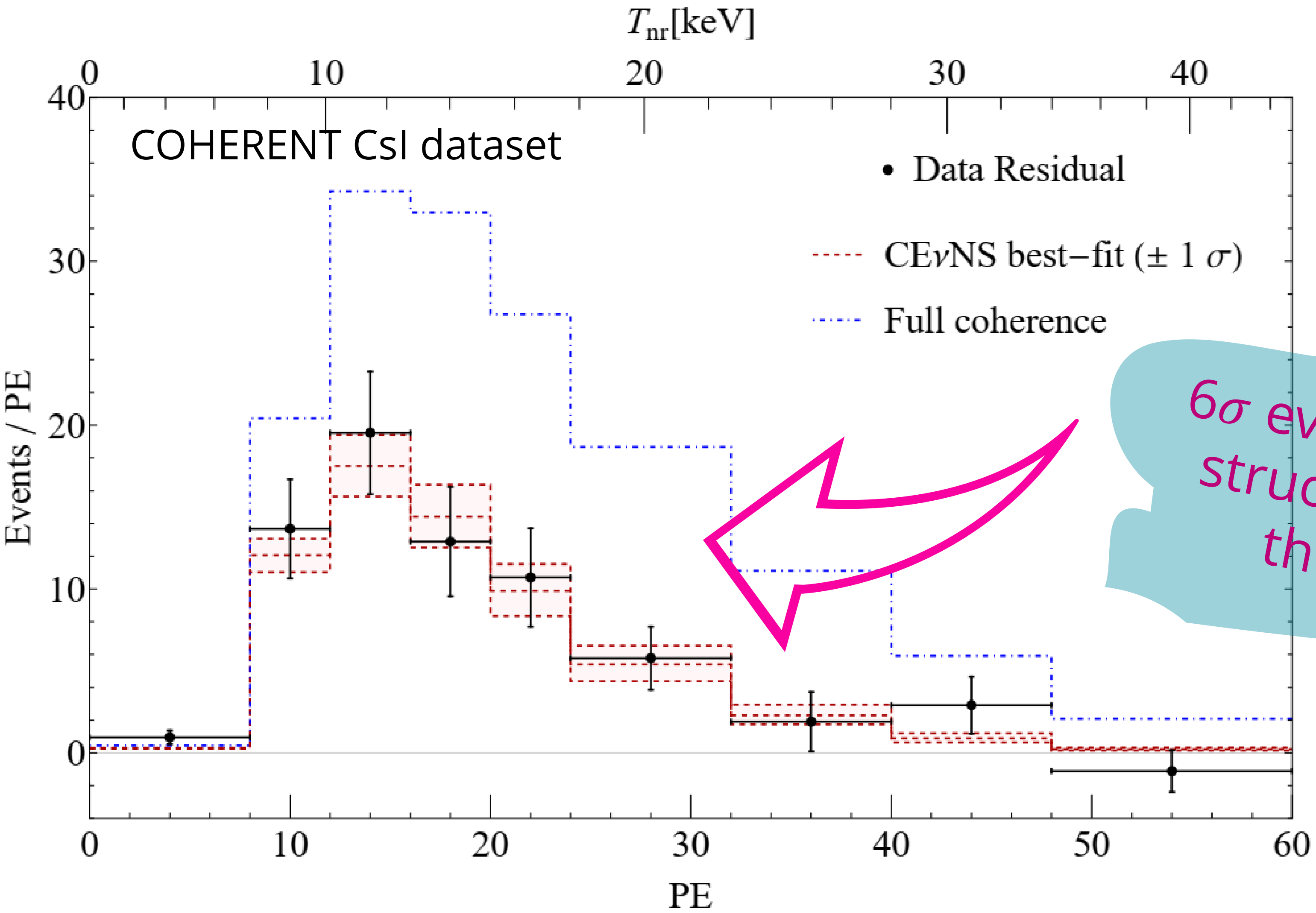

6σ evidence of the nuclear structure suppression of the full coherence!

See also:

Rossi et al. arXiv:2311.17168

De Romeri et al. JHEP04(2023)035 arXiv:2211.11905

D. Papoulias et al., PLB 800 (2020) 135133, arXiv:1903.03722

M. Atzori Corona et al., EPJC 83 (2023) 7, 683 arXiv:2303.09360

The CsI neutron skin

First result Cadeddu et al. Phys. Rev. Lett. 120, 072501 (2018), arXiv:1710.02730

M. Atzori Corona et al., EPJC 83 (2023) 7, 683 arXiv:2303.09360

$$R_n\ (\mathrm{CsI}) = 5.47 \pm 0.38\ \mathrm{fm}$$

$\sim 7\%$ precision

Average proton rms radius for CsI from muonic X-rays data

$$R_p\ (\mathrm{CsI}) \approx 4.78\ \mathrm{fm}$$

G. Fricke et al., Atom. Data Nucl. Data Tabl. **60**, 177 (1995)

Neutron skin: R_n (CsI)- R_p (CsI)

$$\Delta R_{np}(\mathrm{CsI}) = 0.69 \pm 0.38\ \mathrm{fm}$$

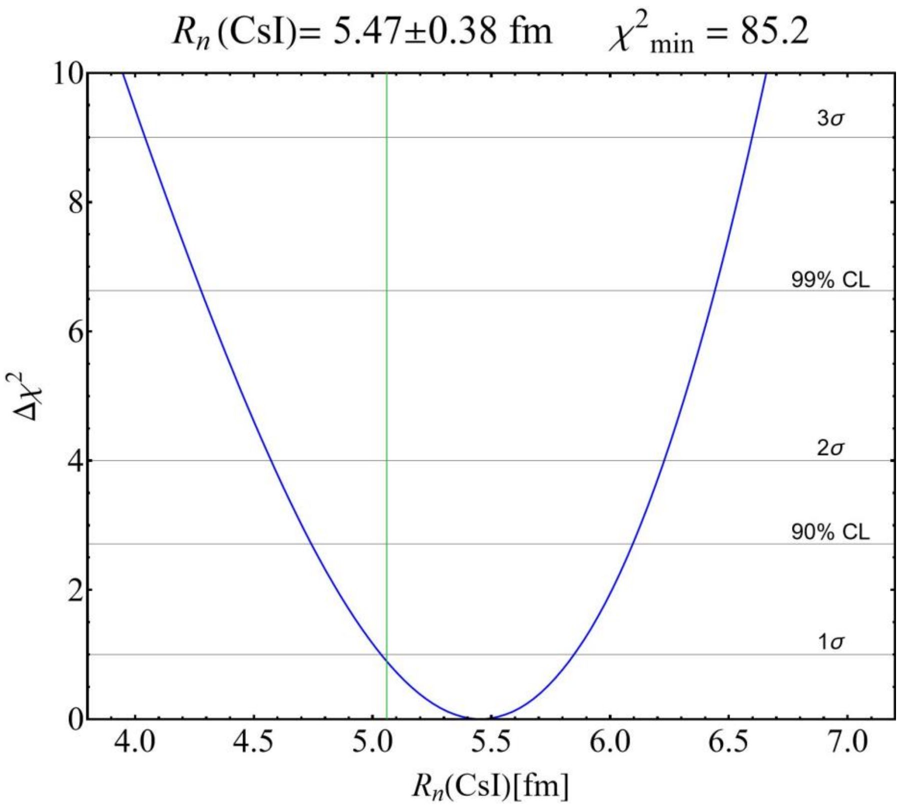

$$R_n(\mathrm{COH-CsI}) = 5.47^{+0.38}_{-0.38}(1\sigma)^{+0.63}_{-0.72}(90\%\mathrm{CL})^{+0.76}_{-0.89}(2\sigma)\ \mathrm{fm},$$

Theoretical values of the neutron skin of Cs and I obtained with nuclear mean field models. The value is compatible with all the models...

$$0.12 < \Delta R_{np}^{CsI} < 0.24\ \mathrm{fm}$$

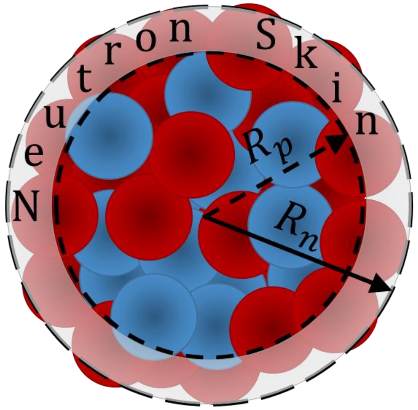

Model	^{127}I						^{133}Cs					
	R_p^{point}	R_p	R_n^{point}	R_n	ΔR_{np}^{point}	ΔR_{np}	R_p^{point}	R_p	R_n^{point}	R_n	ΔR_{np}^{point}	ΔR_{np}
SHF SkI3 [81]	4.68	4.75	4.85	4.92	0.17	0.17	4.74	4.81	4.91	4.98	0.18	0.18
SHF SkI4 [81]	4.67	4.74	4.81	4.88	0.14	0.14	4.73	4.80	4.88	4.95	0.15	0.14
SHF Sly4 [82]	4.71	4.78	4.84	4.91	0.13	0.13	4.78	4.85	4.90	4.98	0.13	0.13
SHF Sly5 [82]	4.70	4.77	4.83	4.90	0.13	0.13	4.77	4.84	4.90	4.97	0.13	0.13
SHF Sly6 [82]	4.70	4.77	4.83	4.90	0.13	0.13	4.77	4.84	4.89	4.97	0.13	0.13
SHF Sly4d [83]	4.71	4.79	4.84	4.91	0.13	0.12	4.78	4.85	4.90	4.97	0.12	0.12
SHF SV-bas [84]	4.68	4.76	4.80	4.88	0.12	0.12	4.74	4.82	4.87	4.94	0.13	0.12
SHF UNEDF0 [85]	4.69	4.76	4.83	4.91	0.14	0.14	4.76	4.83	4.92	4.99	0.16	0.15
SHF UNEDF1 [86]	4.68	4.76	4.83	4.91	0.15	0.15	4.76	4.83	4.90	4.98	0.15	0.15
SHF SkM* [87]	4.71	4.78	4.84	4.91	0.13	0.13	4.76	4.84	4.90	4.97	0.13	0.13
SHF SkP [88]	4.72	4.80	4.84	4.91	0.12	0.12	4.79	4.86	4.91	4.98	0.12	0.12
RMF DD-ME2 [89]	4.67	4.75	4.82	4.89	0.15	0.15	4.74	4.81	4.89	4.96	0.15	0.15
RMF DD-PC1 [90]	4.68	4.75	4.83	4.90	0.15	0.15	4.74	4.82	4.90	4.97	0.16	0.15
RMF NL1 [91]	4.70	4.78	4.94	5.01	0.23	0.23	4.76	4.84	5.01	5.08	0.25	0.24
RMF NL3 [92]	4.69	4.77	4.89	4.96	0.20	0.19	4.75	4.82	4.95	5.03	0.21	0.20
RMF NL-Z2 [93]	4.73	4.80	4.94	5.01	0.21	0.21	4.79	4.86	5.01	5.08	0.22	0.22
RMF NL-SH [94]	4.68	4.75	4.86	4.94	0.19	0.18	4.74	4.81	4.93	5.00	0.19	0.19

Weak mixing angle

M. Atzori Corona et al., EPJC 83 (2023) 7, 683, arXiv:2303:09360

The Weinberg angle, θ_W is a fundamental parameter of the EW theory of the SM. It determines the relative strength of the weak NC vs. the electromagnetic interaction. There are many ways to define it, one of those is the **minimal subtraction scheme** ($\overline{MS}$).

- $\sin^2\hat{\theta}_W(M_Z) \equiv \hat{s}_Z^2 = 0.23122 \pm 0.00004$ ($\overline{MS}$)

The value of $\sin^2\hat{\theta}_W$ runs as a function of the momentum transfer or the energy scale. For low energies it assumes the value $\hat{s}_0^2(0) = 0.23863 \pm 0.00005$ ($\overline{MS}$)

	$\sin^2\vartheta_W$ best-fit$^{+1\sigma+90\%\text{CL}+2\sigma}_{-1\sigma-90\%\text{CL}-2\sigma}$	$\chi^2_{\min}$
COH-CsI	$0.231^{+0.027+0.046+0.058}_{-0.024-0.039-0.047}$	86.0
APV PDG	$0.2375^{+0.0019+0.0031+0.0038}_{-0.0019-0.0031-0.0038}$	-
APV 2021	$0.2399^{+0.0016+0.0026+0.0032}_{-0.0016-0.0026-0.0032}$	-
APV PDG + CsI	$0.2374^{+0.0020+0.0032+0.0039}_{-0.0018-0.0031-0.0037}$	86.0
APV 2021 + CsI	$0.2398^{+0.0016+0.0026+0.0032}_{-0.0015-0.0026-0.0031}$	86.0

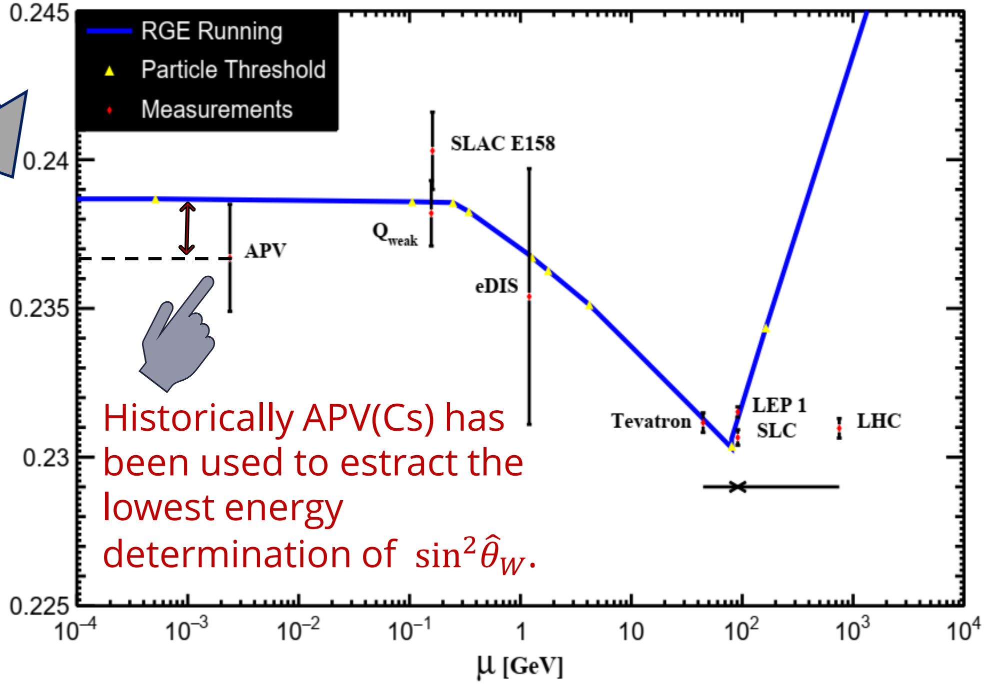

Historically APV(Cs) has been used to estract the lowest energy determination of $\sin^2\hat{\theta}_W$.

R. L. Workman et al. (Particle Data Group), "Review of Particle Physics," PTEP **2022**, 083C01 (2022).

However R_n(Cs) (or the neutron skin) has been taken from **indirect measurements** using antiprotonic atoms, which are known to be affected by considerable model dependencies

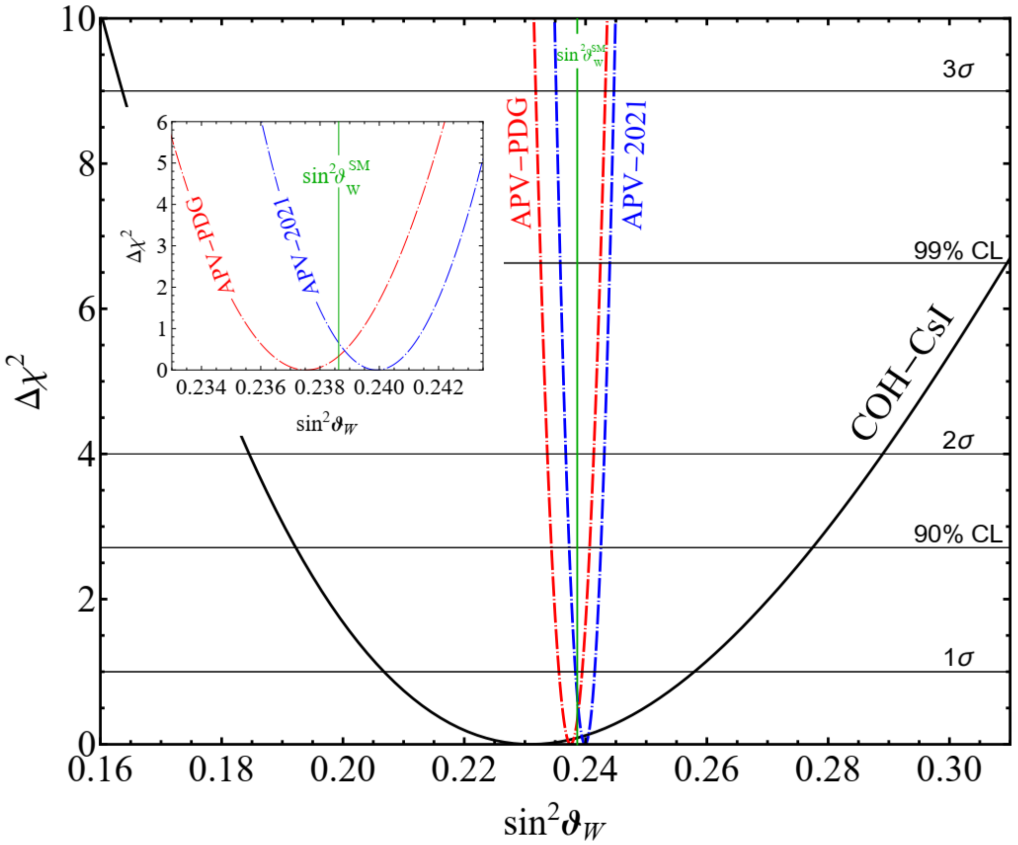

See also Cañas et al. *Phys.Lett.B* 761 (2016) 450-455

Combined 2D fit with COHERENT and APV(Cs)

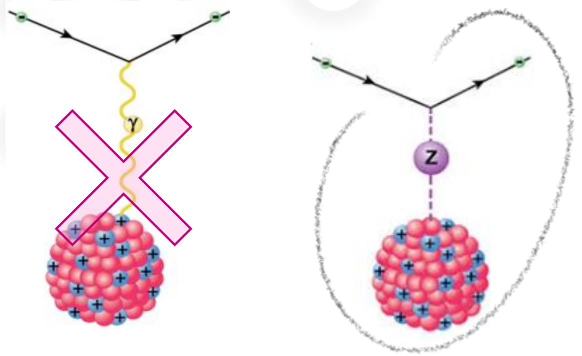

Mediated by photons. Sensitive to the charge (proton) distribution

Mediated by the Z. Mostly sensitive to the weak (neutron) distribution.

M. Cadeddu and F. Dordei, PRD 99, 033010 (2019), arXiv:1808.10202

+ Atomic Parity Violation APV(Cs) and CEνNS depends both on the **weak charge** and thus on R_n(Cs) and $\sin^2\vartheta_W$

$$Q_W^{SM} \approx Z\left(1 - 4\sin^2\theta_W^{SM}\right) - N$$

+ We can combine APV(Cs) and COHERENT(CsI) to obtain a fully data driven measurement of the WMA in the low energy regime!

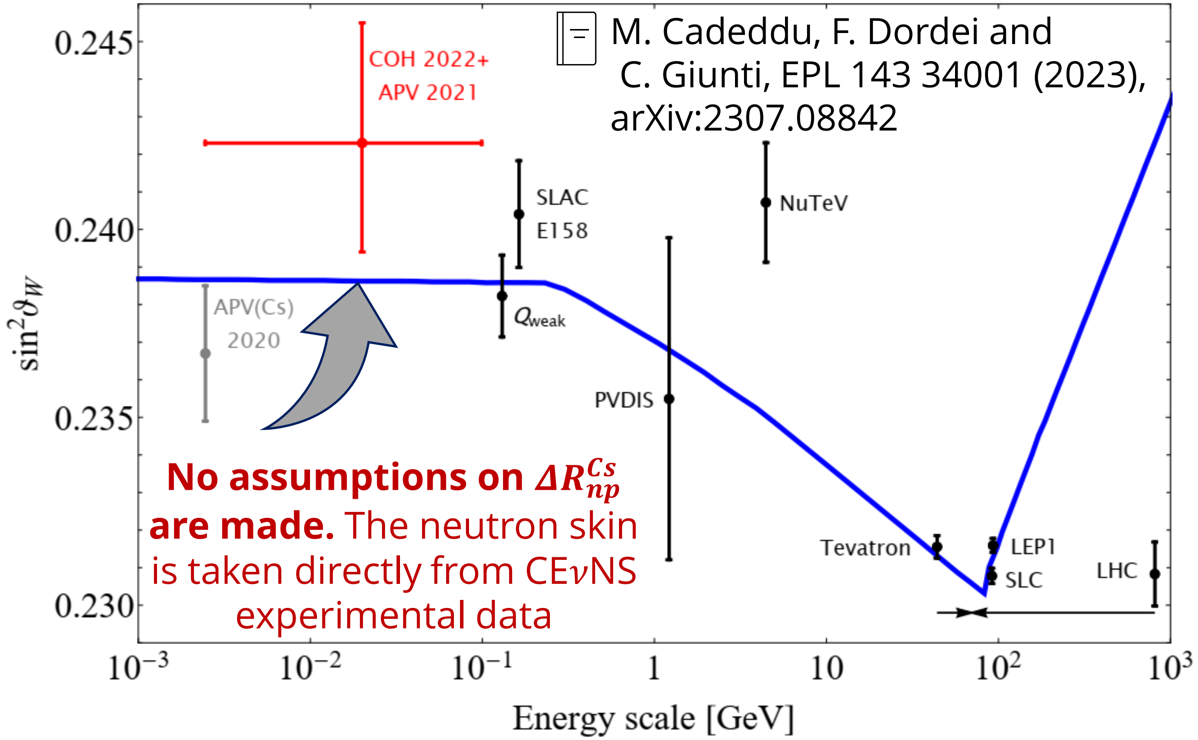

M. Cadeddu, F. Dordei and C. Giunti, EPL 143 34001 (2023), arXiv:2307.08842

No assumptions on ΔR_{np}^{Cs} are made. The neutron skin is taken directly from CEνNS experimental data

M. Cadeddu, N. Cargioli, F. Dordei, C. Giunti, E Picciau PRD 104, 011701 (2021), Arxiv:2104.03280

Measuring the WMA at low energies could reveal the presence of light dark Z bosons that would appear as a deviation of the SM prediction of the running depending on the value of the new mediator mass and kinetic mixing.

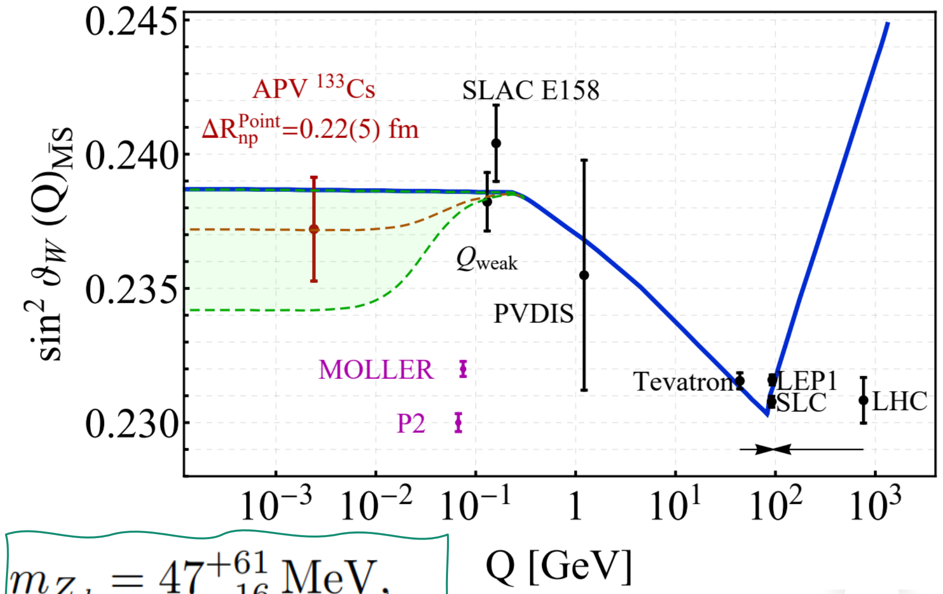

$$m_{Z_d} = 47^{+61}_{-16}\ \text{MeV},$$
$$\varepsilon = 2.3^{+1.1}_{-0.4} \times 10^{-3}$$

Light mediators from SM U(1)' extensions: vector-boson case

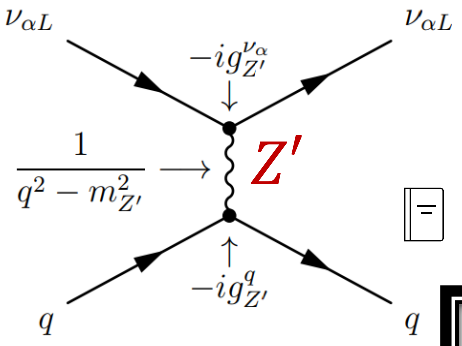

$$\mathcal{L}_{Z'}^{V} = -Z'_\mu \left[\sum_{\ell=e,\mu,\tau} g_{Z'}^{\nu_\ell V}\, \overline{\nu_{\ell L}} \gamma^\mu \nu_{\ell L} + \sum_{q=u,d} g_{Z'}^{qV}\, \bar{q}\gamma^\mu q \right]$$

M. Atzori Corona et al. JHEP 05 (2022)109, arXiv:2202.11002

- Search for anomaly free extensions of the SM (connection with Dark Sectors, Hidden Sectors..)
- Light mediators ~ MeV − few GeVs

Rev.Mod.Phys. 81 (2009) 1199-1228

$$SU(2)_\mathrm{L} \otimes U(1)_Y \otimes SU(3)_\mathrm{c} \rightarrow SU(2)_\mathrm{L} \otimes U(1)_Y \otimes SU(3)_\mathrm{c} \otimes U(1)'$$

- The effect of the new mediator is quantified by additional terms in the weak charge of the nucleus

$$Q_{\ell,\mathrm{SM+V}}^{V} = Q_{\ell,\mathrm{SM}}^{V} + \frac{g_{Z'}^2\, Q'_\ell}{\sqrt{2} G_F \left(|\vec{q}|^2 + M_{Z'}^2\right)} \left[\left(2Q'_u + Q'_d\right) Z F_Z(|\vec{q}|^2) + \left(Q'_u + 2Q'_d\right) N F_N(|\vec{q}|^2) \right]$$

The universal model is not anomaly free

These models are anomaly free if the SM is extended with right-handed neutrinos

Model	Q'_u	Q'_d	Q'_e	Q'_μ	Q'_τ
universal	1	1	1	1	1
$B-L$	$1/3$	$1/3$	-1	-1	-1
$B-3L_e$	$1/3$	$1/3$	-3	0	0
$B-3L_\mu$	$1/3$	$1/3$	0	-3	0
$B-2L_e-L_\mu$	$1/3$	$1/3$	-2	-1	0
$B-L_e-2L_\mu$	$1/3$	$1/3$	-1	-2	0
$B_y+L_\mu+L_\tau$	$1/3$	$1/3$	0	1	1
L_e-L_μ	0	0	1	-1	0
L_e-L_τ	0	0	1	0	-1
$L_\mu-L_\tau$	0	0	0	1	-1

Anomaly-free

The coupling of the new vector boson with the quarks is generated by kinetic mixing of Z' with the photon at the one-loop level

See also:
Miranda et al. Phys. Rev. D 101, 073005 (2020)
Coloma et al. JHEP 01 (2021) 114

Constraints on light mediators from COHERENT data

M. Atzori Corona et al. JHEP 05 (2022)109, arXiv:2202.11002

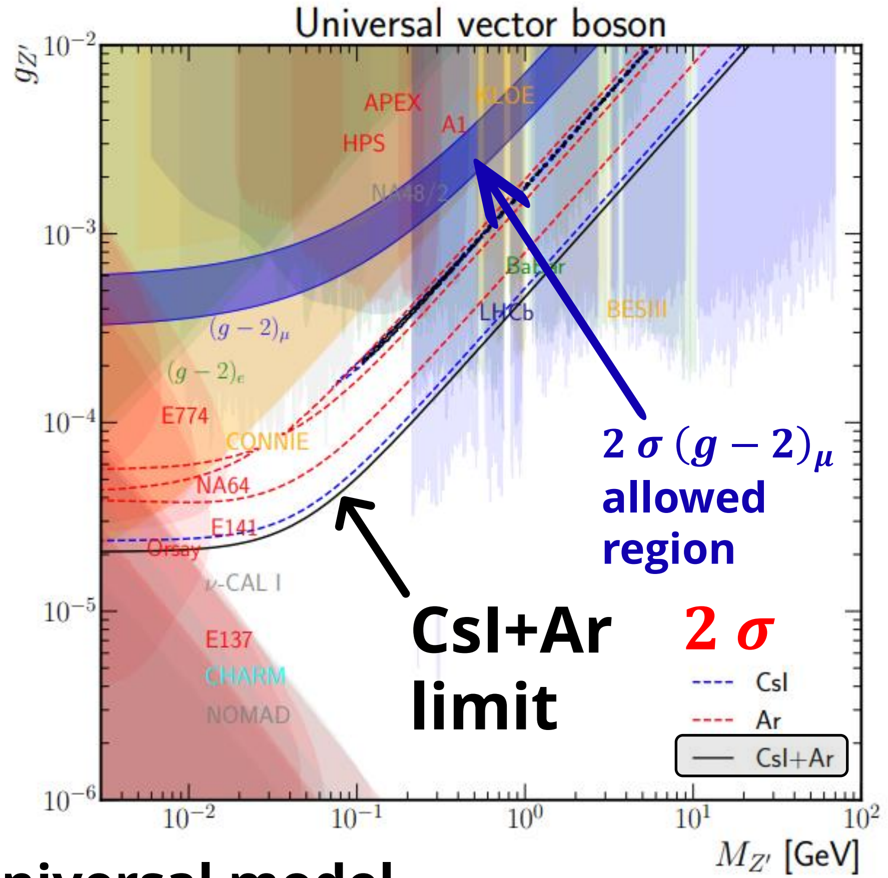

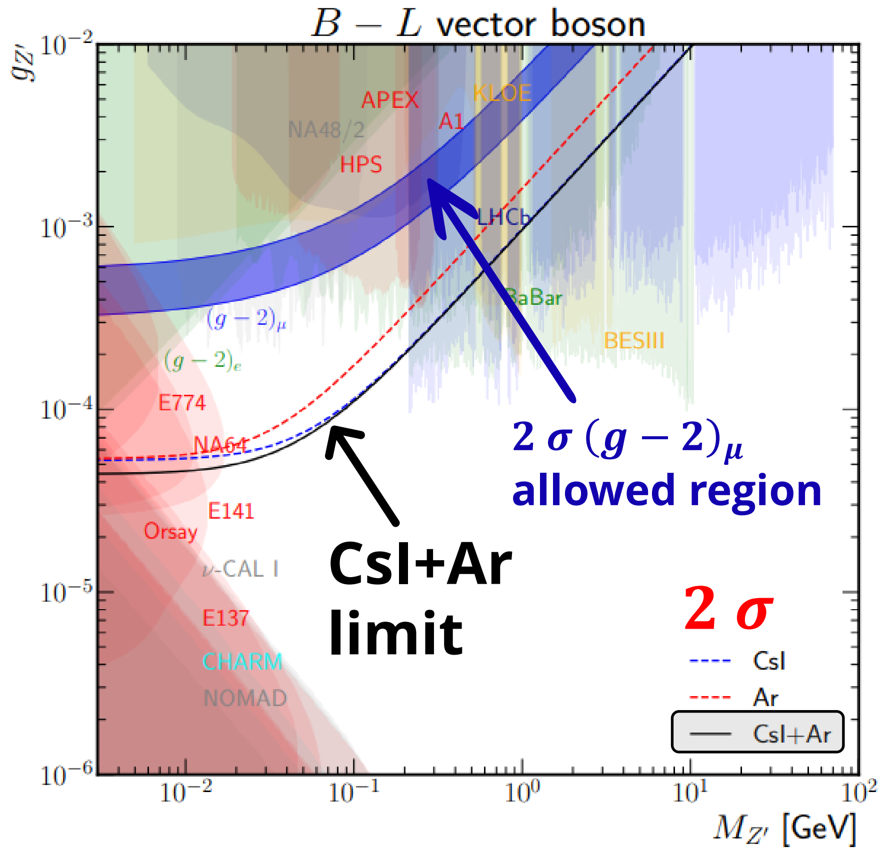

Universal model

- **Same coupling** to all SM fermions
- Improved constraints for 20<$M_{z'}$<200 MeV and 2×10^{-5}<$g_{z'}<10^{-4}$
- $(\boldsymbol{g-2})_{\boldsymbol{\mu}}$ excluded

B-L

- **Quark charge** $Q_q = 1/3$; **Lepton charge** $Q_\ell = -1$
- Improved constraints for 10<$M_{z'}$<200 MeV and 5×10^{-5}<$g_{z'}<3\times10^{-4}$
- $(\boldsymbol{g-2})_{\boldsymbol{\mu}}$ excluded

Constraints on light mediators from COHERENT data

M. Atzori Corona et al. JHEP 05 (2022)109, arXiv:2202.11002

New light scalar boson mediator that is assumed, for simplicity, to have universal coupling with quarks and leptons

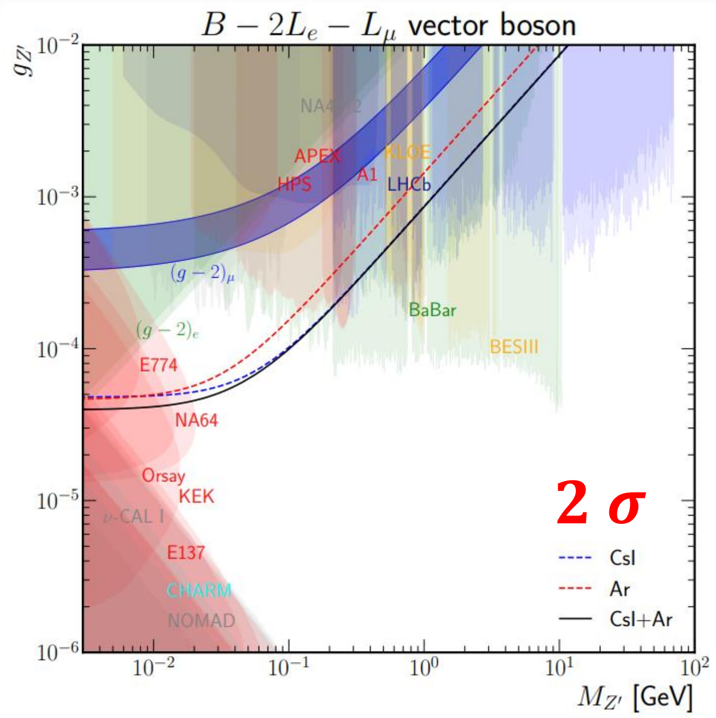

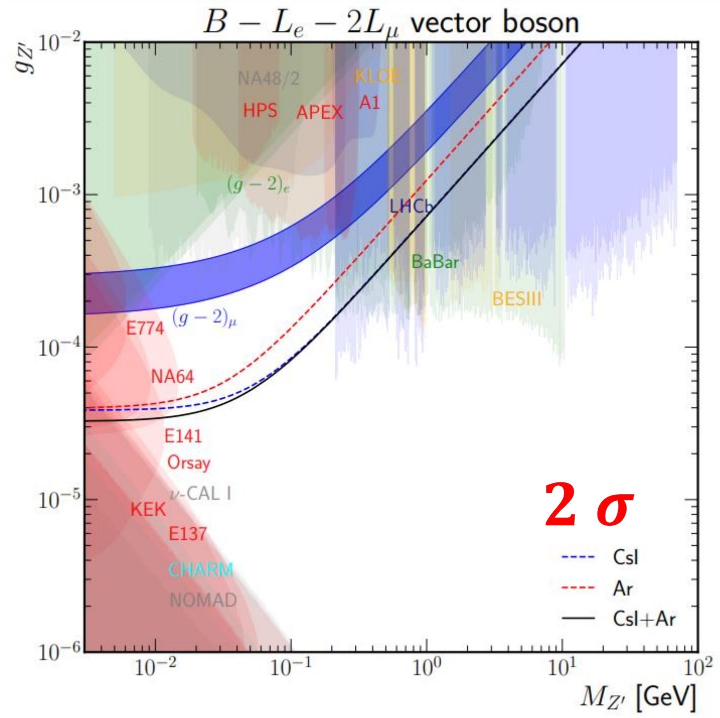

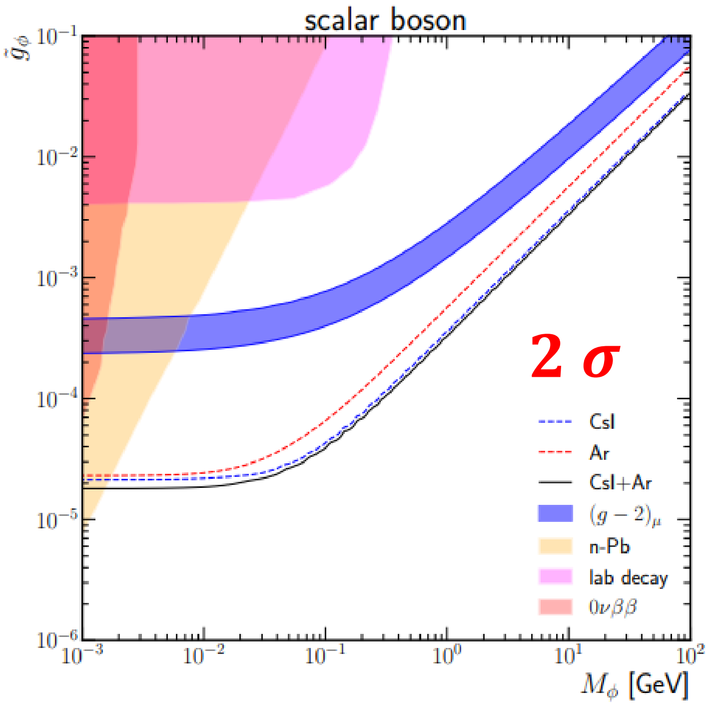

$B-2L_e-L_\mu$

- $Q_q = 1/3$; $Q_e = -2$; $Q_\mu = -1$
- Improved constraints for 10<$M_{Z'}$<100 MeV and 5×10^{-5}<$g_{Z'} < 2\times10^{-4}$
- $(g-2)_\mu$ excluded

$B-L_e-2L_\mu$

- Improved constraints for 20<$M_{Z'}$<200 MeV and 3×10^{-5}<$g_{Z'} < 3\times10^{-4}$
- $(g-2)_\mu$ excluded

Scalar mediator

- Very strong limits with CEνNS for $M_\phi > 2$ MeV
- $(g-2)_\mu$ excluded

The $L_\mu - L_\tau$ scenario

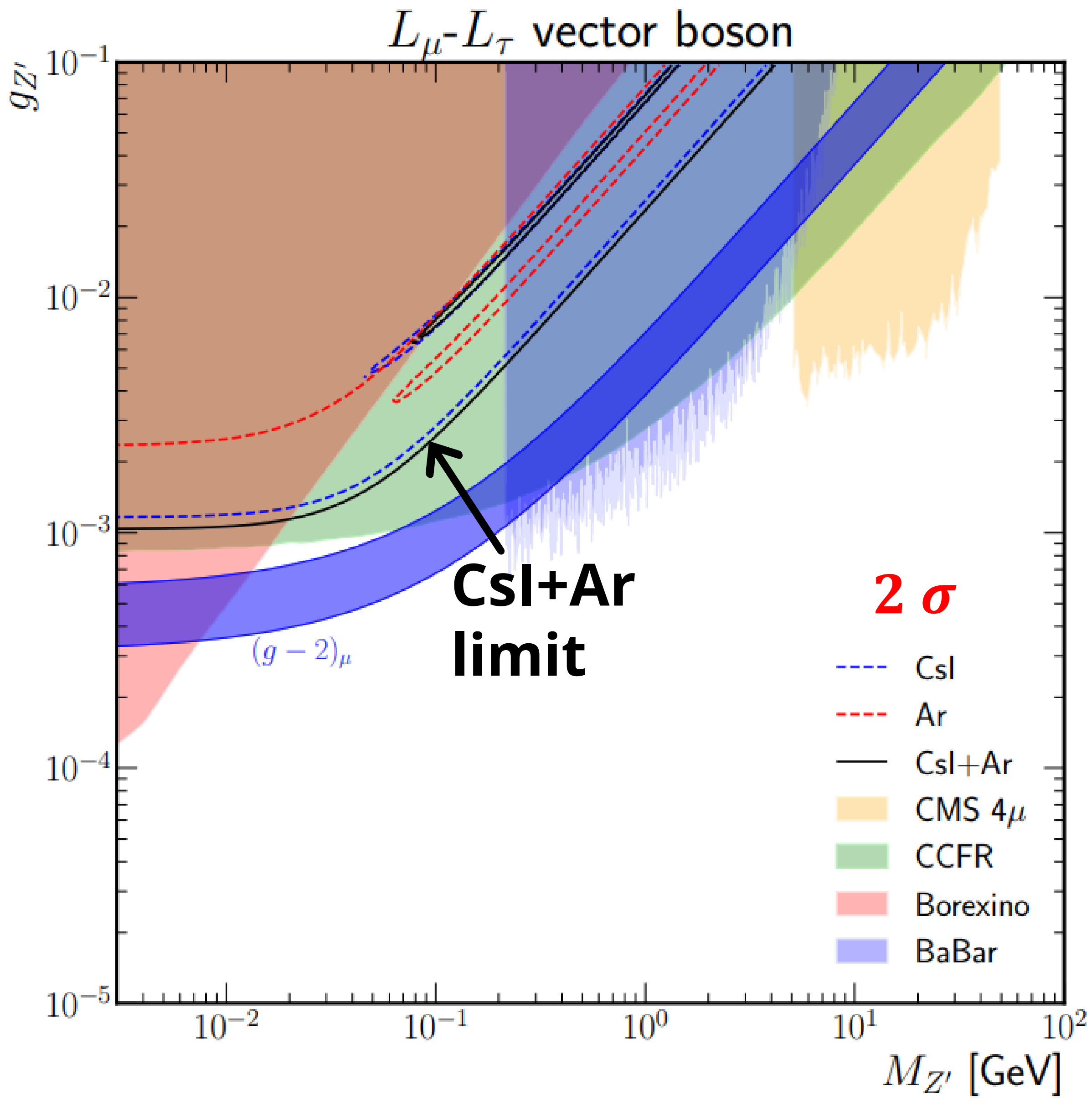

- As for all the $L_\alpha - L_\beta$ models the constraints that we can obtain from CEνNS data are weaker than those in the previous models, because the **interaction with quarks occurs only at loop level**, and hence it is weaker

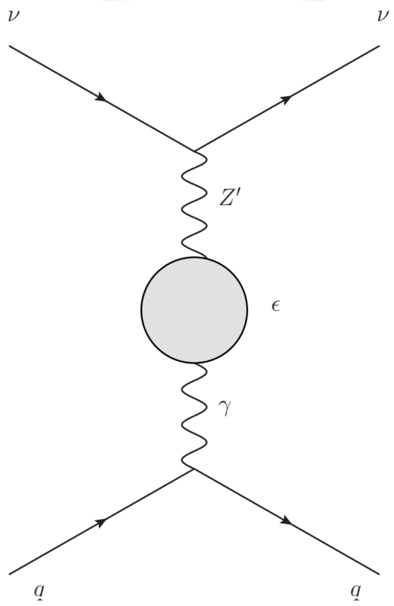

- Coupling only to μ and τ flavor $Q_\mu = 1; Q_\tau = -1$
- One of the most popular model because $(\boldsymbol{g-2})_{\boldsymbol{\mu}}$ band **is not excluded.**
- At the moment CEνNS limits are not competitive!

The $L_\mu - L_\tau$ scenario

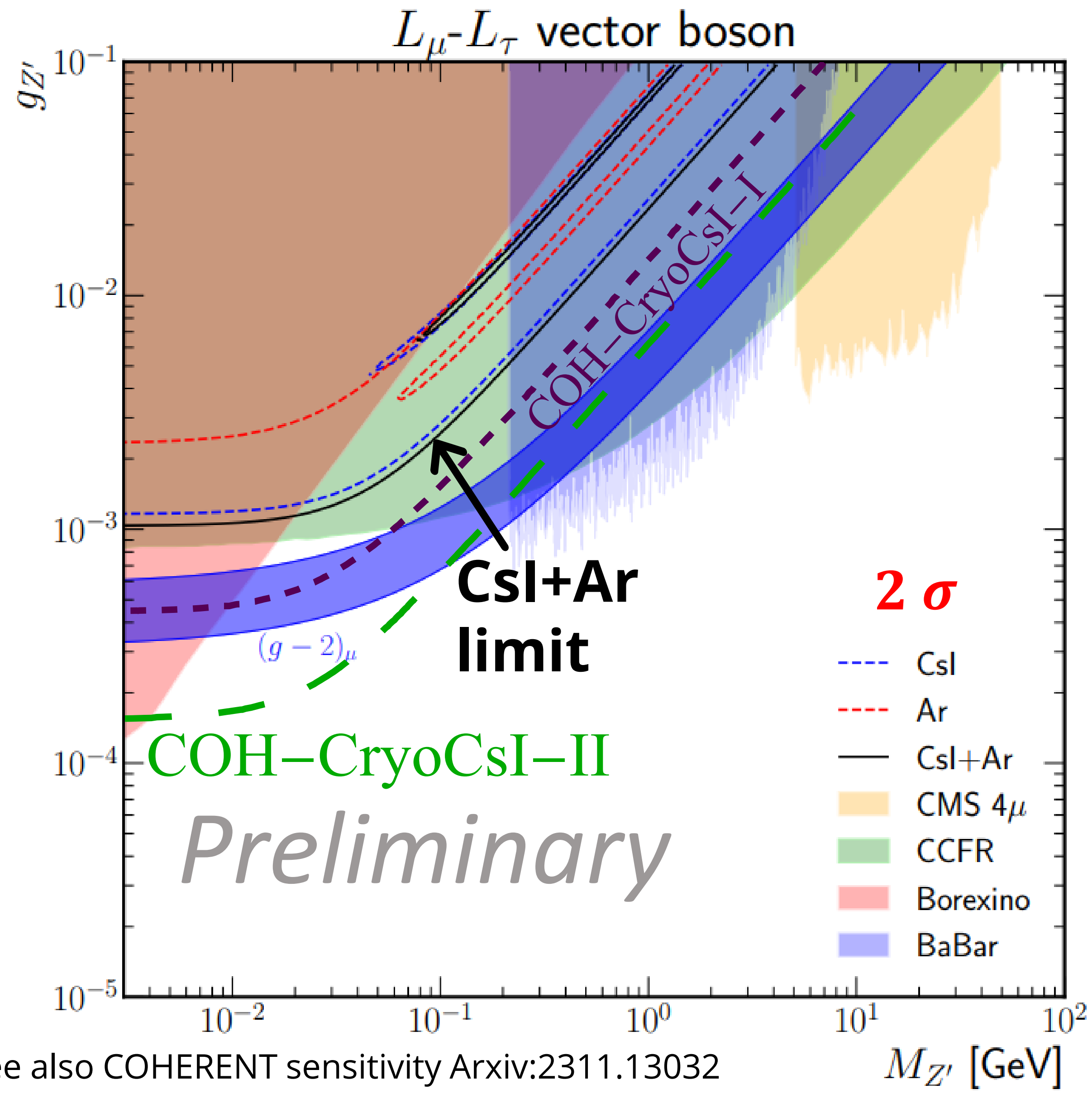

See also COHERENT sensitivity Arxiv:2311.13032

- The **situation will change** in the future thanks to the **COH-Cryo-CsI-I** and **COH-Cryo-CsI-II** detectors (See "The COHERENT Experimental Program" arXiv:2204.04575)
- ~10 kg (COH-CryoCsI-1) and a ~700 kg (COH-CryoCsI-2) cryogenic CsI detector with two target stations.

➢ The $(g-2)_\mu$ band needs to be updated after the recent result by the g-2 Collaboration @Fermilab and the new results on the hadronic vacuum polarzation contribution from lattice. See Arxiv:2308.06230

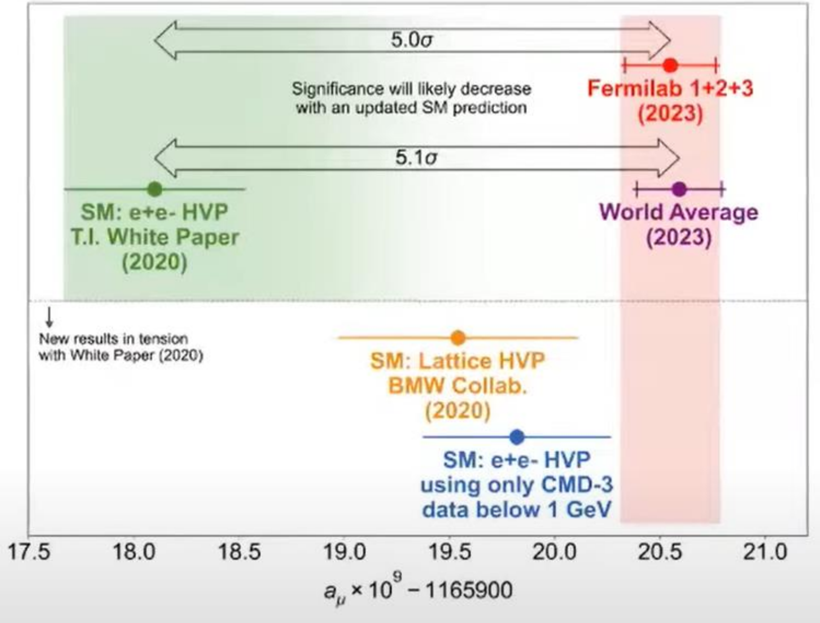

Neutrino charge radius

➢ In the SM the effective vertex reduces to $\gamma_\mu F(q^2)$ since the contribution $q_\mu \gamma^\mu q_\mu / q^2$ vanishes in the coupling with a conserved current

$$\Lambda_\mu(q) = (\gamma_\mu - q_\mu \gamma^\mu q_\mu / q^2) F(q^2)$$

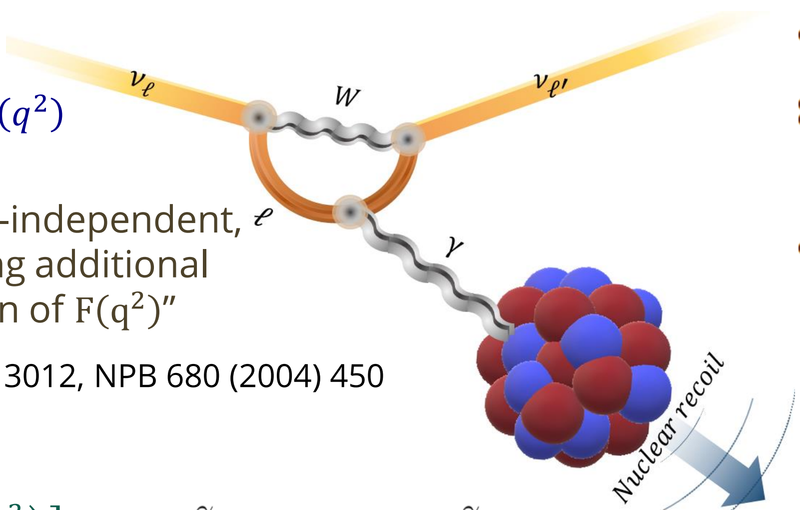

"A charge radius that is gauge-independent, finite is achieved by including additional diagrams in the calculation of $F(q^2)$"

Bernabeu et al, PRD 62 (2000) 113012, NPB 680 (2004) 450

➢ In the Standard Model

$$\langle r^2_{\nu_l} \rangle_{SM} = -\frac{G_F}{2\sqrt{2}\pi^2}\left[3 - 2\log\left(\frac{m_e^2}{m_W^2}\right)\right]$$

$$\langle r^2_{\nu_e} \rangle_{SM} = -8.2 \times 10^{-33}\ \mathrm{cm}^2$$

$$\langle r^2_{\nu_\mu} \rangle_{SM} = -4.8 \times 10^{-33}\ \mathrm{cm}^2$$

$$\langle r^2_{\nu_\tau} \rangle_{SM} = -3.0 \times 10^{-33}\ \mathrm{cm}^2$$

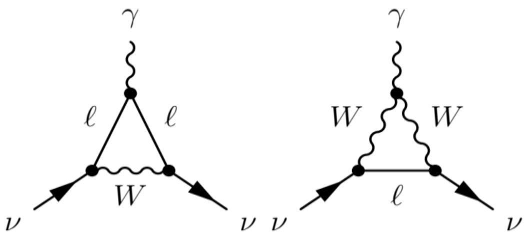

R. L. Workman et al. (Particle Data Group), "Review of Particle Physics," PTEP **2022**, 083C01 (2022).

VALUE (10^{-32} cm^2)	*CL%*	*DOCUMENT ID*		*TECN*	*COMMENT*
−2.1 to 3.3	90	[1] DENIZ	2010	TEXO	Reactor $\bar{\nu}_e e$
• • We do not use the following data for averages, fits, limits, etc. • •					
−27.5 to 3	90	[2] CADEDDU	2018		ν_μ coherent scat. on CsI
−0.53 to 0.68	90	[3] HIRSCH	2003		$\nu_\mu e$ scat.

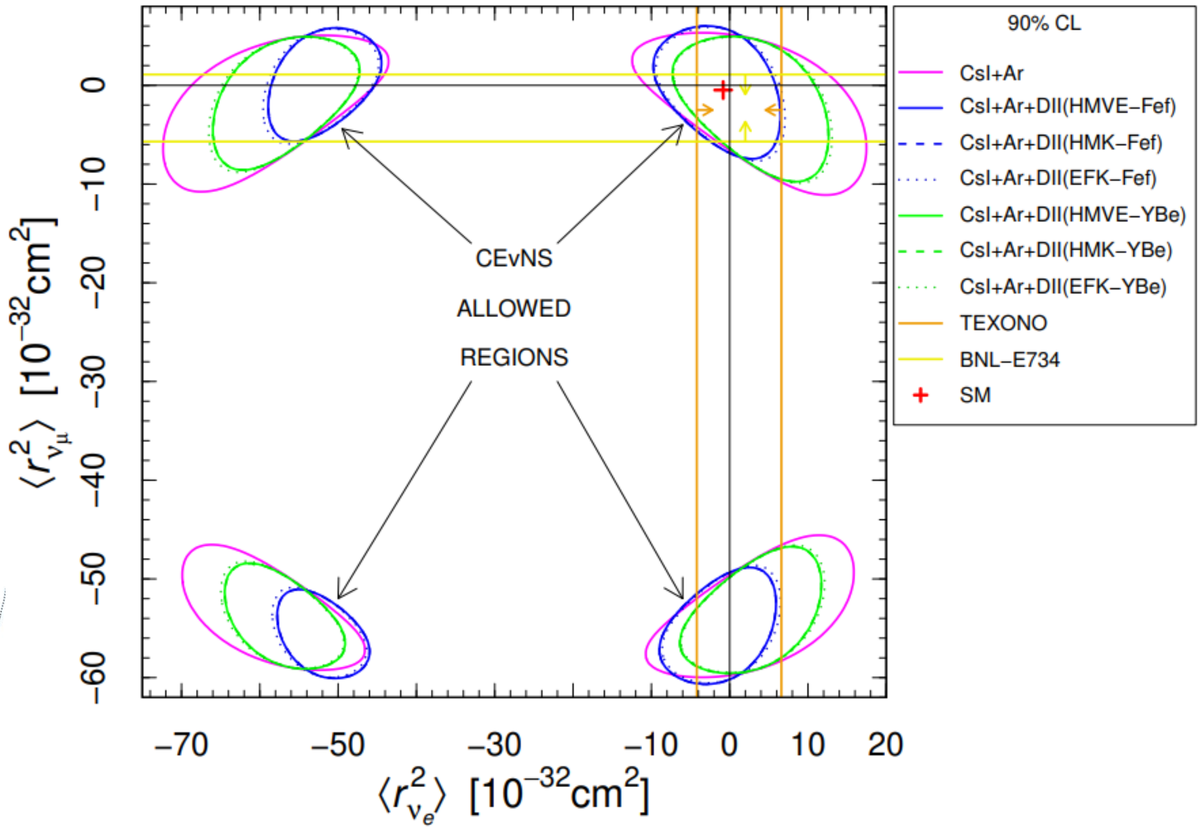

$-7.1 < \langle r^2_{\nu_e} \rangle [10^{-32}\ \mathrm{cm}^2] < 5$ @ 90% CL

M. Atzori Corona et al. **JHEP** 09 (2022) 164, arXiv:2205.09484

Current best limits:
accelerator $\nu_{e/\mu} - e$ scattering

- **TEXONO** $-4.2 < \langle r^2_{\nu_e} \rangle < \mathbf{6.6}\ [10^{-32}\mathrm{cm}^2]$
- **BNL-E734** $-5.7 < \langle r^2_{\nu_\mu} \rangle < 1.1\ [10^{-32}\mathrm{cm}^2]$ @90% CL

Limits on ν magnetic moment and millicharge

In the SM the channel due to neutrino-electron scattering is negligible with respect to that of CEvNS, however the contribution due to the magnetic moment and the millicharge grows as 1/T. Dark matter-searching experiments such as LZ, XENONnT that observe solar neutrinos are sensitive to these quantities

M. Atzori Corona et al. PRD **107**, 053001 (2023), arXiv:2207.05036

See also:
Giunti, Ternes, PRD 108 9, 095044 (2023)
Miranda et al. JHEP 12 (2021) 191
Miranda et al. PLB 808 (2020) 135685
Miranda et al. JHEP07(2019)103

$$\frac{d\sigma^{\mathrm{MM}}_{\nu_\ell}}{dT_{\mathrm{e}}}(E, T_{\mathrm{e}}) = Z^{\mathrm{Xe}}_{\mathrm{eff}}(T_{\mathrm{e}}) \frac{\pi\alpha^2}{m_e^2}\left(\frac{1}{T_{\mathrm{e}}} - \frac{1}{E}\right)\left|\frac{\mu_{\nu_\ell}}{\mu_{\mathrm{B}}}\right|^2$$

$$\left.\frac{d\sigma_{\nu_\ell}}{dT_{\mathrm{e}}}\right|^{\mathrm{EC}}_{\mathrm{EPA}} = \frac{2\alpha}{\pi}\frac{\sigma_\gamma(T_e)}{T_e}\log\left[\frac{E_\nu}{m_\nu}\right] q^2_{\nu_\ell}$$

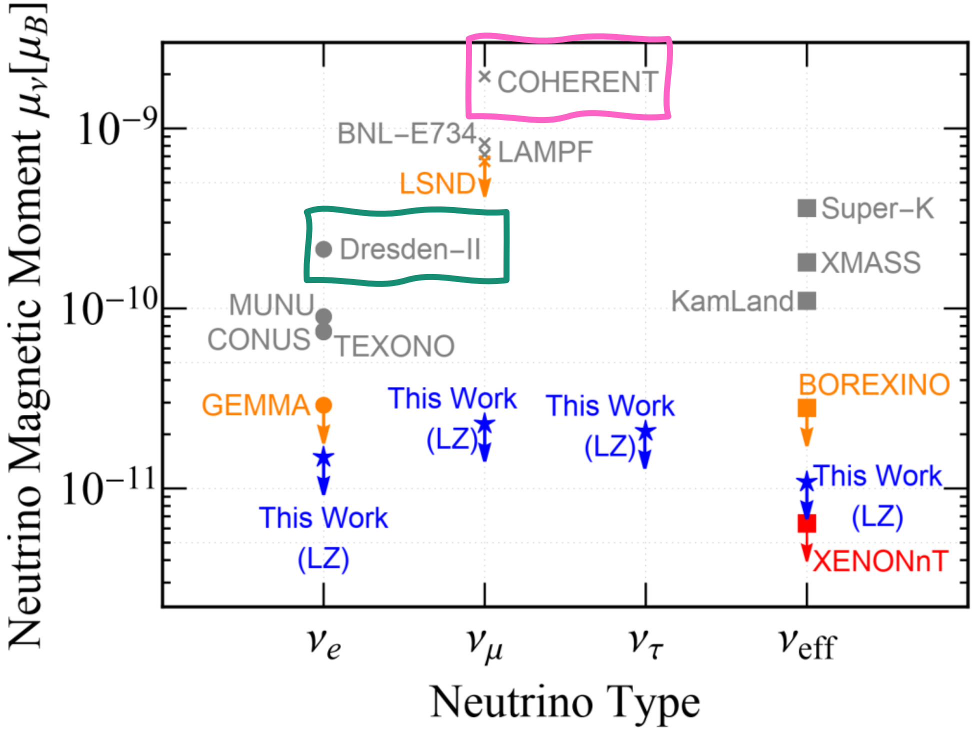

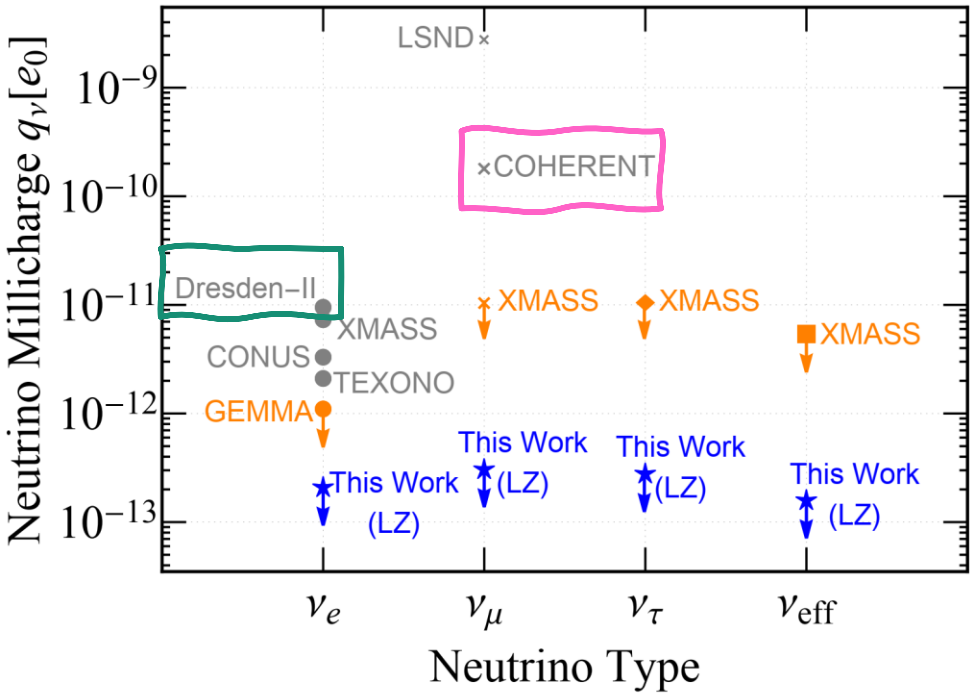

$$\mu_\nu = \frac{3e_0 G_F}{8\sqrt{2}\pi^2} m_\nu \simeq 3.2 \times 10^{-19}\left(\frac{m_\nu}{\mathrm{eV}}\right)\mu_B$$

- CEvNS limits from COHERENT and Dresden-II detectors competitive. Dresden-II profits from the very low threshold, however the CEvNS signal in Dresden-II is debated…

Migdal contribution in reactor CEvNS experiments

New paper
[arXiv:2307.12911]

- The first observation of CEvNS at reactors by Dresden-II [PRL129 211802 (2022)] relies on an unexpected enhancement at low energies [PRD 103, 122003] of the measured quenching factor (QF) with respect to the Lindhard prediction (k=0.157).
- The QF quantifies the reduction of the ionization yield produced by a nuclear recoil with respect to an electron recoil of the same energy.
- Since the Dresden-II result implies an extra observable ionization signal produced after the nuclear recoil, some authors [PRD 104, 015005 , PRD 106, L031702] have cleverly interpreted this enhancement as due to the so called Migdal effect

SuperCDMS Coll. Arxiv:2202.07043

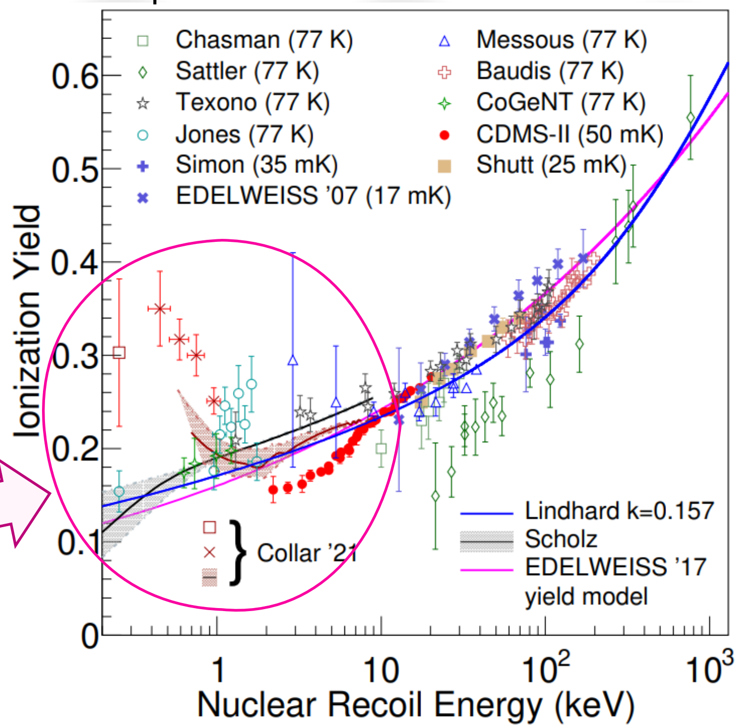

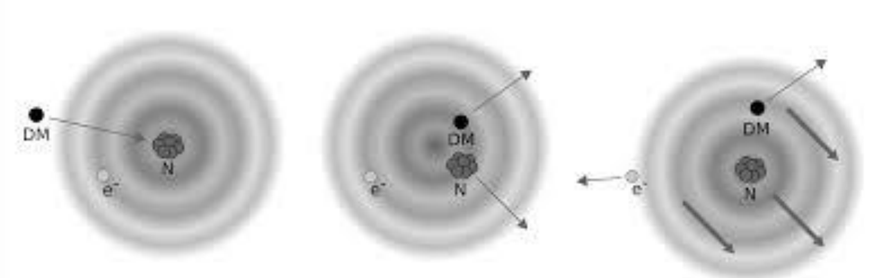

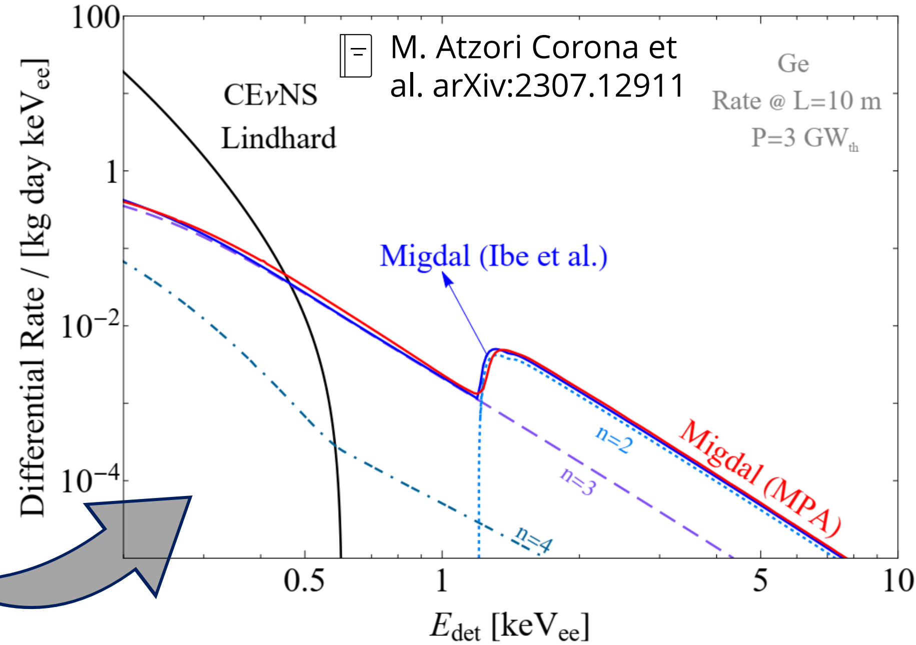

✓ In our last work we study in detail the impact of the Migdal contribution to the standard CEvNS signal calculated with the Lindhard quenching factor. To this purpose, we compare different formalisms, that of Ibe et al. (JHEP 03, 194) and Migdal photo-absorption (PRD 102, 121303) that nicely show a perfect agreement, making our findings robust.

Migdal contribution

$$\left(\frac{d\sigma_{\bar{\nu}_e\text{-}\mathcal{N}}}{dT_{\rm nr}}\right)^{\text{Ibe } et\ al.}_{\rm Migdal} = \frac{G_F^2 M}{\pi}\left(1-\frac{M T_{\rm nr}}{2E_\nu^2}\right) Q_W^2 \times |Z_{\rm ion}(q_e)|^2\,,$$

Where Z_{ion} is the ionization rate of an individual electron in the target

$$|Z_{\rm ion}(q_e)|^2 = \frac{1}{2\pi}\sum_{n,\ell}\int dT_e \frac{d}{dT_e} p^c_{q_e}(n\ell \to T_e)$$

p^c are the ionization probabilities for an atomic electron with quantum numbers n and ℓ that is ionized with a final energy T_e.

- The formalism developed in PRD 102, 121303 relates the **photoabsorption cross section σ_γ** to the Migdal dipole matrix element without requiring any many-body calculation.
- ➢ Photoabsorption cross section is experimentally known, such that the Migdal rate suffers from very small uncertainties

$$\left(\frac{d^2\sigma_{\bar{\nu}_e\text{-}\mathcal{N}}}{dT_{\rm nr}dE_r}\right)^{\rm MPA}_{\rm Migdal} = \frac{G_F^2 M}{\pi}\left(1-\frac{M T_{\rm nr}}{2E_\nu^2}\right) Q_W^2 \times \frac{1}{2\pi^2\alpha_{\rm EM}}\frac{m_e^2}{M}\frac{T_{\rm nr}}{E_r}\sigma_\gamma^{\rm Ge}(E_r),$$

- ✓ The Migdal contribution to the standard CEνNS signal calculated with the Lindhard quenching factor is completely negligible for observed energies below ~0.3 keV where the signal is detectable, and thus unable to provide any contribution to CEνNS searches in this energy regime.

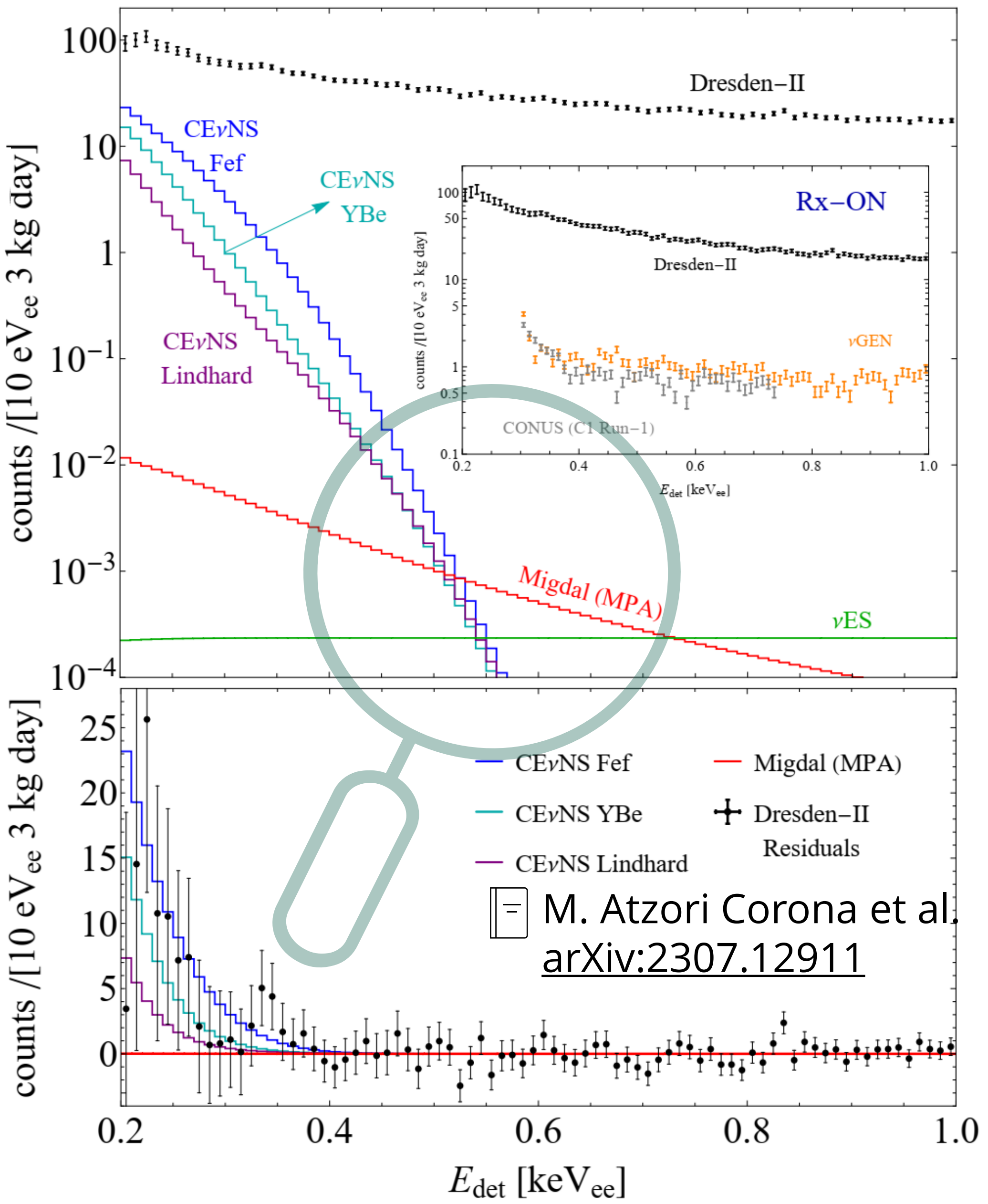

M. Atzori Corona et al. arXiv:2307.12911

✓ A different explanation is thus required!

Conclusions

- CEνNS is a powerful tool for measuring the neutron form factor (R_n meausered with a 7% precsion). Very important to know when fitting for BSM physics.
- On the other hand CEνNS is not so sensitive to the $\sin^2\vartheta_W$, but, in combination with APV(Cs) provides a complete data-driven value of $\sin^2\vartheta_W$ (historically APV uses a R_n(Cs) which is extrapolated)
- BSM physics, expecially light new physics, can show up in the running of $\sin^2\vartheta_W$.
- CEνNS data (COHERENT CsI+Ar) is able to put strong constraints for different light Z boson models like the universal, B-L and other anomaly free models excluding the possibile interpretation of the muon g-2 results
- Good prospects are expected for the popular $L_\mu - L_\tau$ model in the upgrade phase of COHERENT CsI experiment. Waiting for a clarification of the $(\boldsymbol{g-2})_{\boldsymbol{\mu}}$ theoretical prediction.
- CEνNS is also powerful in constraing BSM neutrino properties, e.g. neutrino charge radius (best limit on the electron neutrino), neutrino magnetic moment and millicharge.
- In combination with neutrino-electron scattering data in COHERENT, DRESDEN-II and direct dark matter experiments like LZ we achieve very competitive limits on neutrino magnetic moment and millicharge.
- Thanks to the lower energy threshold achieved, Dresden-II Ge detector is very powerful in constraing BSM physics, however the signal relies on an unexpected increase of the quenching factor.
- The **extra ionization could be due to the Migdal effect**, however in arXiv:2307.12911 we show that the standard Migdal effect is negligible with respect to CEvNS, thus a different explanation is required.

The future is bright!


THANK YOU FOR YOUR ATTENTION!

BACKUP

Accessing new physics with an undoped, cryogenic

COHERENT Coll.
arXiv:2311.13032v1 (2023)

The COHERENT CsI detector that first observed CEvNS achieved a light yield of 13.35 PE/keVee, but it was only able to achieve a threshold of ≈ 700 eVee due to a 9 PE coincidence cut to remove both Cherenkov light in the photomultiplier tube (PMT) and the prominent afterglow observed in doped CsI[Na] crystals [45] at room temperature. There are three strategies to improve threshold relative to the original CsI detector: switch from PMT to silicon photomultiplier (SiPM) light detectors, reduce the afterglow scintillation rate, or increase the light yield. By switching to a SiPM readout for COH-CryoCsI-1, all three of these will be simultaneously met for **undoped CsI crystals operating near 40 K** where light yield is optimized.

[...] Though data analysis is underway, preliminary estimates point to a roughly energy independent **quenching factor of ≈ 15%**. We further assume a 10% relative uncertainty on that central value, achievable in past measurements of quenching in inorganic scintillators. With this, COH-CryoCsI1 would have **a ≈ 500 eVnr threshold for nuclear recoils**.

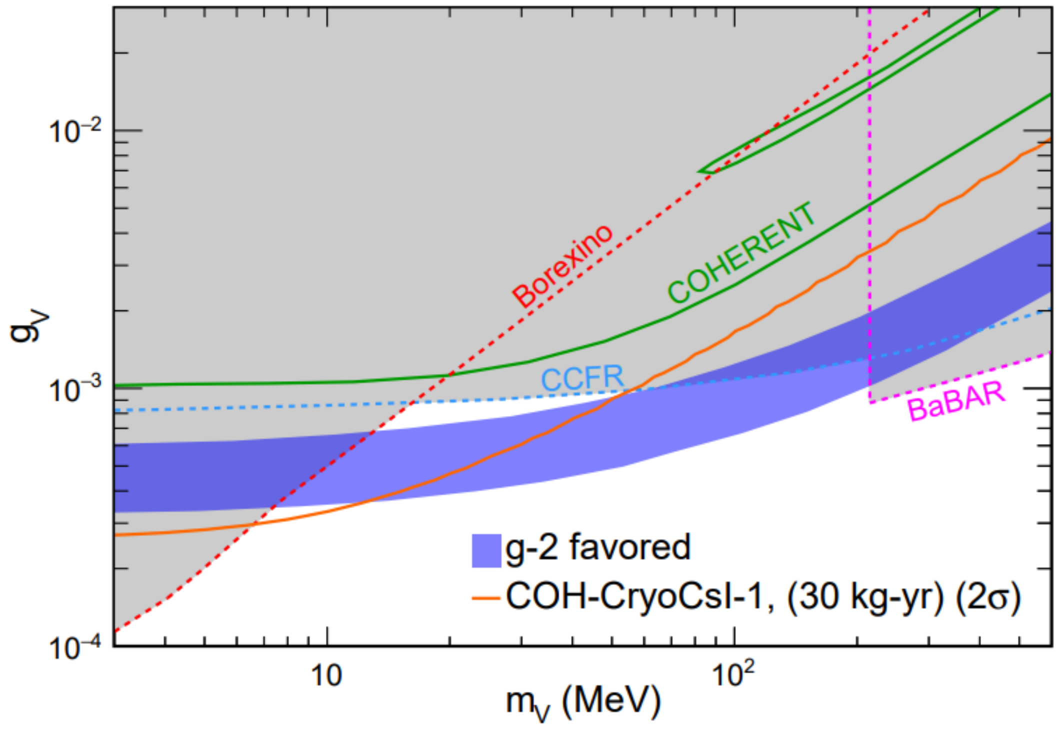

Figure 7. Sensitivity of COH-CryoCsI-1 to a $L_\mu - L_\tau$ mediator compared to current constraints from CEvNS (solid lines) and other experiments (dashed lines). Such a model would resolve the reported $g-2$ anomaly in the parameter space given by the blue shaded region.

Neutron nuclear radius in argon

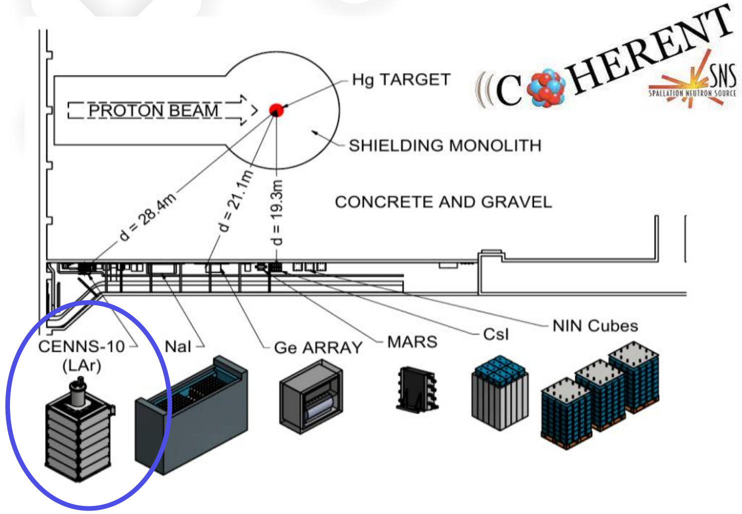

Combined fit in (time, energy, PSP) space suggest >3σ CEvNS detection significance

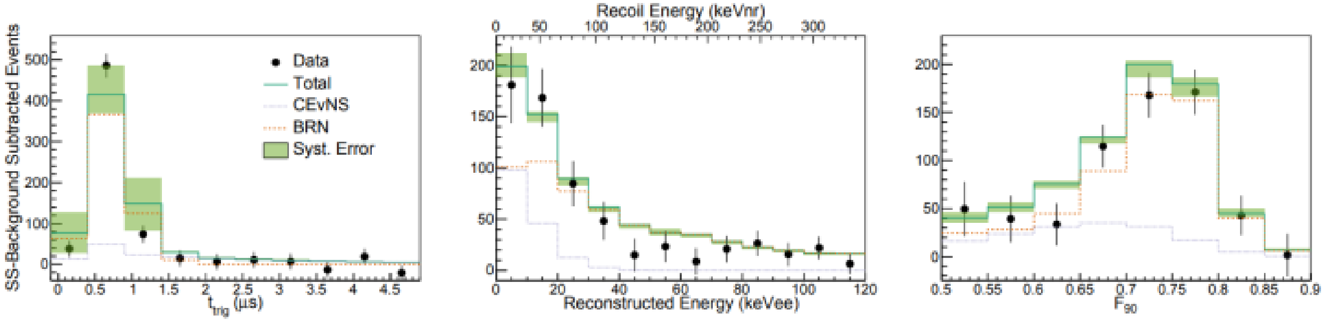

Dominant backgrounds:

1. ^{39}Ar beta decay
2. Beam related neutrons

Akimov et al, COHERENT Coll. PRL 126, 01002 (2021)

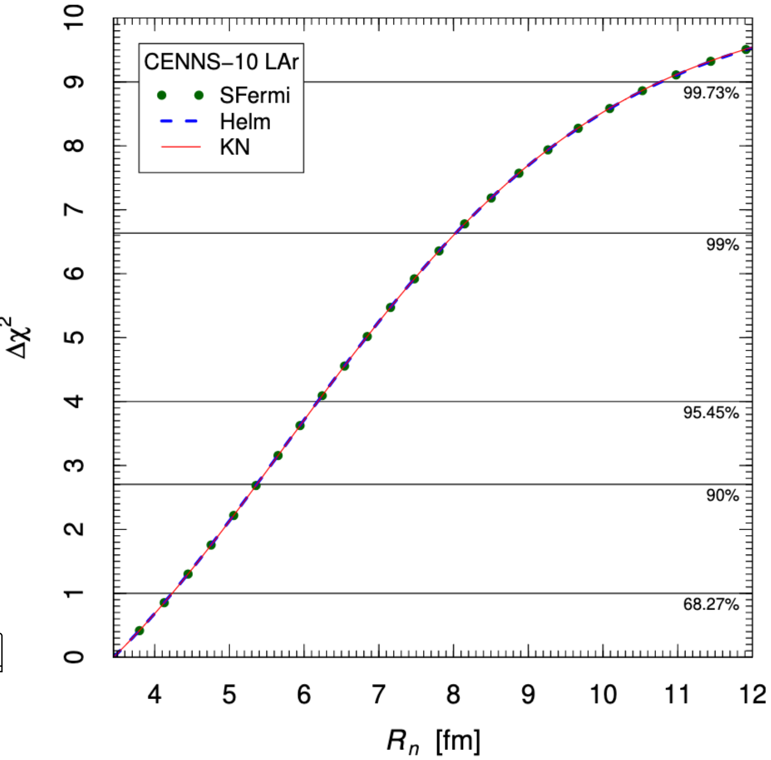

Cadeddu et al., PRD 102, 015030 (2020)

COHERENT Argon

$$R_n(^{40}\mathrm{Ar}) < 4.2\ \mathrm{fm}$$

More statistics needed.

Theoretical values

Interaction		$R_p^{\rm point}$	$R_n^{\rm point}$
Sky3D			
SkI3	[37]	3.33	3.43
SkI4	[37]	3.31	3.41
Sly4	[38]	3.38	3.46
Sly5	[38]	3.37	3.45
Sly6	[38]	3.36	3.44
Sly4d	[39]	3.35	3.44
SV-bas	[40]	3.33	3.42
UNEDF0	[41]	3.37	3.47
UNEDF1	[42]	3.33	3.43
SkM*	[43]	3.37	3.45
SkP	[44]	3.40	3.48

See also:
Payne et al.,
PRC 100, 061304 (2019)

See also:
Miranda et al.,
JHEP 05 (2020) 130

COHERENT future argon: "COH-Ar-750"
LAr based detector for precision CEνNS

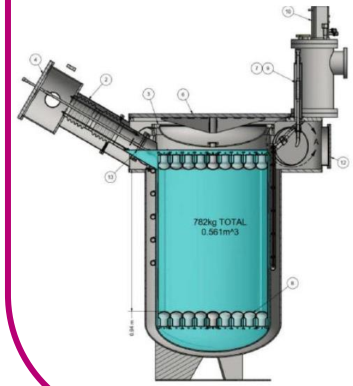

- Single phase, scintillation only, 750 kg total (610 kg fiducial)
- 3000 CEνNS/year

Interplay between nuclear and electroweak physics

+ This feature is always present when dealing with electroweak processes.

- Atomic Parity Violation (APV): atomic electrons interacting with nuclei. Cesium available.
- Parity Violation Electron Scattering (PVES): polarized electron scattering on nuclei. PREX(Pb), CREX(Ca)
- Coherent elastic neutrino-nucleus scattering (CEνNS). Cesium-iodide (CsI), argon (Ar) and germanium (Ge) available.

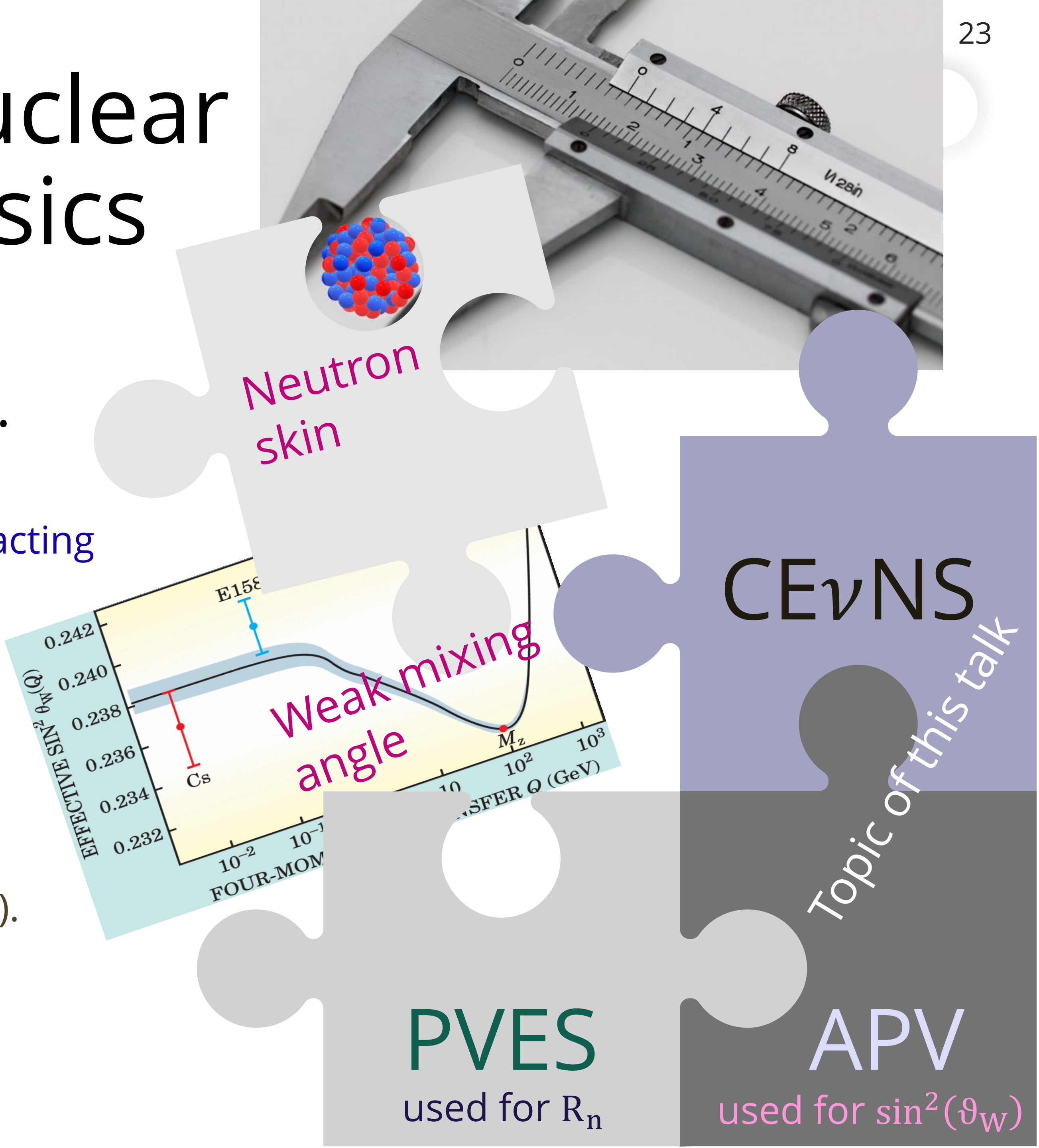

First average CsI neutron radius measurement (2018)

+ Using the first CsI dataset from D. Akimov et al. **Science** 357.6356 (2017)

M. Cadeddu, C. Giunti, Y.F. Li, Y.Y. Zhang, PRL 120 072501, (**2018**), arXiv:1710.02730

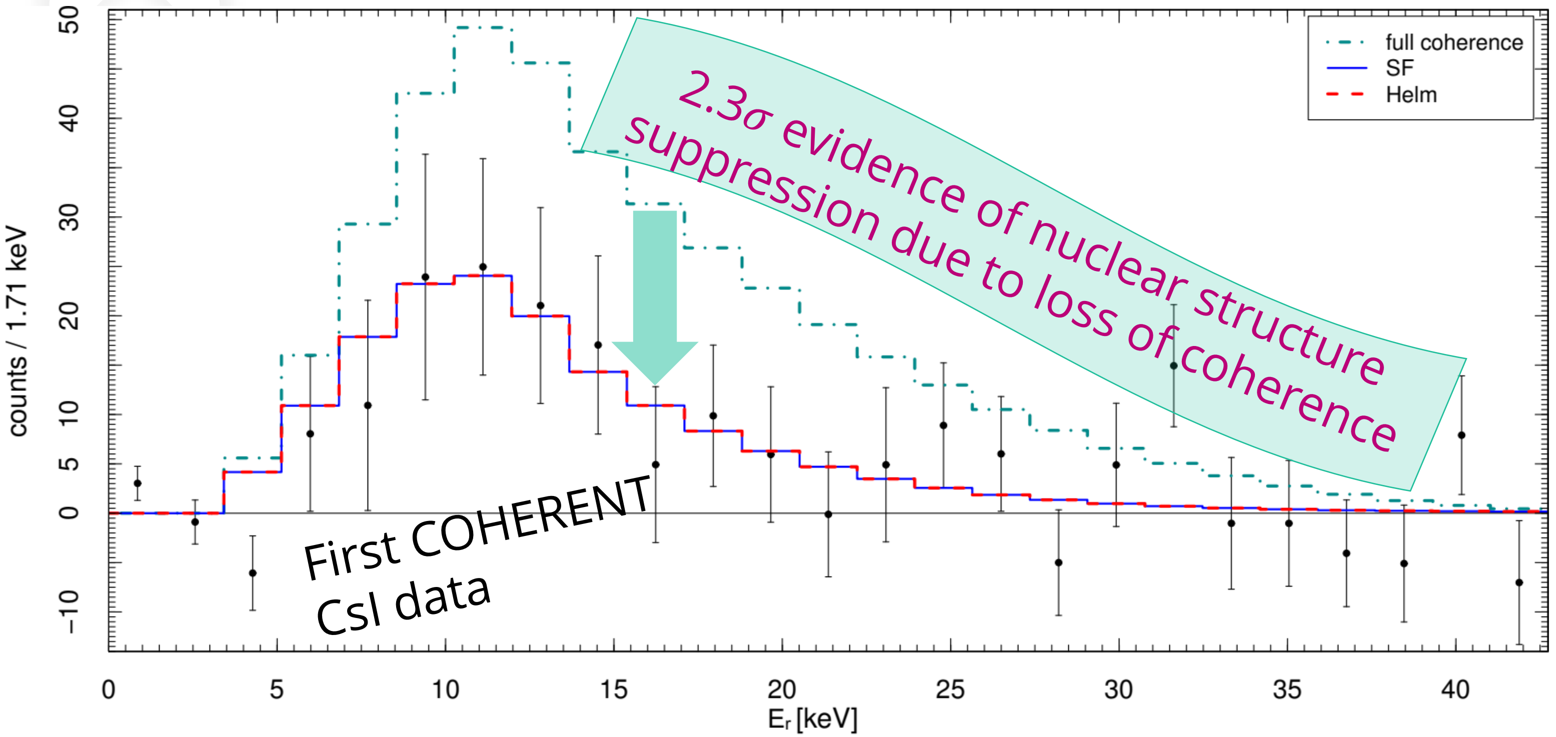

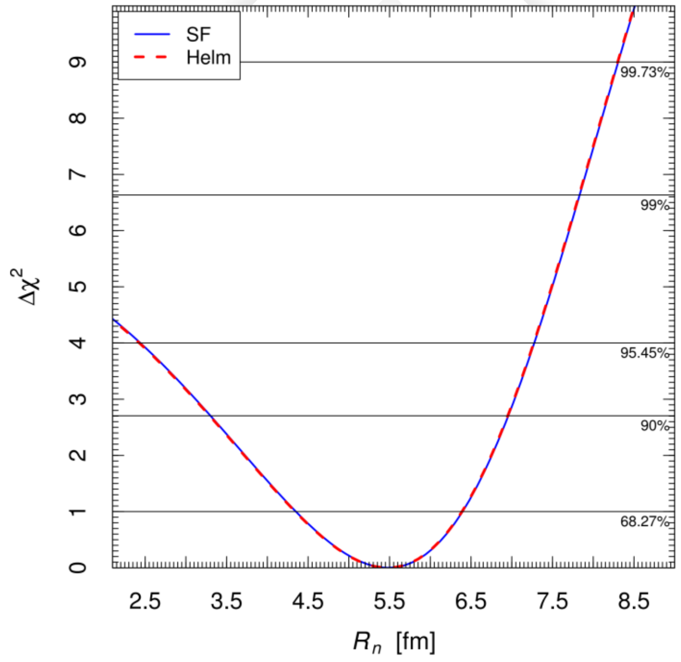

$$R_n^{CsI} = 5.5^{+0.9}_{-1.1}\ \mathrm{fm}$$

- We first compared the data with the predictions in the case of full coherence, i.e. all nuclear form factors equal to unity: the corresponding histogram does not fit the data.
- We fitted the COHERENT data in order to get information on the value of the neutron rms radius R_n, which is determined by the minimization of the χ^2 using the symmetrized Fermi (t=2.3 fm) and Helm form factors (s=0.9 fm).

✓ Only energy information used
x No energy resolution
x No time information
x Small dataset and big syst. uncer.

Improvements with the latest CsI dataset

+ New quenching factor

$$E_{ee} = f(E_{nr}) = aE_{nr} + bE_{nr}^2 + cE_{nr}^3 + dE_{nr}^4.$$

a=0.05546, b=4.307, c= -111.7, d=840.4

Akimov et al. (COHERENT Coll), arXiv:2111.02477, JINST 17 P10034 (2022)

+ 2D fit, arrival time information included

$$N_{ij}^{\mathrm{CE}\nu\mathrm{NS}} = (N_i^{\mathrm{CE}\nu\mathrm{NS}})_{\nu_\mu} P_j^{(\nu_\mu)} + (N_i^{\mathrm{CE}\nu\mathrm{NS}})_{\nu_e,\bar{\nu}_\mu} P_j^{(\nu_e,\bar{\nu}_\mu)}$$

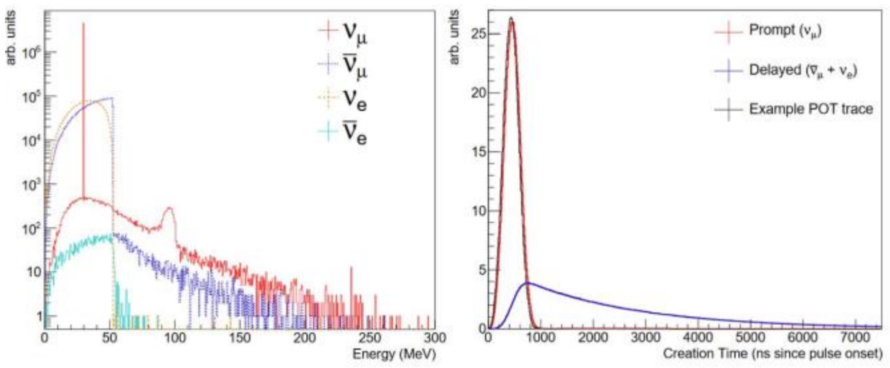

+ Doubled the statistics and reduced syst. uncertainties

$$\sigma_{\mathrm{CE}\nu\mathrm{NS}} = 13\%, \sigma_{\mathrm{BRN}} = 0.9\%,$$
$$\text{and } \sigma_{\mathrm{SS}} = 3\%$$

➢ Theoretical number of CEvNS events

$$\boxed{N_i^{\mathrm{CE}\nu\mathrm{NS}} = N(\mathrm{CsI}) \int_{T_{\mathrm{nr}}^i}^{T_{\mathrm{nr}}^{i+1}} dT_{\mathrm{nr}}\, A(T_{\mathrm{nr}}) \int_0^{T'^{\max}_{\mathrm{nr}}} dT'_{\mathrm{nr}}\, R(T_{\mathrm{nr}}, T'_{\mathrm{nr}}) \int_{E_{\min}(T'_{\mathrm{nr}})}^{E_{\max}} dE \times \sum_{\nu=\nu_e,\nu_\mu,\bar{\nu}_\mu} \frac{dN_\nu}{dE}(E) \frac{d\sigma_{\nu\text{-CsI}}}{dT'_{\mathrm{nr}}}(E, T'_{\mathrm{nr}}),}$$

➢ With the inclusion of energy resolution

$$\boxed{R(N_{\mathrm{PE}}, N'_{\mathrm{PE}}) = \frac{[a_R(1+b_R)]^{1+b_R}}{\Gamma(1+b_R)} N_{\mathrm{PE}}^{b_R}\, e^{-a_R(1+b_R)N_{\mathrm{PE}}}}$$

✓ Analysis with a Gaussian least-square function

$$\boxed{\chi^2_{\mathrm{C}} = \sum_{i=2}^{9} \sum_{j=1}^{11} \left(\frac{N_{ij}^{\exp} - \sum_{z=1}^{3}(1+\eta_z) N_{ij}^z}{\sigma_{ij}} \right)^2 + \sum_{z=1}^{3} \left(\frac{\eta_z}{\sigma_z} \right)^2,}$$

Cadeddu et al., PRC 104, 065502 (2021), arXiv:2102.06153

Analysis updated in this talk using a Poissonian least-square function after the COHERENT data release!

arXiv:2303.09360

Atomic Parity Violation in cesium APV(Cs)

M. Cadeddu and F. Dordei, PRD 99, 033010 (2019), arXiv:1808.10202

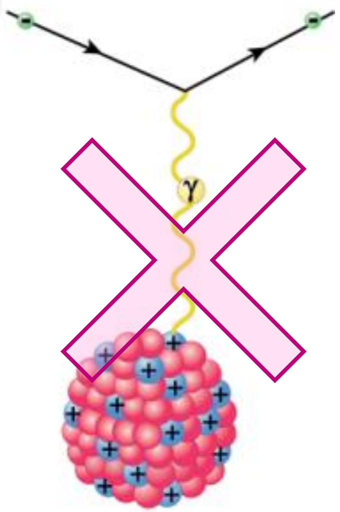

Interaction mediated by the photon and so mostly sensitive to the charge (proton) distribution

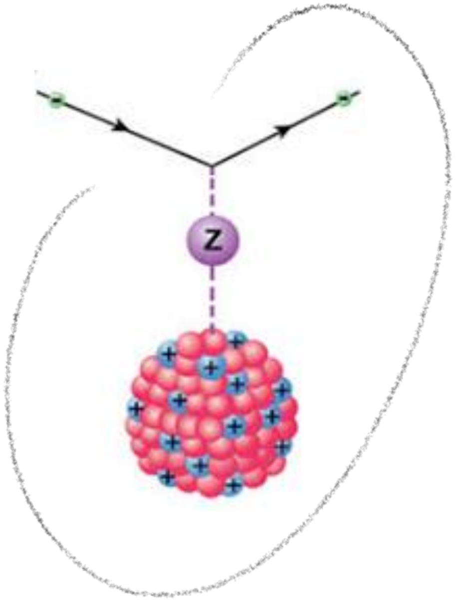

Interaction mediated by the Z boson and so mostly sensitive to the weak (neutron) distribution.

+ Parity violation in an atomic system can be observed as an **electric dipole transition amplitude between two atomic states with the same parity**, such as the $6S$ and $7S$ states in cesium.

  ➢ Indeed, a transition between two atomic states with same parity is forbidden by the parity selection rule and cannot happen with the exchange of a photon.

  ✓ However, an electric dipole transition amplitude can be induced by a Z boson exchange between atomic electrons and nucleons → Atomic Parity Violation (APV) or Parity Non Conserving (PNC).

+ The quantity that is measured is the usual **weak charge**

$$Q_W^{SM} \approx Z\left(1 - 4\sin^2\theta_W^{SM}\right) - N$$

Extracting the weak charge from APV

$$Q_W = N\left(\frac{\mathrm{Im}\,E_{\mathrm{PNC}}}{\beta}\right)_{\mathrm{exp.}}\left(\frac{Q_W}{N\,\mathrm{Im}\,E_{\mathrm{PNC}}}\right)_{\mathrm{th.}}\beta_{\mathrm{exp.+th.}}$$

+ Experimental value of electric dipole transition amplitude between 6S and 7S states in Cs

C. S. Wood et al., Science **275**, 1759 (1997)

J. Guena, et al., PRA **71**, 042108 (2005)

PDG2020 average

$$\mathrm{Im}\left(\frac{E_{\mathrm{PNC}}}{\beta}\right) = -1.5924(55)\ \mathrm{mV/cm}$$

✓ Theoretical amplitude of the electric dipole transition

$$E_{\mathrm{PNC}} = \sum_n \left[\frac{\langle 6s|H_{\mathrm{PNC}}|np_{1/2}\rangle\langle np_{1/2}|\mathbf{d}|7s\rangle}{E_{6s}-E_{np_{1/2}}} + \frac{\langle 6s|\mathbf{d}|np_{1/2}\rangle\langle np_{1/2}|H_{\mathrm{PNC}}|7s\rangle}{E_{7s}-E_{np_{1/2}}}\right],$$

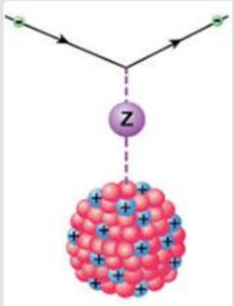

➢ where ***d*** is the electric dipole operator, and

$$H_{\mathrm{PNC}} = -\frac{G_F}{2\sqrt{2}}Q_W\gamma_5\rho(\mathbf{r})$$

Value of ImE_{PNC} used by PDG (V. Dzuba *et al.*, PRL 109, 203003 (2012))

$$\mathrm{Im}\,E_{\mathrm{PNC}} = (0.8977 \pm 0.0040)\times 10^{-11}|e|\,a_B\,Q_W/N$$

see also

nuclear Hamiltonian describing the **electron-nucleus weak interaction**

$\rho(\mathbf{r}) = \rho_p(\mathbf{r}) = \rho_n(\mathbf{r}) \rightarrow$ **neutron skin correction** needed

β: tensor transition polarizability

It characterizes the size of the Stark mixing induced electric dipole amplitude (external electric field)

Bennet & Wieman, PRL 82, 2484 (1999)
Dzuba & Flambaum, PRA 62 052101 (2000)

PDG2020 average

β = 27.064 (33) a_B^3

NEW result on ImE_{PNC} !

➢ I will refer with APV2021 when usign Im E_{PNC} from B. K. Sahoo et al. PRD 103, L111303 (2021)

Weak mixing angle from APV(Cs)

R. L. Workman et al. (Particle Data Group), "Review of Particle Physics," PTEP **2022**, 083C01 (2022).

Historically APV(Cs) has been used to estract the lowest energy determination of the weak mixing angle.

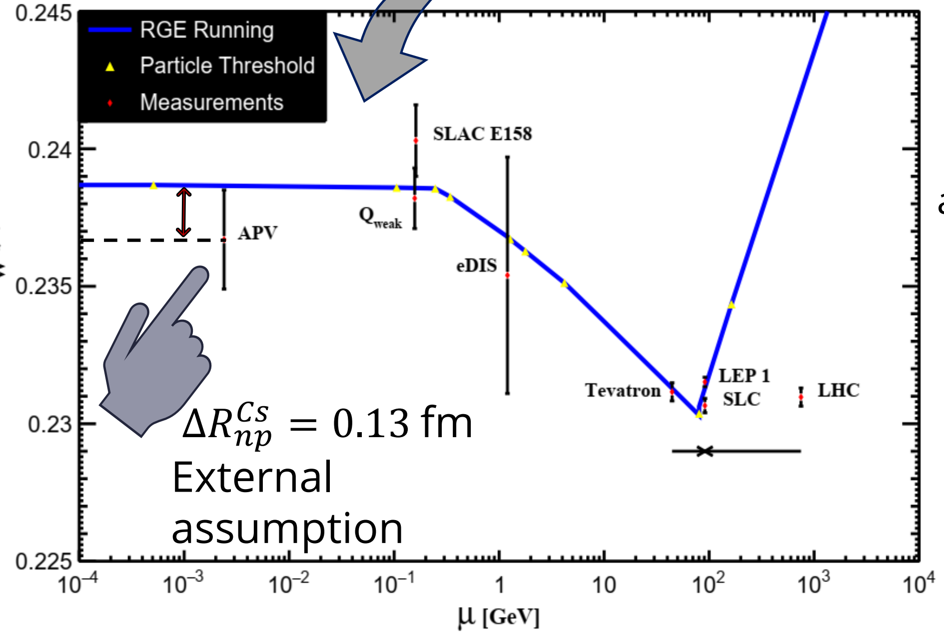

However R_n(Cs) (or the neutron skin) has been taken from **indirect measurements** using antiprotonic atoms, which are known to be affected by considerable model dependencies

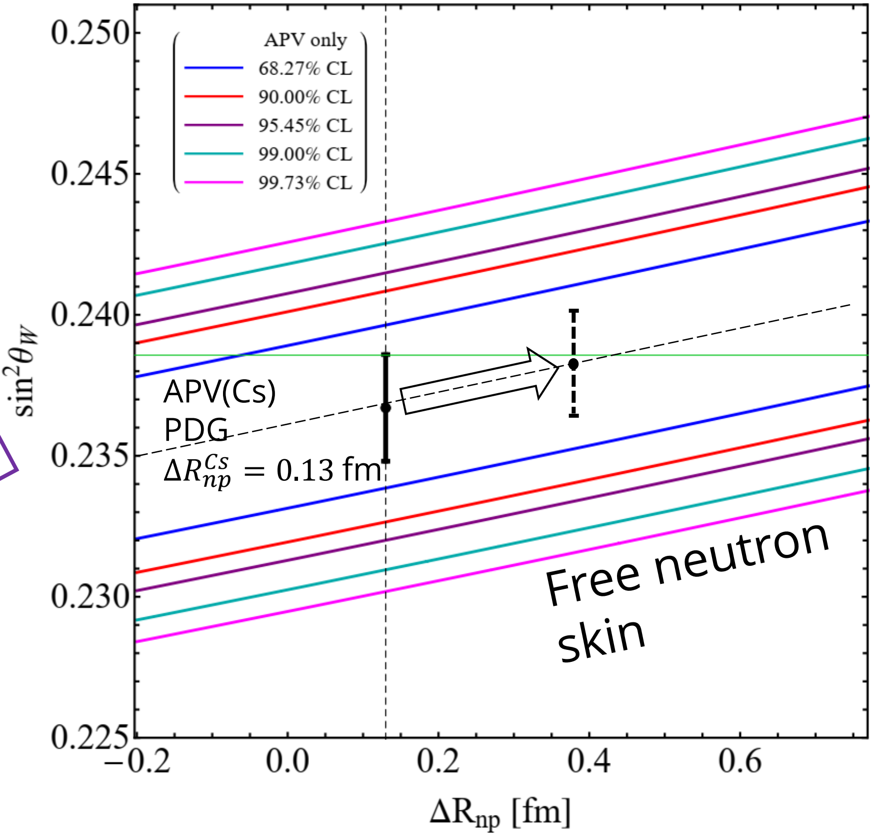

+ In order to measure R_n one has to subtract to the so-called "neutron skin" correction in order to obtain

$$\delta E_{\mathrm{PNC}}^{\mathrm{n.s.}}(R_n) = [(\mathrm{N}/Q_W)\,(1-(q_n(R_n)/q_p))\,E_{\mathrm{PNC}}^{\mathrm{w.n.s.}}]$$

$$q_{p,n} = 4\pi\int_0^\infty \rho_{p,n}(r) f(r) r^2 \mathrm{d}r$$

Where **ρ(r) are the proton and neutron densities** in the nucleus.

✓ The theoretical PNC amplitude of the electric dipole transition is calculated from atomic theory to be

$$\mathrm{Im}\,E_{\mathrm{PNC}} = (0.8977 \pm 0.0040) \times 10^{-11} |e|\, a_B\, Q_W/N$$

Value of ImE_{PNC} used by PDG (V. Dzuba *et al.*, PRL 109, 203003 (2012))
I will refer to it with "APV PDG".

But, we also use

NEW result on ImE_{PNC} !

- I will refer with APV 2021 when usign Im E_{PNC} from B. K. Sahoo et al. PRD 103, L111303 (2021)

Atomic Parity Violation for weak mixing angle measurements

✓ Weak charge in the SM including radiative corrections

Using SM prediction at low energy
$\sin^2\hat{\theta}_W(0) = 0.23857(5)$

$$Q_W^{SM+\text{r.c.}} \equiv -2\left[Z\left(g_{AV}^{ep} + 0.00005\right) + N\left(g_{AV}^{en} + 0.00006\right)\right]\left(1 - \frac{\alpha}{2\pi}\right) \approx Z\left(1 - \ 4\sin^2\theta_W^{SM}\right) - N$$

Theoretically

$$Q_W^{SM\ \text{th}}\left({}^{133}_{55}Cs\right) = -73.23(1)$$

1σ difference

Experimentally

$$Q_W^{\text{exp.}}\left({}^{133}_{55}Cs\right) = -72.82(42)$$

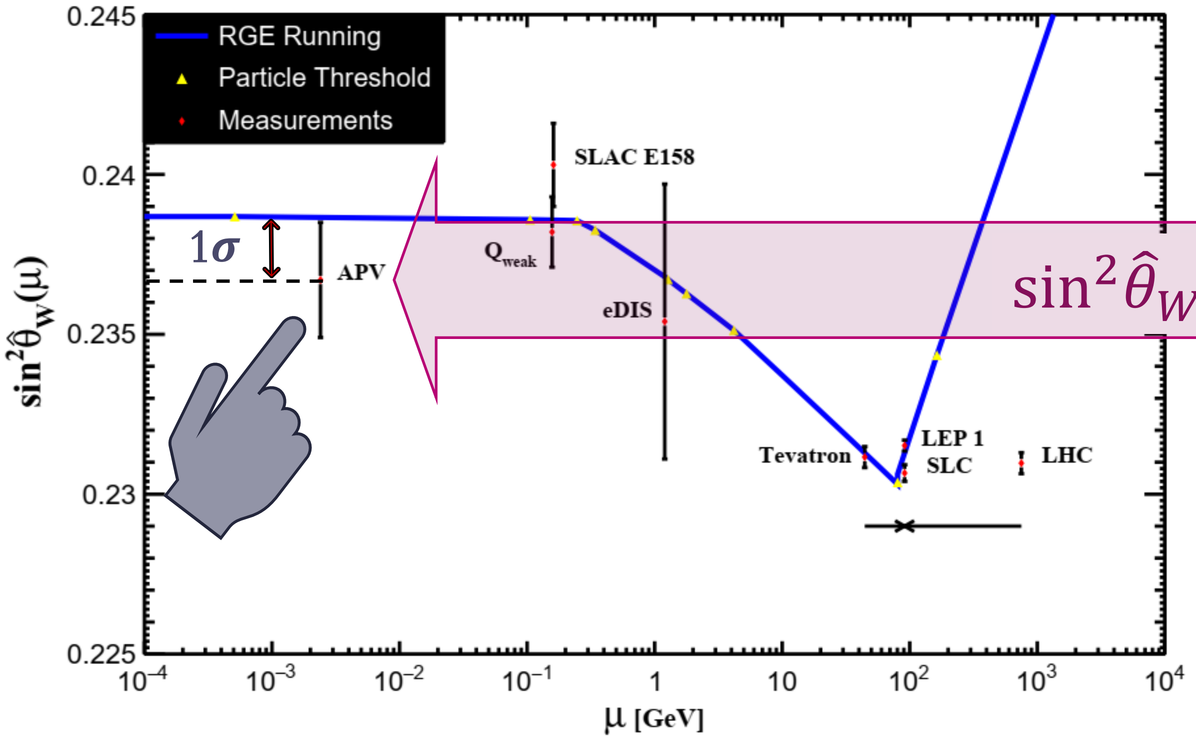

$\sin^2\hat{\theta}_W(2.4\ \text{MeV})=0.2367\pm0.0018$

But which Cs neutron skin correction is used?

R. L. Workman et al. (Particle Data Group), "Review of Particle Physics," PTEP **2022**, 083C01 (2022).

The dilemma

APV (Cs)

- Sensitive to the weak mixing angle
- Similarly sensitive to the neutron skin

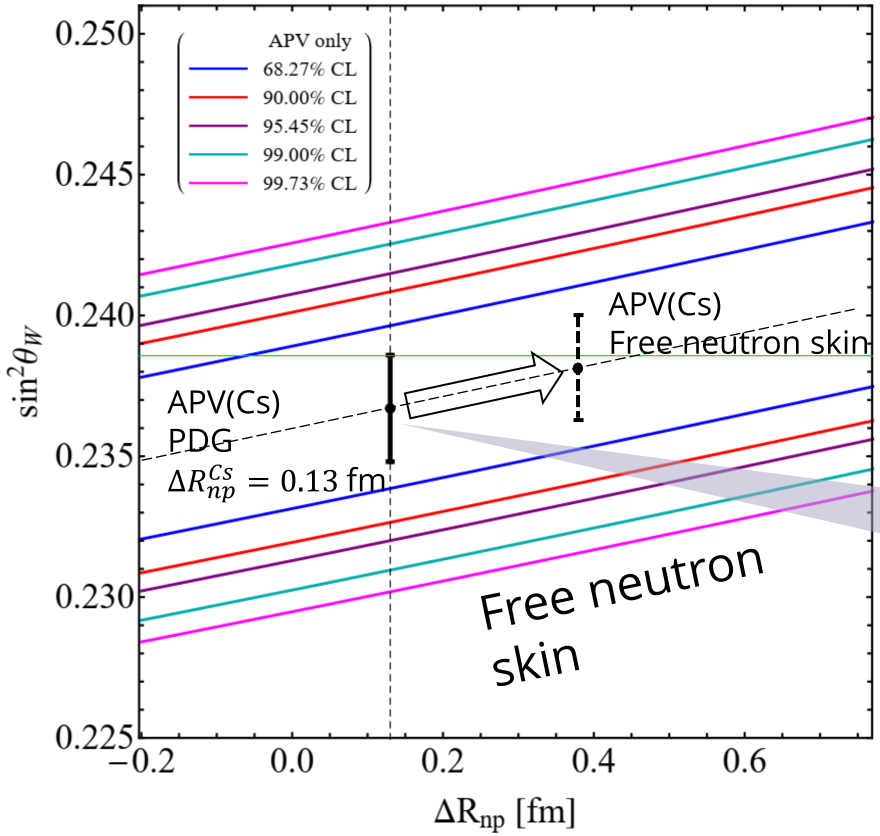

APV(Cs) PDG corresponds to $\Delta R_{np}^{Cs}(\mathrm{Extr.}) = 0.13$ fm

Extrapolated from antiprotonic atoms…

COHERENT (CsI)

- CEνNS is sensitive to the neutron skin
- But less sensitive to the weak mixing angle

$$\sin^2\vartheta_W(\mathrm{COH-CsI}) = 0.231^{+0.027}_{-0.024}(1\sigma)^{+0.046}_{-0.039}(90\%\mathrm{CL})^{+0.058}_{-0.047}(2\sigma)$$

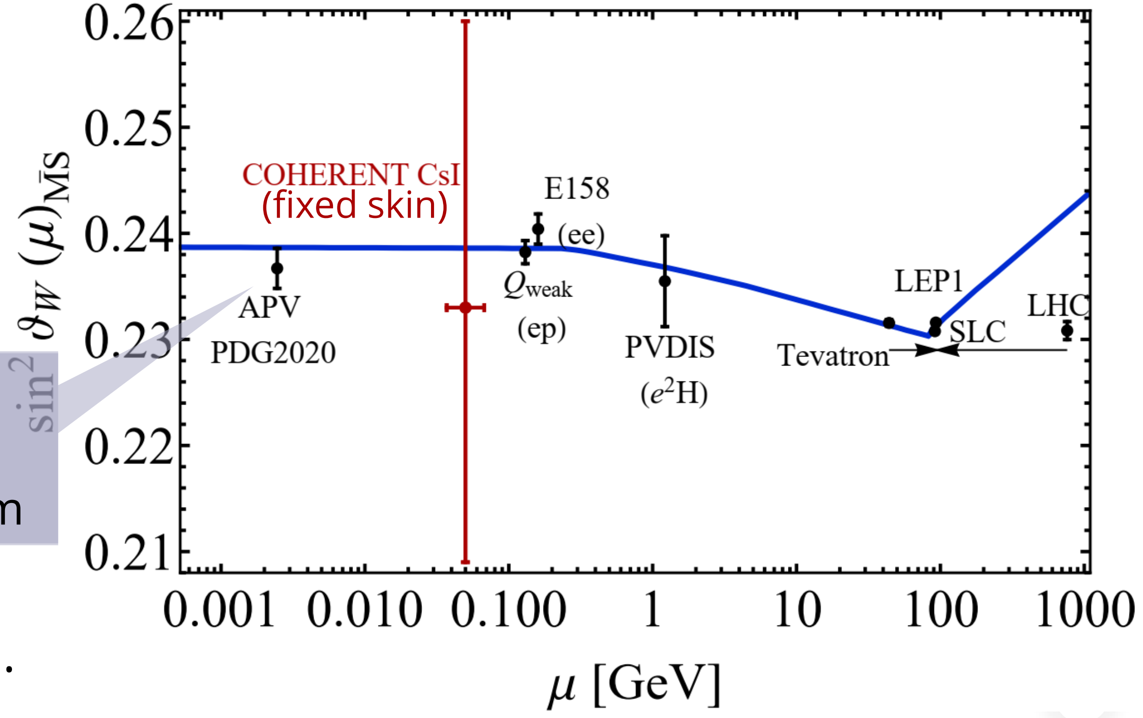

Extrapolated value of ΔR_{np}^{Cs}

+ Neutron-skin of a variety of nuclei as extracted from **antiprotonic data** as a function of the asymmetry parameter, I.

✓ From this **linear fit** one obtains the relation for the neutron skin for every nuclei

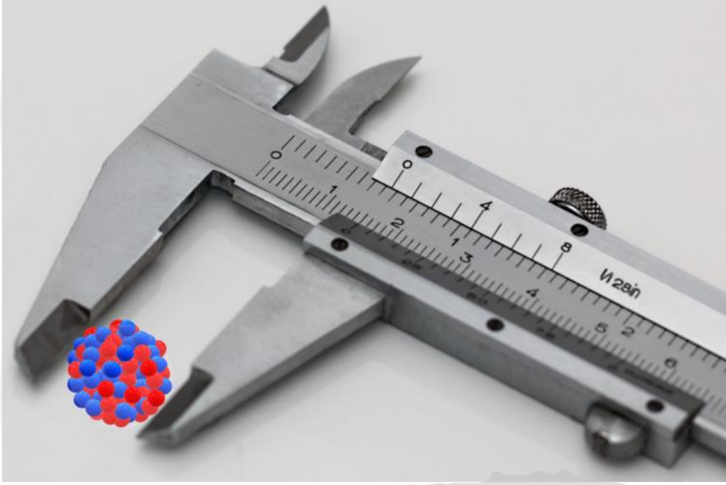

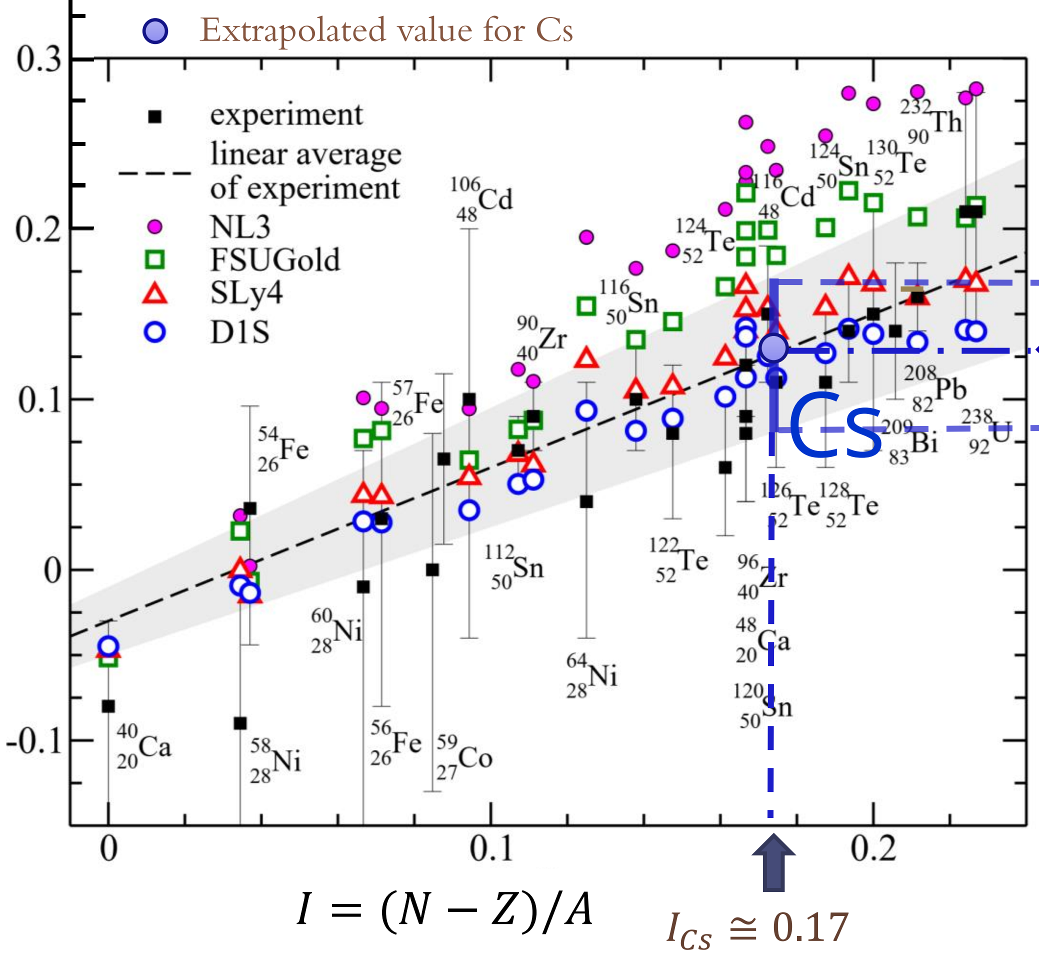

A. Trzcinska et al. s, PRL. 87, 082501 (2001)

$$\Delta R_{np}[\text{fm}] = -(0.04 \pm 0.03) + (1.01 \pm 0.15)\frac{N-Z}{A}$$

For cesium it gives

$$\Delta R_{np}^{Cs}(\text{extrap}) \cong 0.13 \pm 0.04 \text{ fm}$$

Extrapolated (not measured) value for cesium! ⚠

Antiprotonic data: radiochemical and the other based on x-ray data constraining the neutron distribution at the nuclear periphery

M. Thiel et al., Journal of Physics G, 46, 9 (2019), arXiv:1904.12269v1

Extrapolated value of ΔR_{np}^{Cs}

PREX-I & PREX-II

$\Delta R_{np}^{Pb} = 0.283 \pm 0.071$ fm

D. Adhikari *et al.* PRL 126, 172502 (2021)

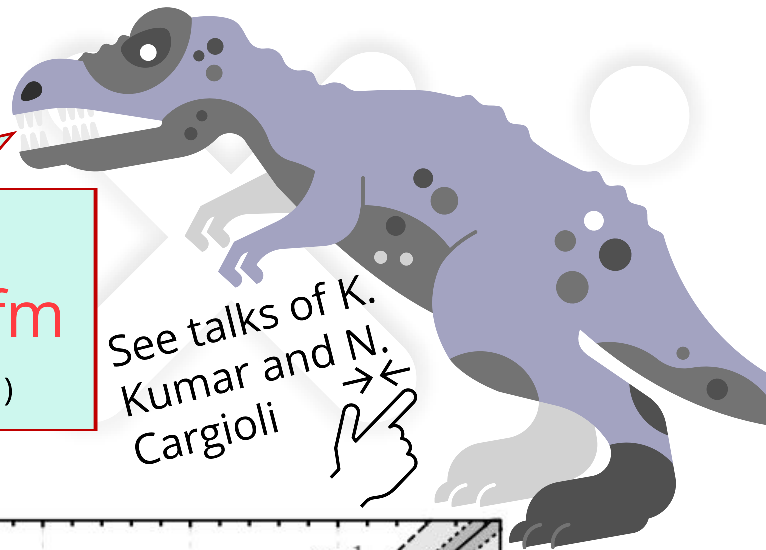

See talks of K. Kumar and N. Cargioli

A. Trzcinska et al. s, PRL. 87, 082501 (2001

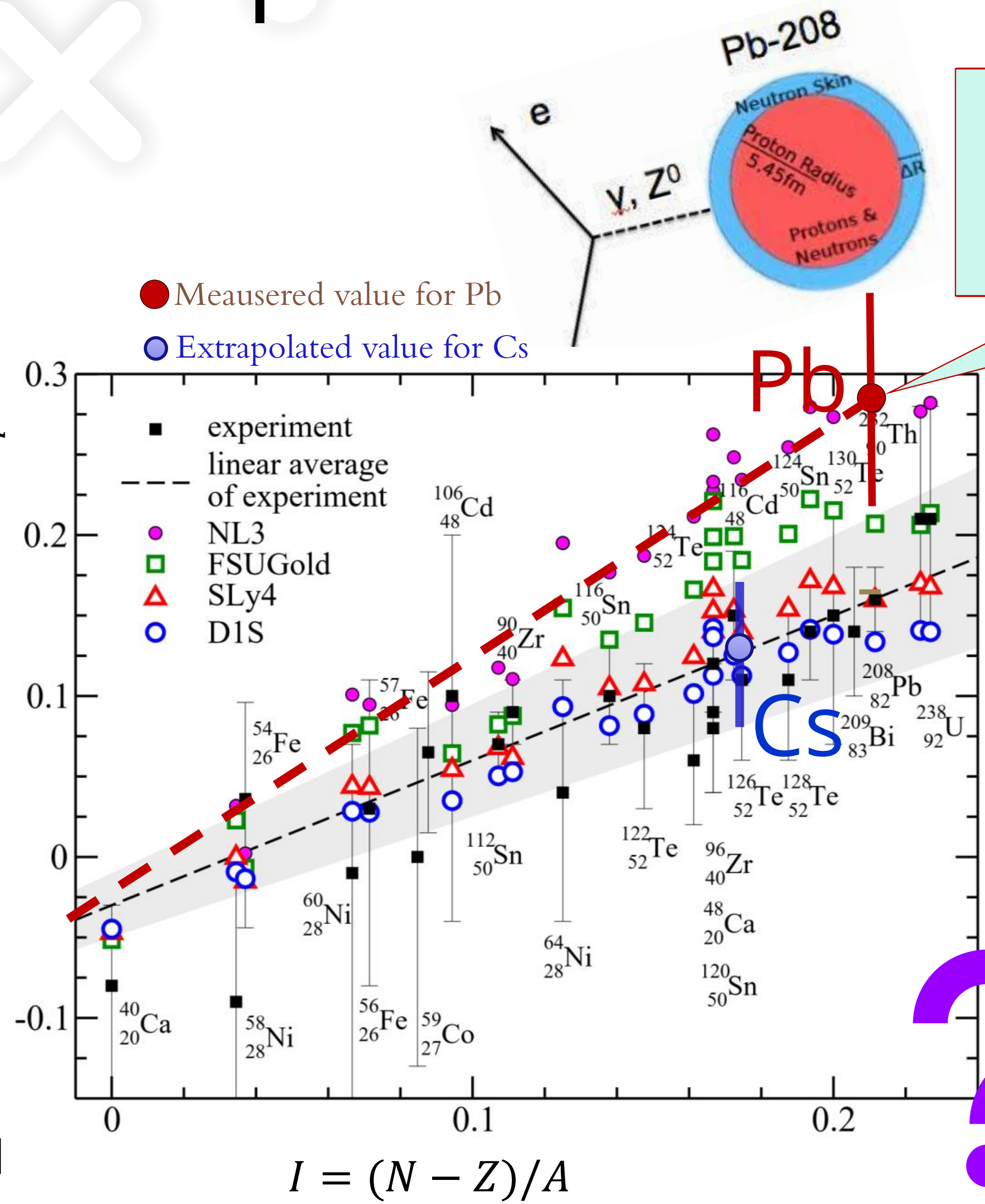

?

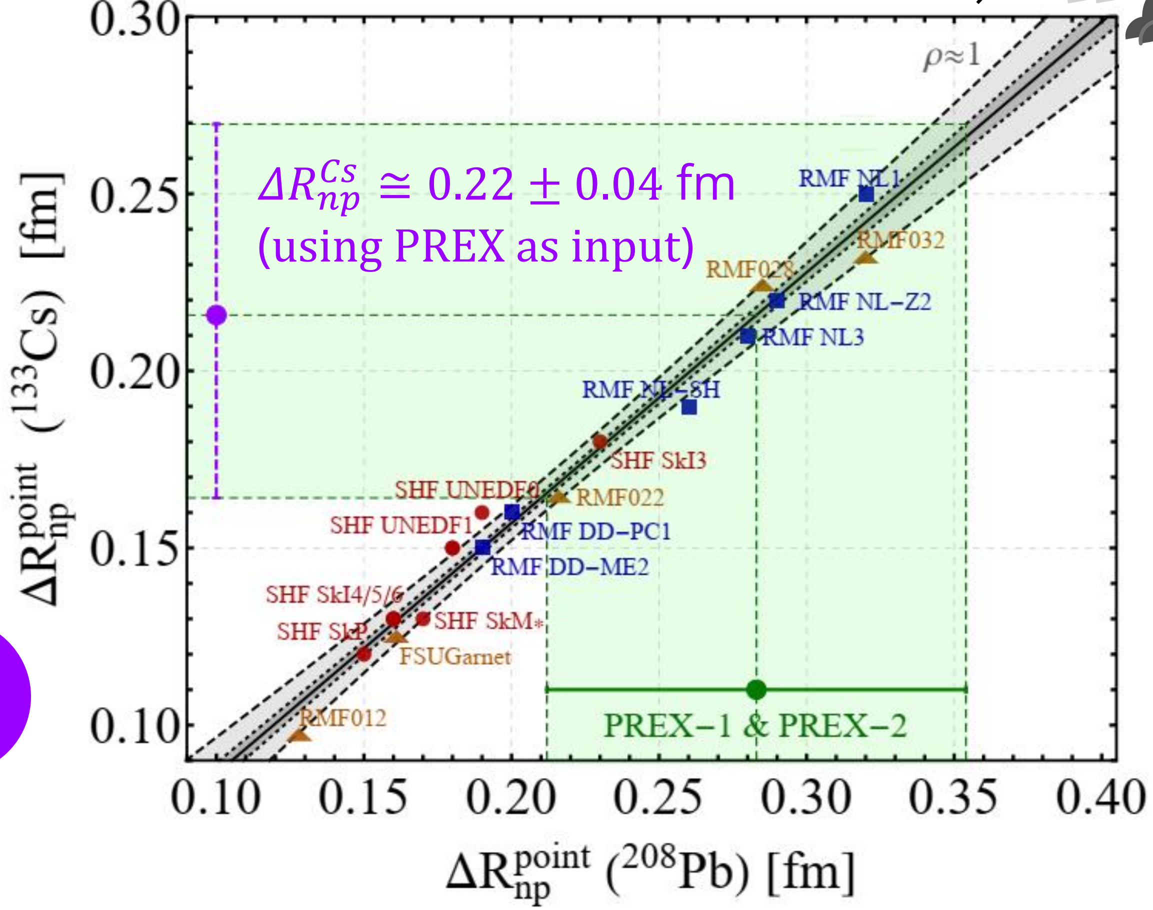

M. Cadeddu et al. PRD 104, L011701 (2021), arXiv:2104.03280

1D fits

R_n fixed to theory*
$\sin^2\vartheta_W$ free to vary

$R_n^{NSM}(\text{CsI}) \approx 5.06$ fm

* Nuclear shell model

$\sin^2\vartheta_W$ fixed to theory
$\sin^2\vartheta_W(0) = 0.23863(5)$
R_n free to vary

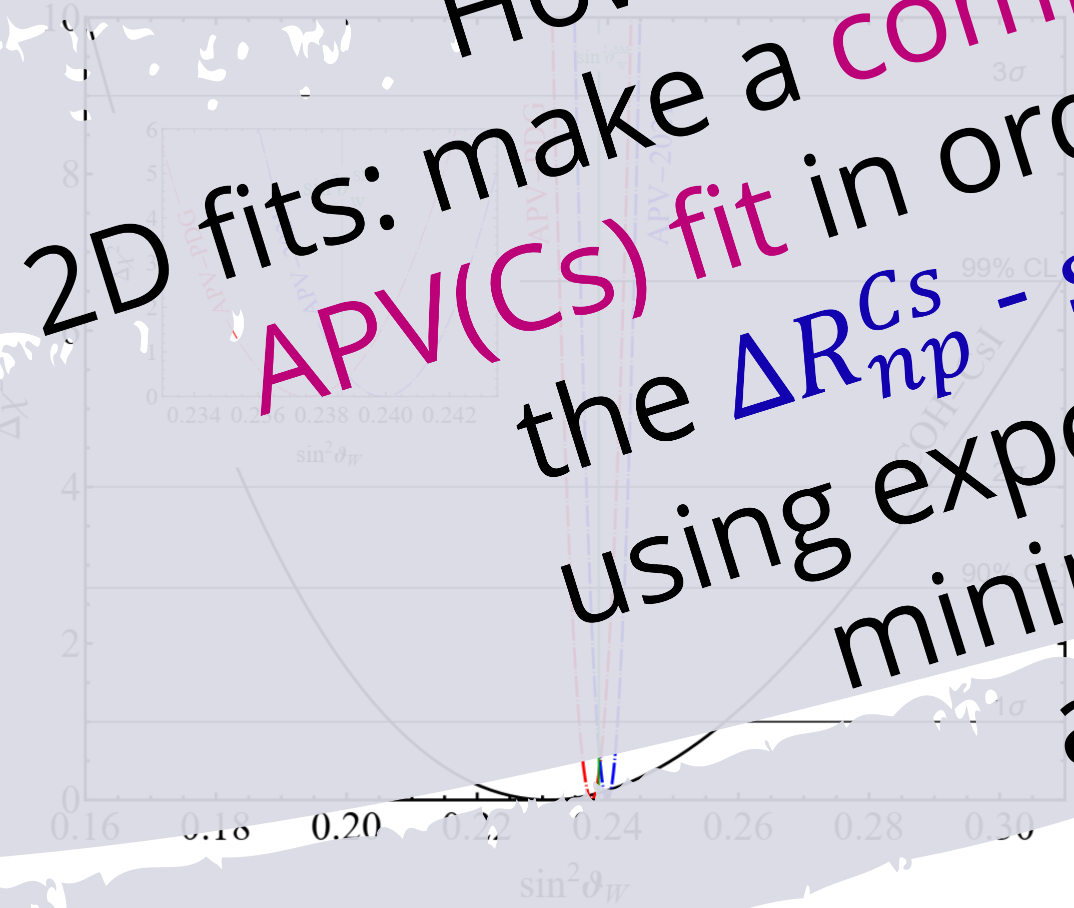

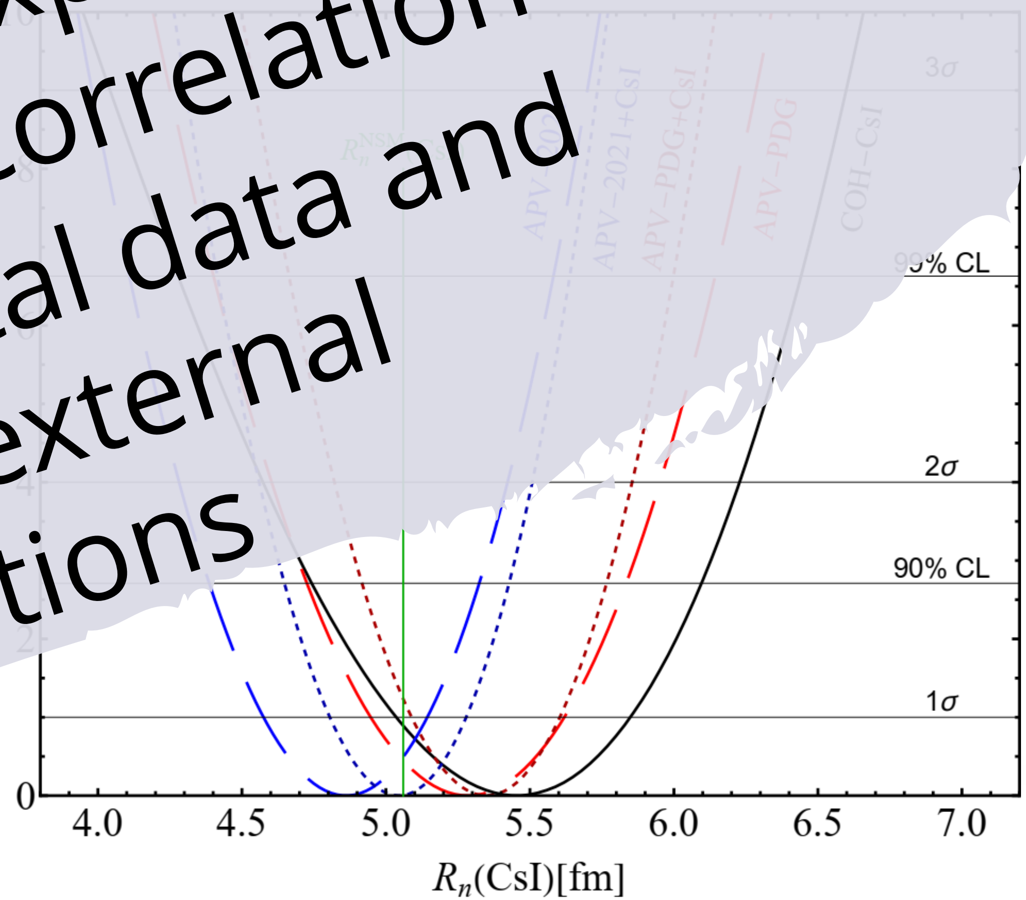

However, we can do more!

2D fits: make a combined COHERENT (CsI) & APV(Cs) fit in order to exploit properly the ΔR_{np}^{Cs} - $\sin^2\vartheta_W$ correlation using experimental data and minimizing external assumptions

1st advantage: $R_n(Cs)$ & $R_n(I)$ separation

Even if theoretical nuclear models predict a similar neutron radius for Cs and I, i.e. $R_n(Cs) = 5.09\ \mathrm{fm} \approx R_n(I) = 5.03\ \mathrm{fm}$, meaning that the use of $R_n(CsI)$ is OK for current precision, it is interesting to try to separate the cesium and iodine contributions.

Assuming to know the value of the weak mixing angle at low energy $\sin^2\hat{\theta}_W(0) = 0.23863(5)$

COHERENT χ^2 APV χ^2

$$\chi^2 = \chi^2_{\mathrm{C}} + \left(\frac{Q_W^{\mathrm{Cs\,ns}}(R_n) - Q_W^{\mathrm{th}}(\sin^2\vartheta_W)}{\sigma_{\mathrm{APV}}(R_n, \sin^2\vartheta_W)} \right)^2$$

$$\Delta R_{np}(^{127}\mathrm{I}) = R_n - R_p = 0.57^{+1.0}_{-0.8}\ \mathrm{fm}$$

$$\Delta R_{np}(^{133}\mathrm{Cs}) = R_n - R_p = 0.2^{+0.31}_{-0.34}\ \mathrm{fm}$$

Contribution of Cs and I disentangled!!

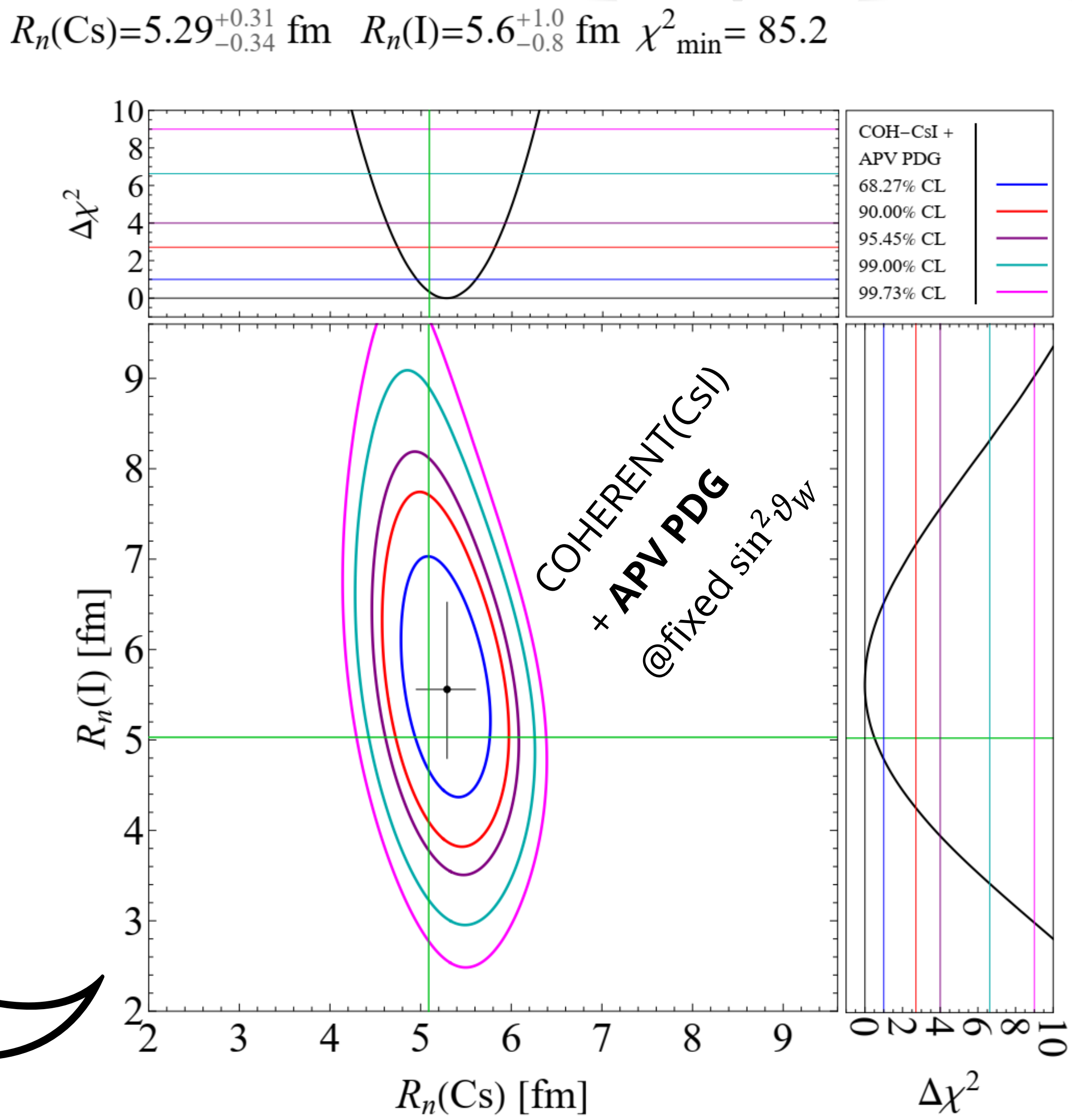

M. Atzori Corona et al., arXiv:2303.09360

1^{st} advantage: $R_n(Cs)$ & $R_n(I)$ separation

Even if theoretical nuclear models predict a similar neutron radius for Cs and I, i.e. $R_n(Cs) = 5.09\ \mathrm{fm} \approx R_n(I) = 5.03\ \mathrm{fm}$, meaning that the use of $R_n(CsI)$ is OK for current precision, it is interesting to try to separate the cesium and iodine contributions.

Using ImE_{PNC} form B. K. Sahoo et al. PRD 103, L111303 (2021) (**APV 2021**)

$$\Delta R_{np}(^{127}\mathrm{I}) = R_n - R_p = 0.97^{+0.9}_{-0.9}\ \mathrm{fm}$$

$$\Delta R_{np}(^{133}\mathrm{Cs}) = R_n - R_p = -0.24^{+0.30}_{-0.25}\ \mathrm{fm}$$

Contribution of Cs and I disentangled!!

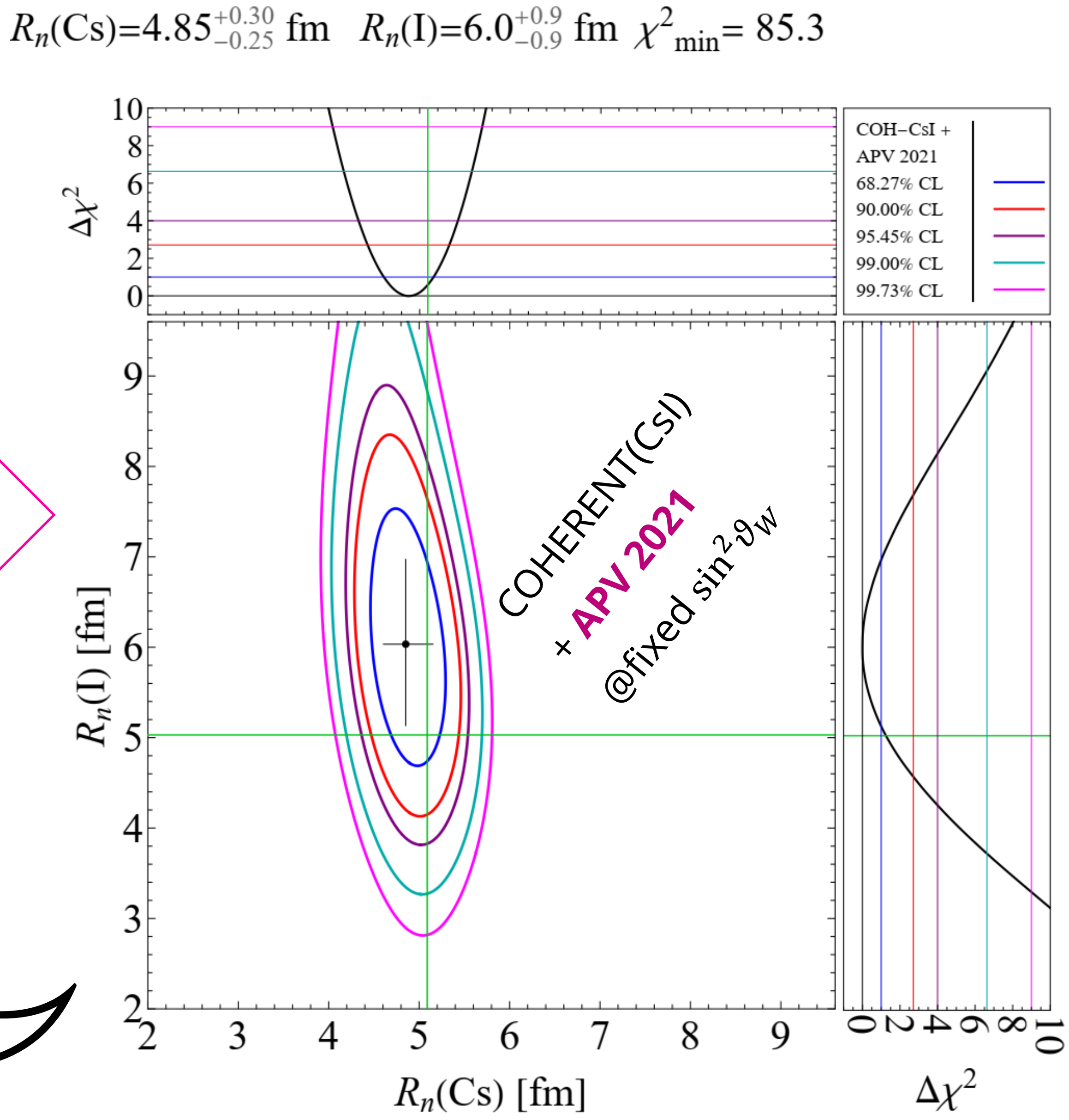

M. Atzori Corona et al., arXiv:2303.09360

2D fit: leaving both the weak mixing angle and the nuclear neutron radius* free to vary

*average CsI neutron radius

2^{nd} advantage: extract both R_n(CsI) and $\sin^2\vartheta_W$ from data

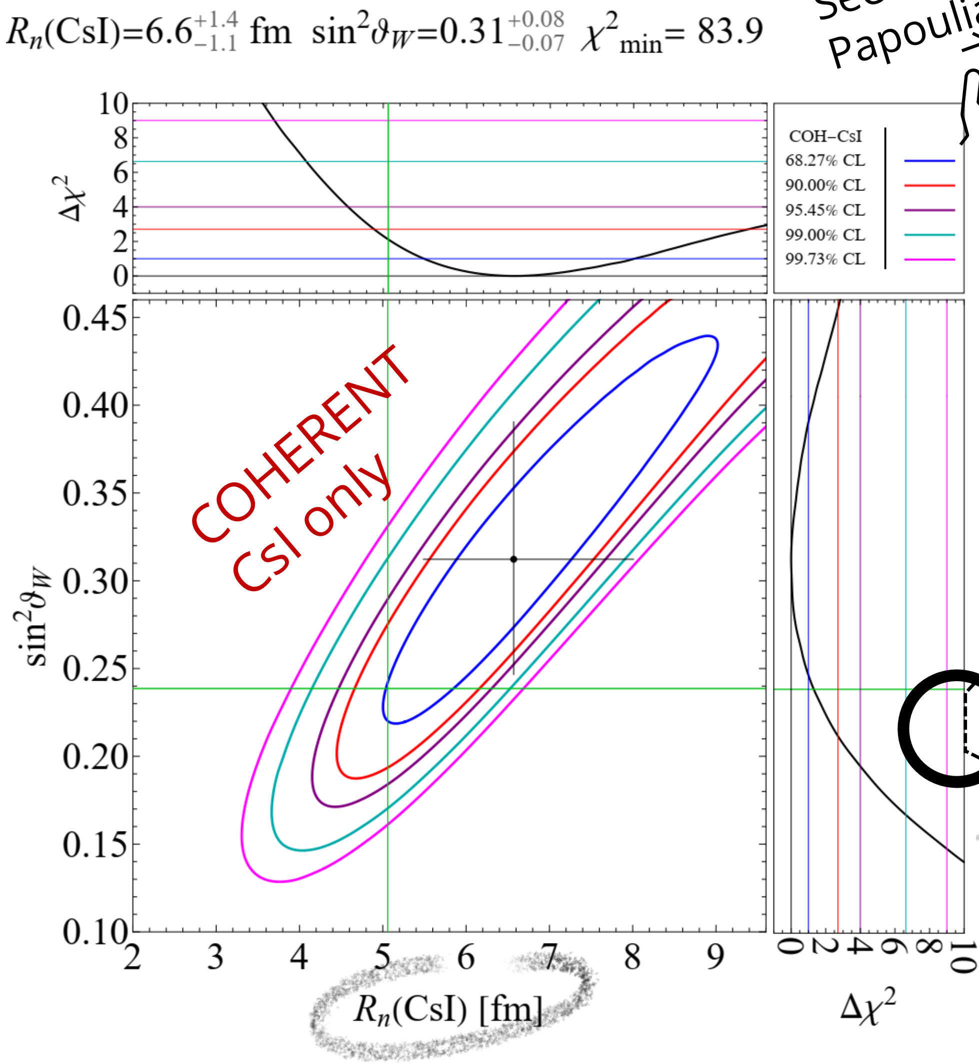

See also D. Papoulias's talk

+APV(Cs) PDG

MIND THE SCALE

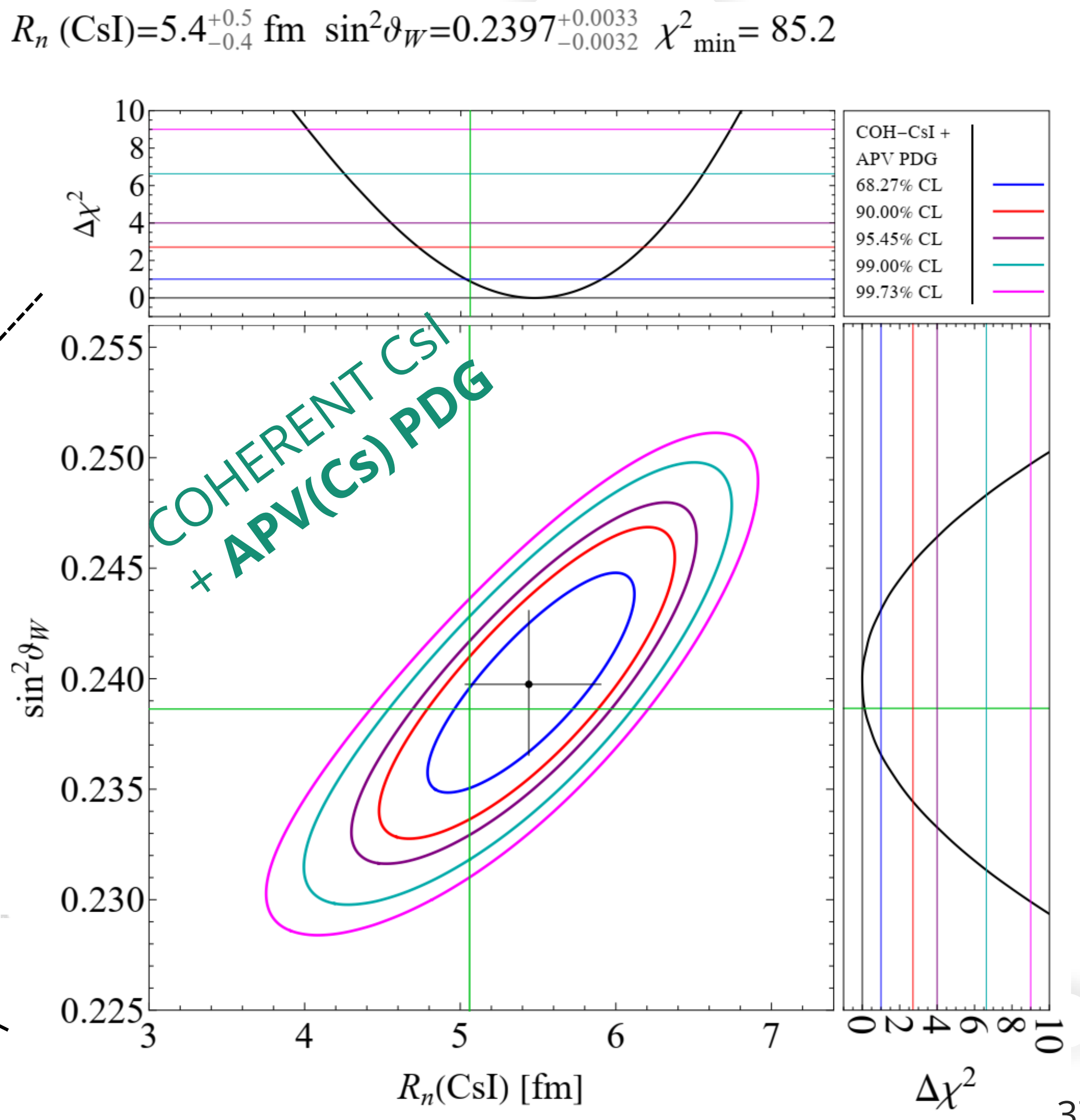

2^{nd} advantage: extract both R_n(CsI) & $\sin^2\vartheta_W$ from data

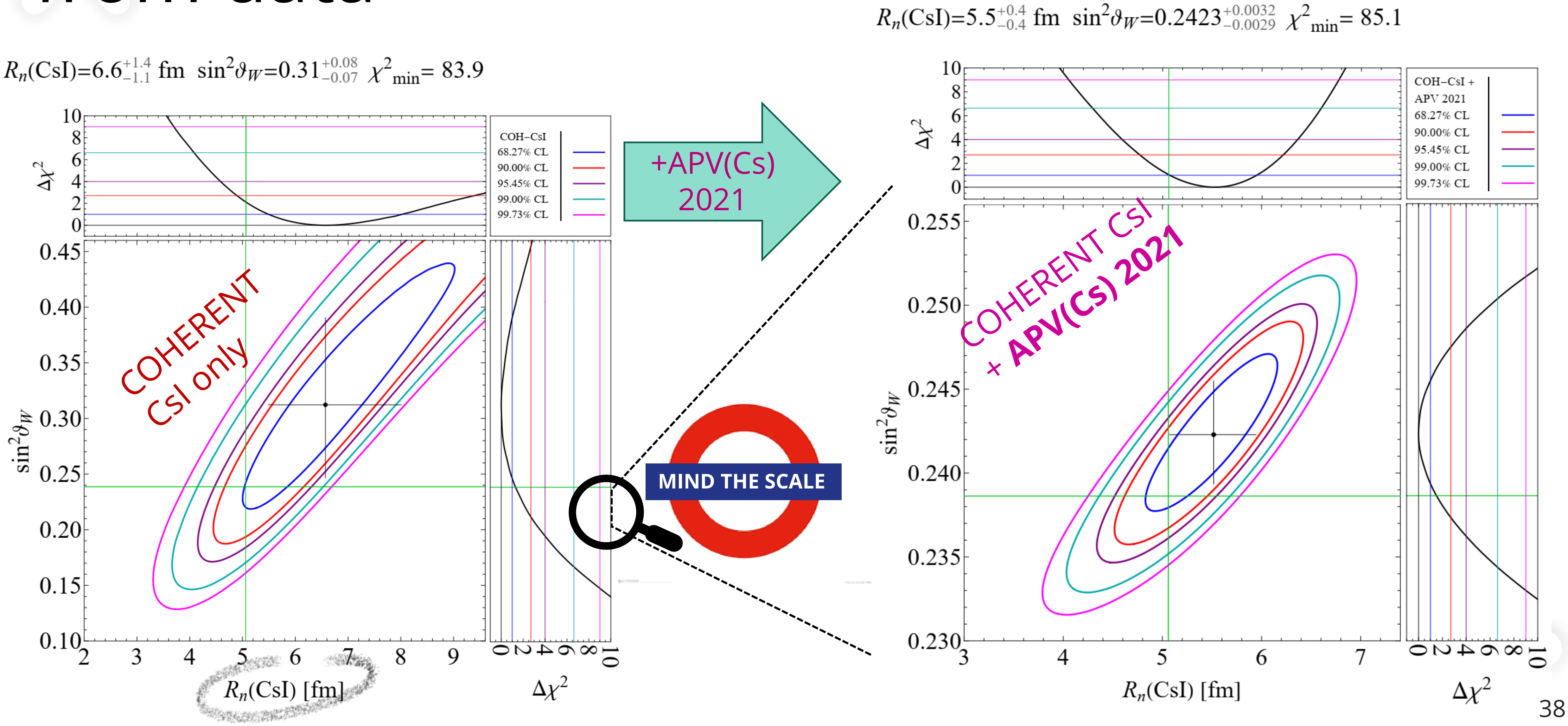

Weak mixing angle determination from APV without any assumption on R_n(Cs)

No assumptions on ΔR_{np}^{Cs} are made. The skin is taken directly from CEνNS experimental data

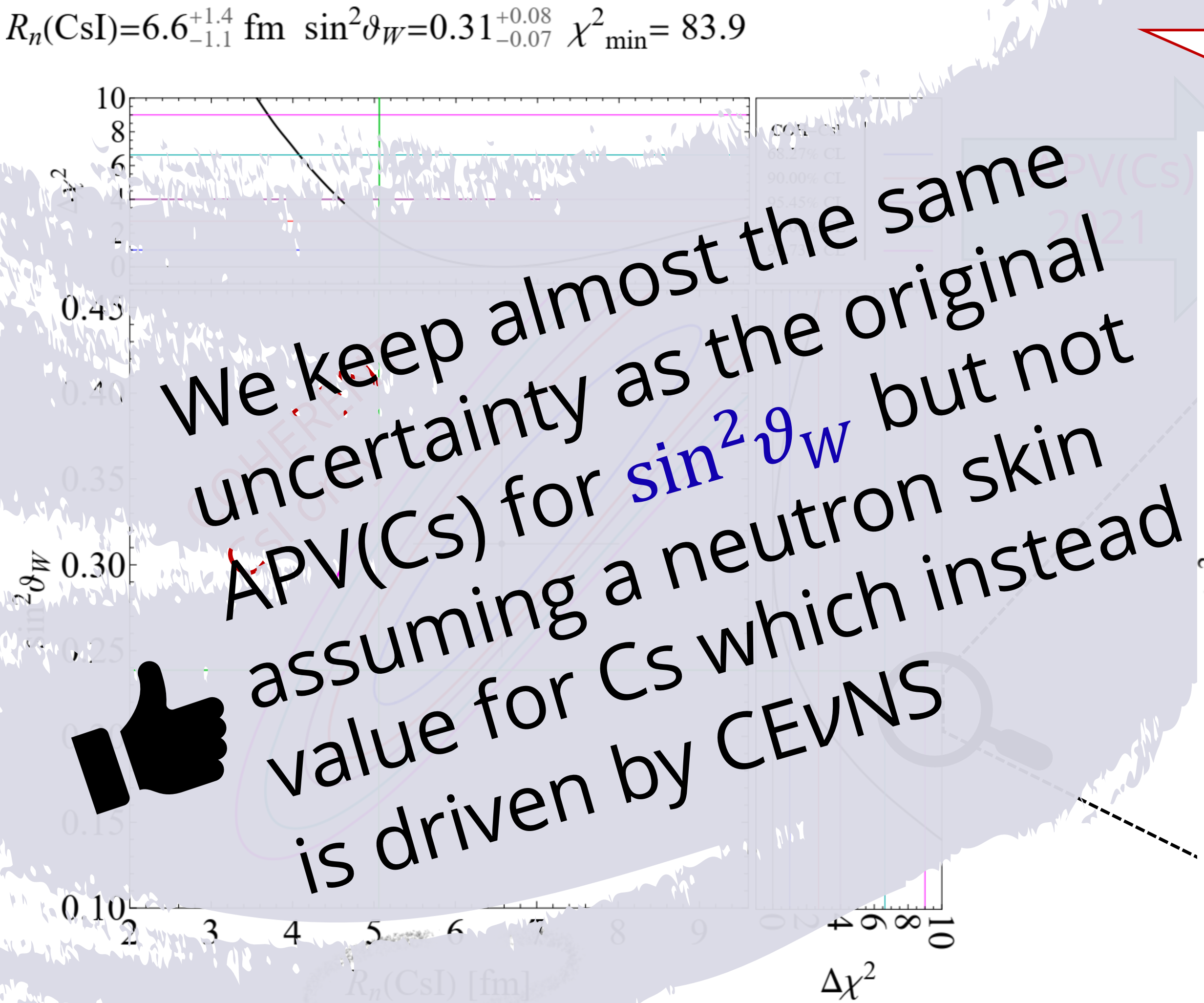

We keep almost the same uncertainty as the original APV(Cs) for $\sin^2\vartheta_W$ but not assuming a neutron skin value for Cs which instead is driven by CEνNS

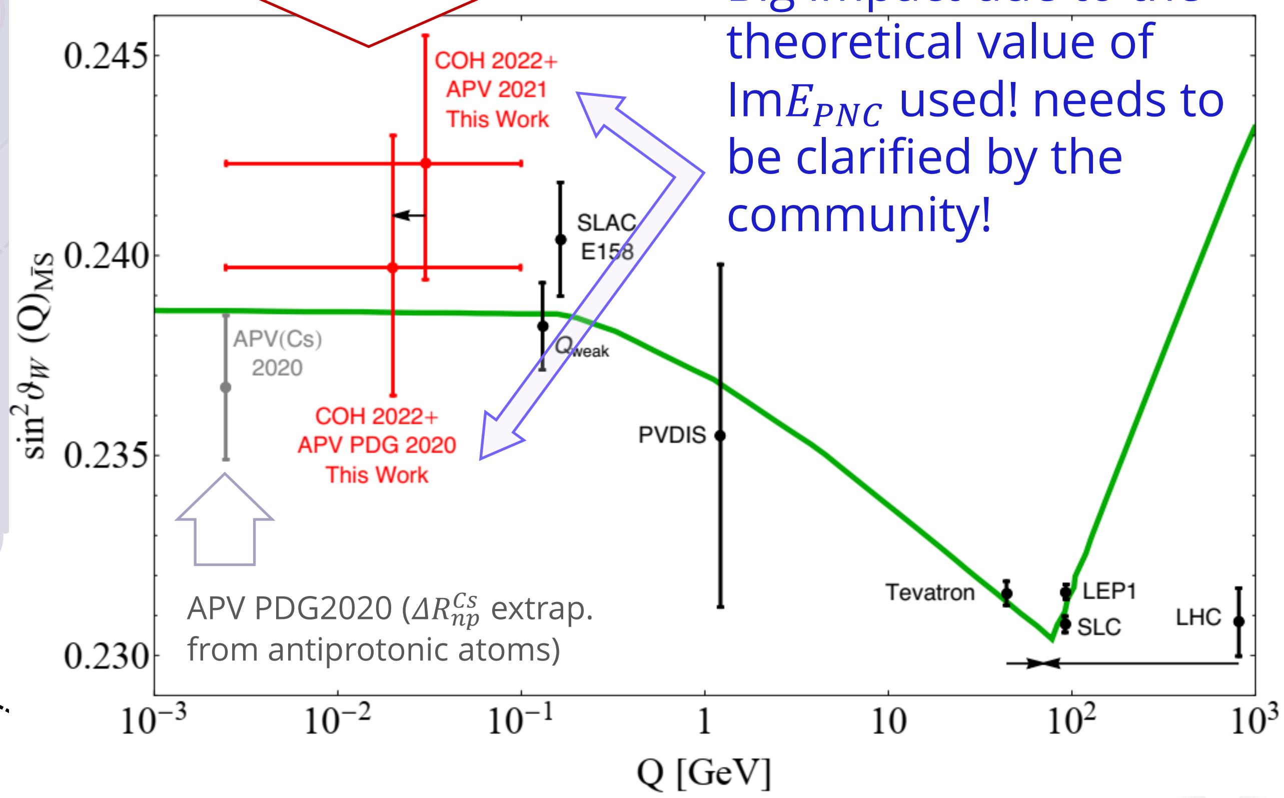

Big impact due to the theoretical value of ImE_{PNC} used! needs to be clarified by the community!

Summary of nuclear neutron radius measurements

- APVPDG: Using ImE_{PNC} from V. Dzuba *et al.*, PRL 109, 203003 (2012)

Despite the different fit configurations used to extract the values of R_n(CsI), R_n(Cs) and R_n(I), a coherent picture emerges with an overall agreement between COHERENT and APV results and the theoretical predictions.

Using APV PDG we obtain on average larger values on the radii, still compatible within uncertainties

- APV2021: using ImE_{PNC} from B. K. Sahoo et al. PRD 103, L111303 (2021)

On the contrary, APV 2021 shifts downwards the measured radii towards the predictions, but in the simultaneous 2D fit with $\sin^2\vartheta_W$ where the correlation with the latter increases the extracted central value of R_n(CsI).

2D fit COHERENT(CsI)+APV(Cs) is stable against ImE_{PNC} choice. Precision of ~7% is reached even if letting $sin^2\vartheta_W$ free to vary!

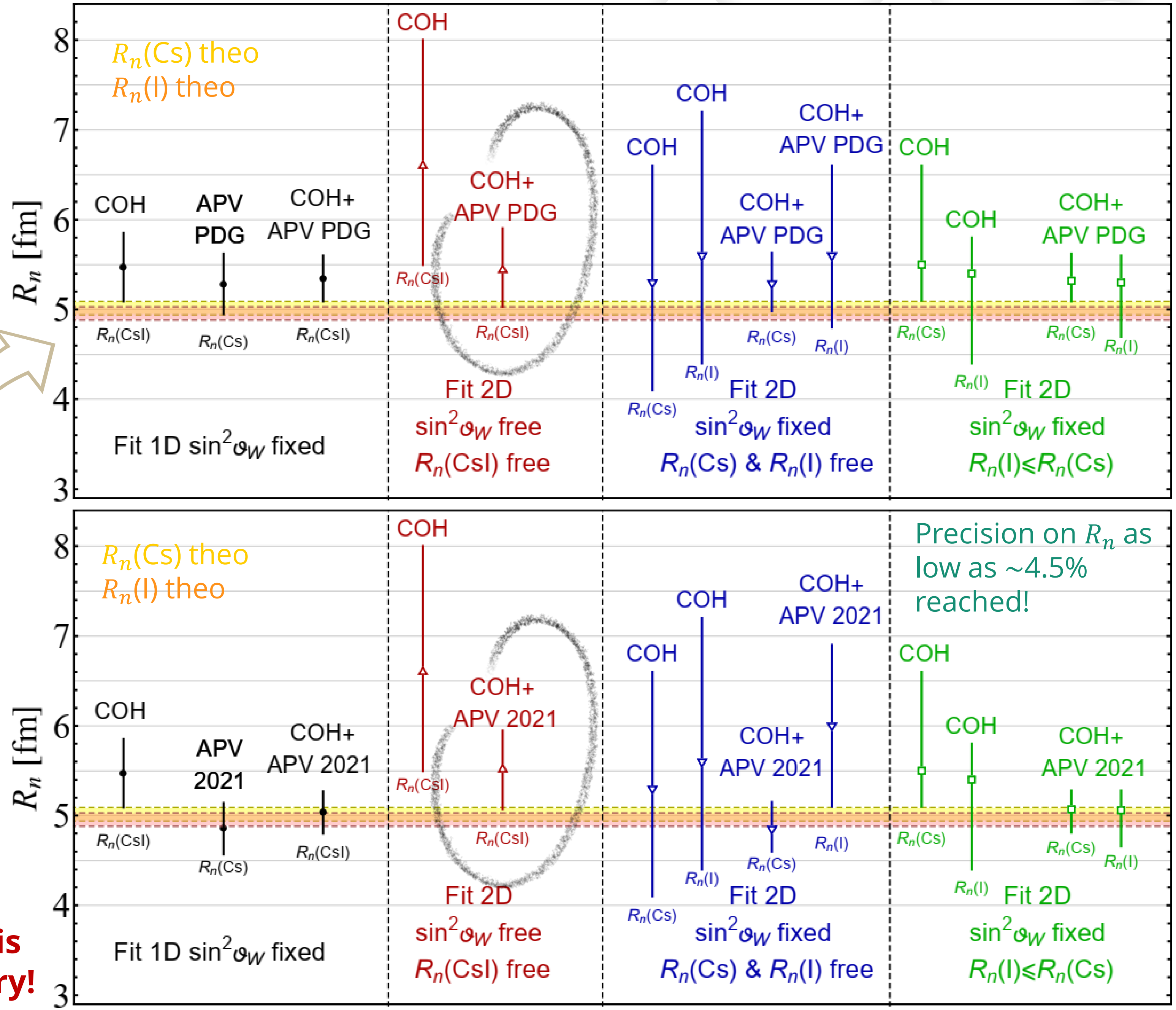

The past, present and future of R_n measurements with CEνNS and PVES

See details in **D. Akimov et al., arXiv:2204.04575 (2022)**

- **COH-CryoCsI-I**: 10 kg, cryogenic temperature ($\sim 40K$), twice the light yield of present CsI crystal at 300K
- **COH-CryoCsI-II**: 700 kg undoped CsI detector. Both lower energy threshold of 1.4 keVnr while keeping the shape of the energy efficiency of the present COHERENT CsI.

COHERENT future argon: "COH-LAr-750"
LAr based detector for precision CEνNS

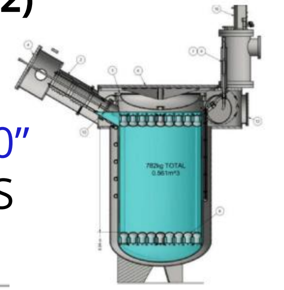

Single phase, scintillation only, 750 kg total (610 kg fiducial)
✓ 3000 CEνNS/year

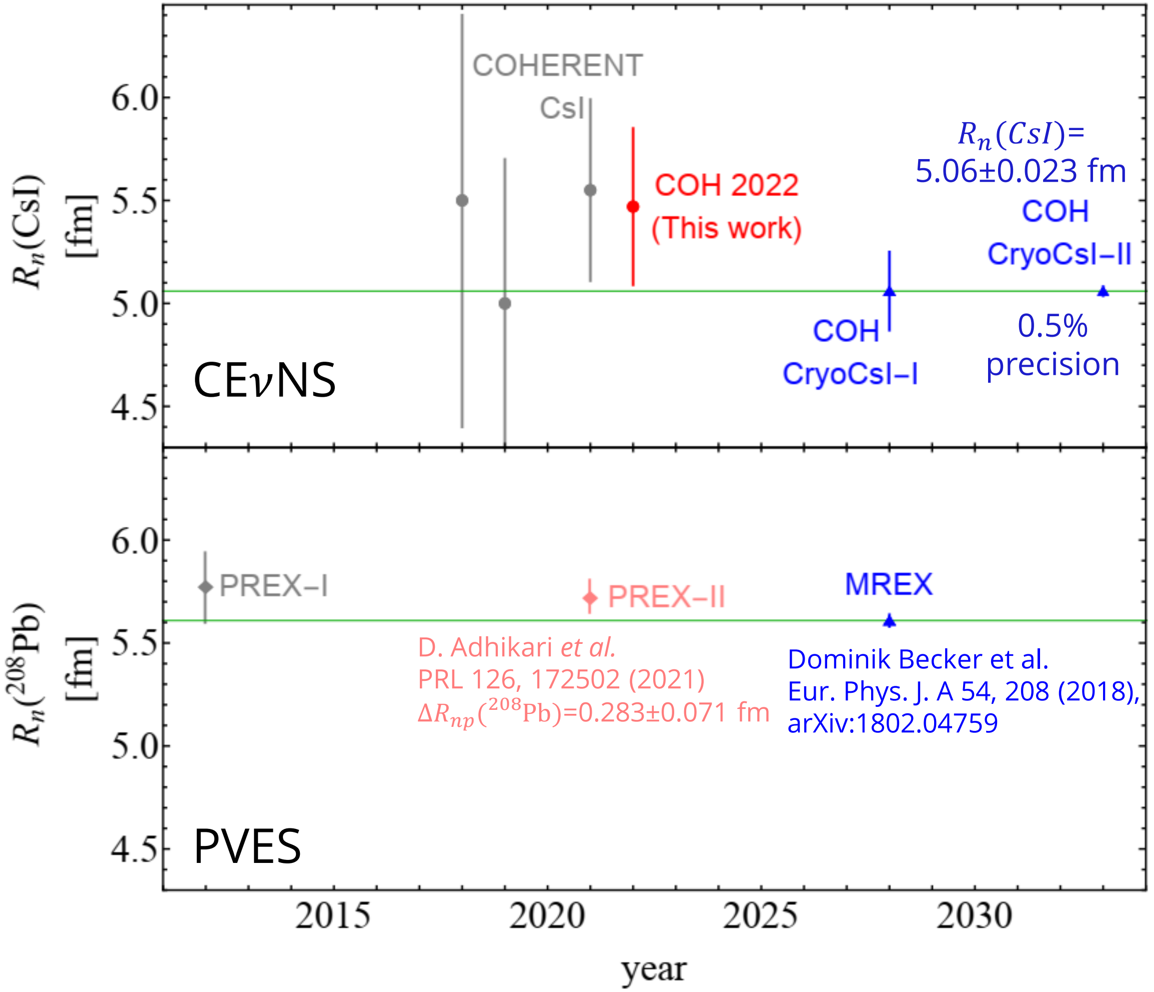

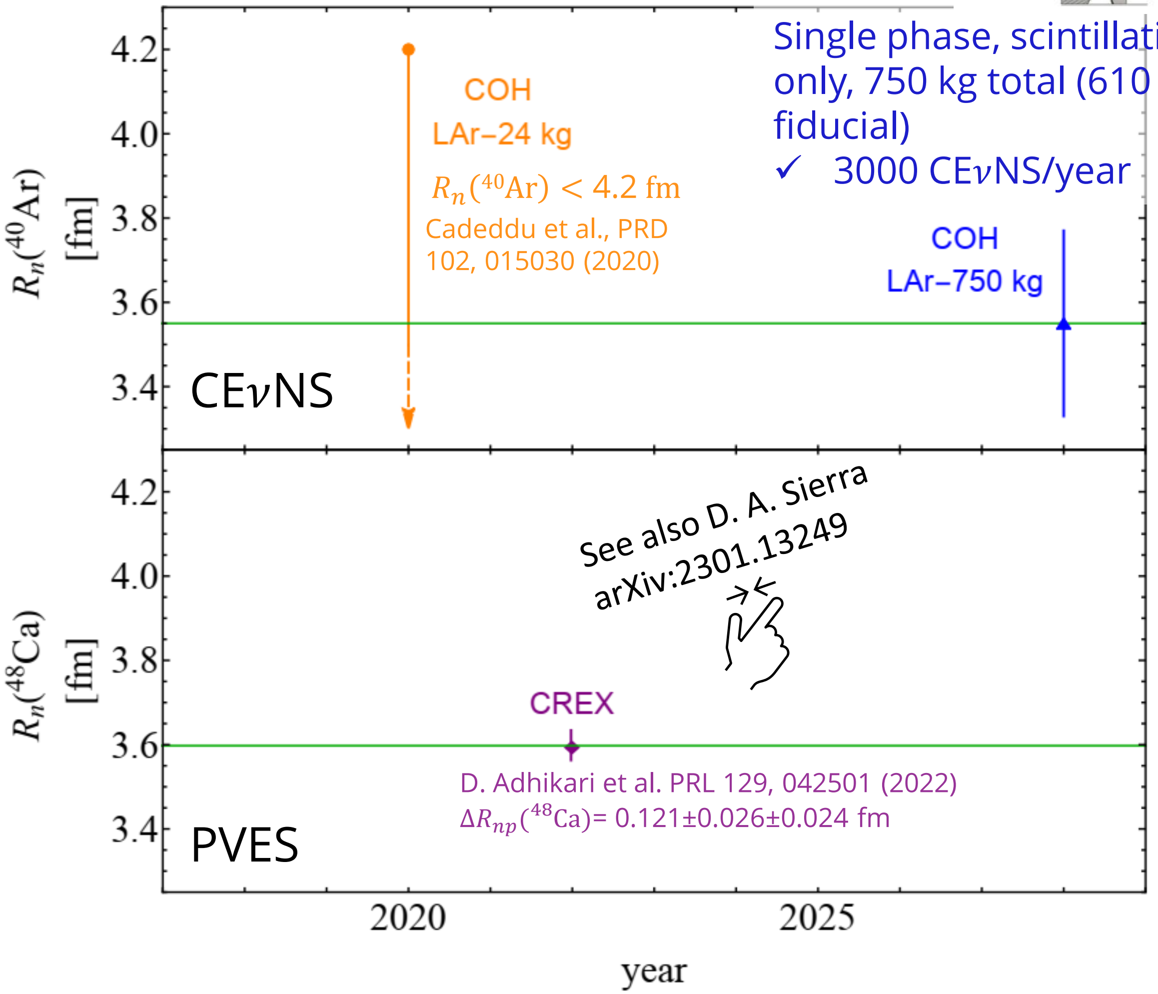

The past, present and future of $\sin^2\vartheta_W$ with CEνNS and APV

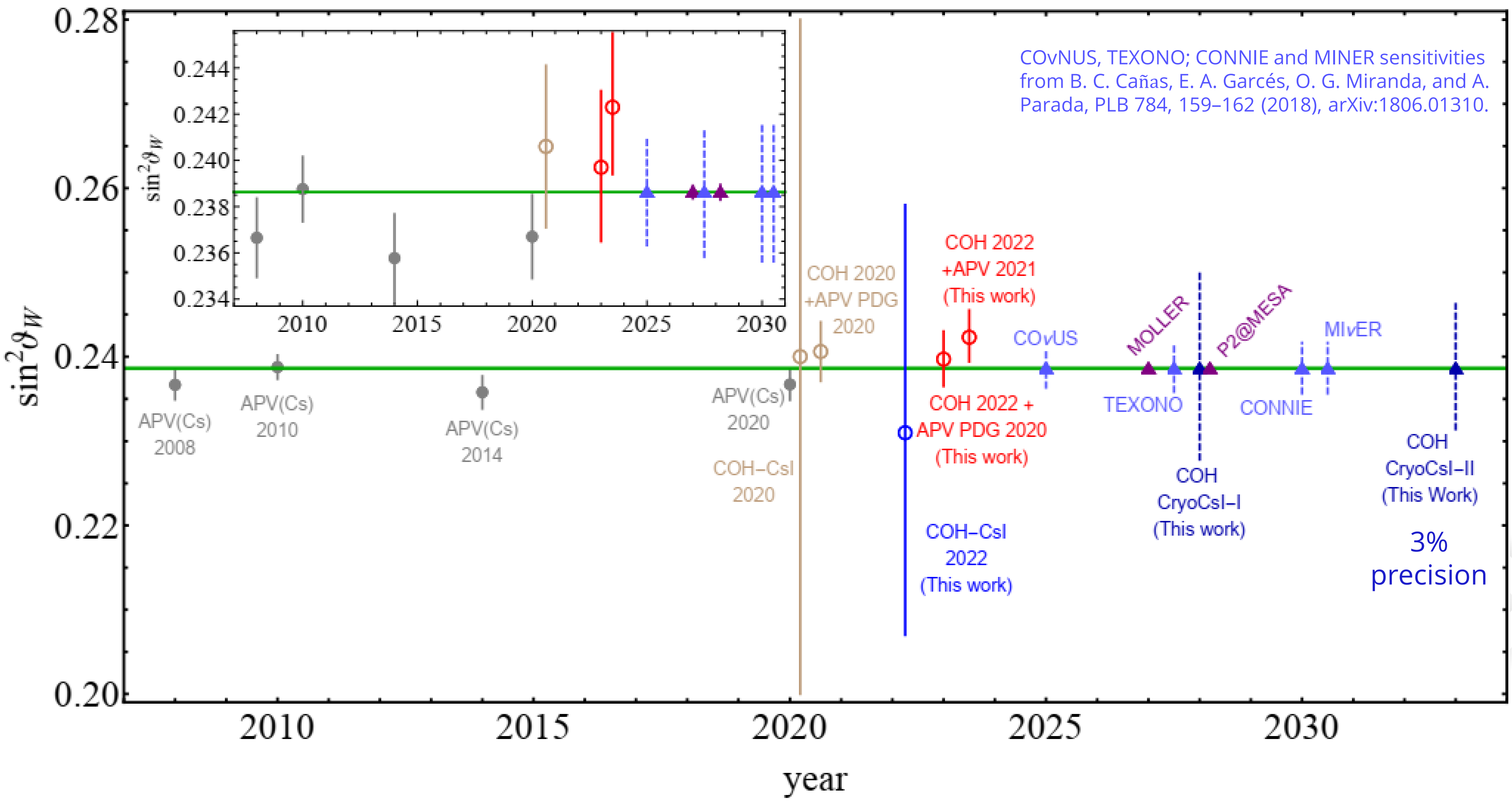

$R_n(\mathrm{Cs})=5.3^{+1.3}_{-1.2}$ fm $R_n(\mathrm{I})=5.6^{+1.6}_{-1.2}$ fm $\chi^2{}_{\mathrm{min}}= 85.2$

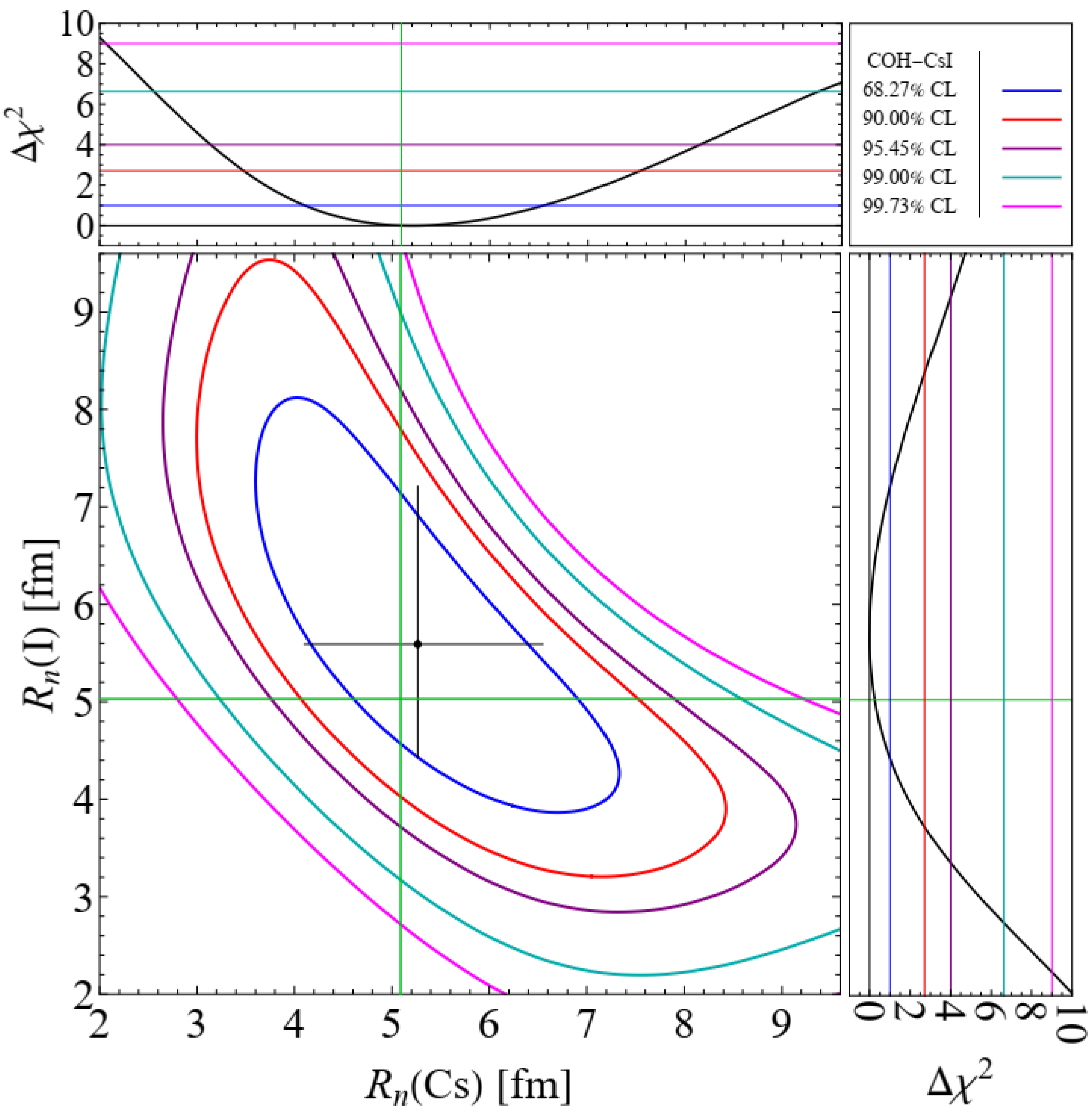

Leptophilic models

In the $\boldsymbol{L_\alpha - L_\beta}$ (where α and β are two leptons flavors) models there is **no direct coupling** between a $L_\alpha - L_\beta$ gauge boson and quarks

$$\left(\frac{d\sigma}{dT_{\rm nr}}\right)^{\nu_\ell-\mathcal{N}}_{L_\alpha-L_\beta}(E,T_{\rm nr}) = \frac{G_F^2 M}{\pi}\left(1-\frac{MT_{\rm nr}}{2E^2}\right) \times \left\{\left[g_V^p(\nu_\ell) + \frac{\sqrt{2}\alpha_{\rm EM} g_{Z'}^2\left(\delta_{\ell\alpha}\varepsilon_{\beta\alpha}(|\vec{q}|) + \delta_{\ell\beta}\varepsilon_{\alpha\beta}(|\vec{q}|)\right)}{\pi G_F\left(|\vec{q}|^2 + M_{Z'}^2\right)}\right] Z F_Z(|\vec{q}|^2) + g_V^n N F_N(|\vec{q}|^2)\right\}^2$$

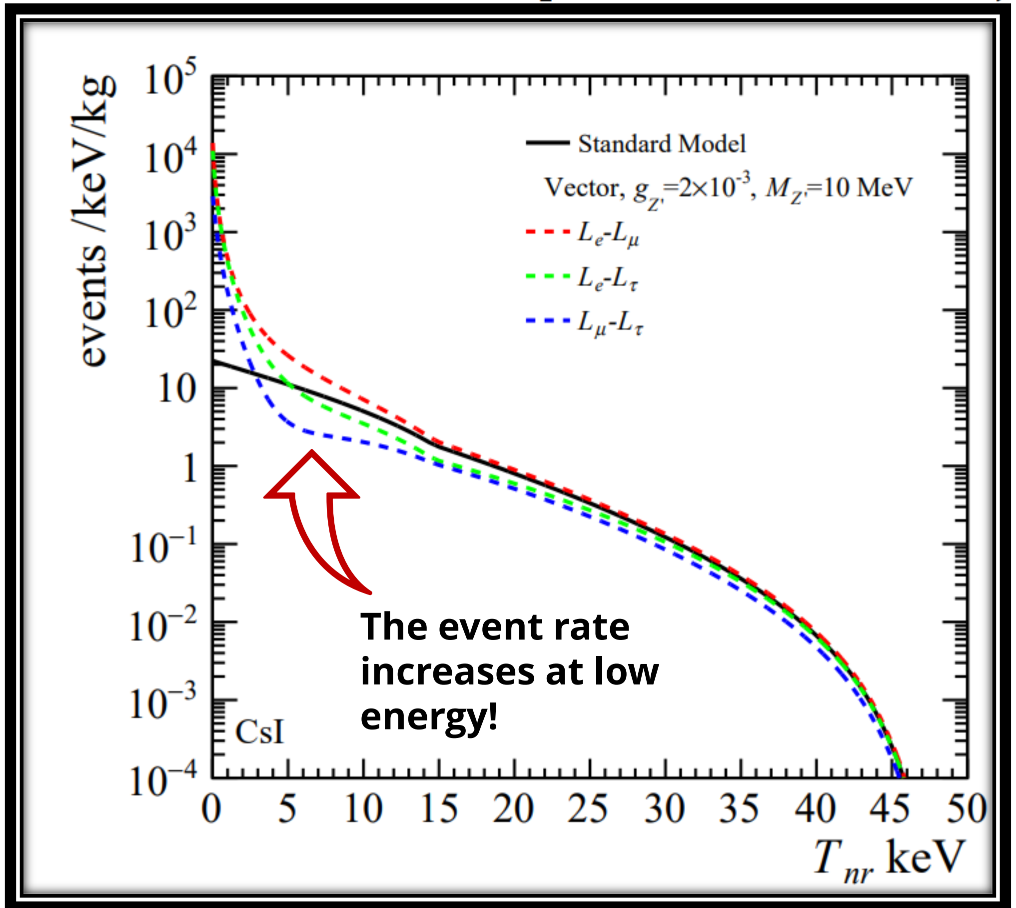

The coupling between neutrinos and quark is due to 1-loop effects

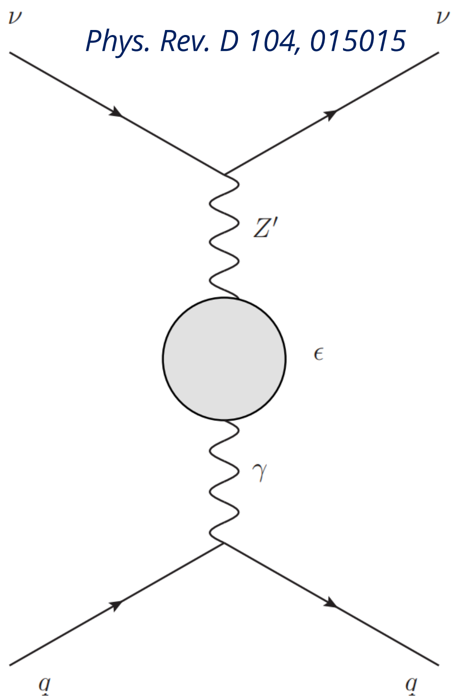

The scalar mediator case

+ The interaction can be mediated by a scalar field ϕ
+ We assume a scalar boson with $g_\phi^d = g_\phi^u \doteq g_\phi^q$ and $g_\phi^{\nu_e} = g_\phi^{\nu_\mu} \doteq g_\phi^{\nu_\ell}$
+ The contribution of the scalar boson to CEνNS is incoherent

JHEP 05 (2018) 066

$$\frac{d\sigma_{\nu_\ell\text{-}\mathcal{N}}}{dT_{\mathrm{nr}}} = \left(\frac{d\sigma_{\nu_\ell\text{-}\mathcal{N}}}{dT_{\mathrm{nr}}}\right)_{\mathrm{SM}} + \left(\frac{d\sigma_{\nu_\ell\text{-}\mathcal{N}}}{dT_{\mathrm{nr}}}\right)_{\mathrm{scalar}}$$

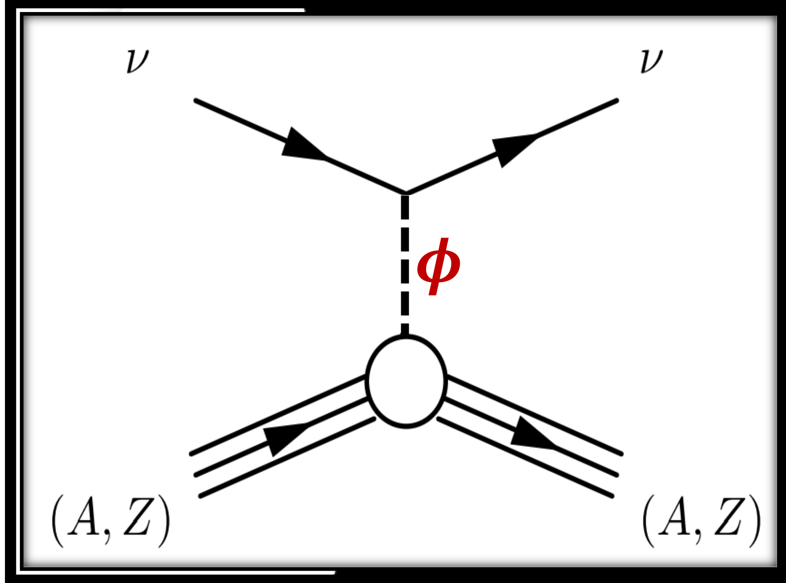

$$\left(\frac{d\sigma_{\nu_\ell\text{-}\mathcal{N}}}{dT_{\mathrm{nr}}}\right)_{\mathrm{scalar}} = \frac{M^2 T_{\mathrm{nr}}}{4\pi E^2} \frac{\boxed{\tilde{g}_\phi^4}}{(|\vec{q}|^2 + \boxed{M_\phi^2})^2} \boxed{\left(\frac{\sigma_{\pi N}}{\overline{m}_{ud}}\right)_{\mathrm{ref}}^2} \left[Z F_Z(|\vec{q}|^2) + N F_N(|\vec{q}|^2)\right]^2$$

Reference value of $\sim 17{,}3$ *Phys. Rev. Lett. 115, 092301*
Particle Data Group, PTEP 2022, 083C01 (2022)

Radiative corrections

$F_N\left(|\vec{q}|^2\right)$. Thus, in this paper, we calculated the couplings taking into account the radiative corrections in the $\overline{\text{MS}}$ scheme following Refs. [51, 62]

$$
\begin{aligned}
g_V^{\nu_\ell\, p} &= \rho\left(\frac{1}{2} - 2\sin^2\vartheta_{\mathrm{W}}\right) + 2\,⧖_{WW} + \square_{WW} - 2\varnothing_{\nu_\ell W} + \rho(2\,\boxtimes_{ZZ}^{uL} + \boxtimes_{ZZ}^{dL} - 2\,\boxtimes_{ZZ}^{uR} - \boxtimes_{ZZ}^{dR}), \\
g_V^{\nu_\ell\, n} &= -\frac{\rho}{2} + 2\square_{WW} + ⧖_{WW} + \rho(2\,\boxtimes_{ZZ}^{dL} + \boxtimes_{ZZ}^{uL} - 2\,\boxtimes_{ZZ}^{dR} - \boxtimes_{ZZ}^{uR}).
\end{aligned}
\tag{2}
$$

The quantities in Eq. (2), $\square_{WW}, ⧖_{WW}$ and $\boxtimes_{ZZ}^{fX}$, with $f \in \{u, d\}$ and $X \in \{L, R\}$, are the radiative corrections associated with the WW box diagram, the WW crossed-box and the ZZ box respectively, while $\rho = 1.00063$ is a parameter of electroweak interactions. Moreover, $\varnothing_{\nu_\ell W}$ describes the neutrino charge radius contribution and introduces a dependence on the neutrino flavour ℓ (see Ref. [62] or the appendix B of Ref. [63] for further information on such quantities). Numerically, the values of these couplings correspond to $g_V^p(\nu_e) = 0.0382$, $g_V^p(\nu_\mu) = 0.0300$, and $g_V^n = -0.5117$.

M. Atzori Corona et al., EPJC 83 (2023) 7, 683, arXiv:2303:09360

COHERENT CsI χ^2

+ Poissonian least-square function:

+ Since in some energy-time bins the number of events is zero, we used the Poissonian least-squares function

$$\chi^2_{\mathrm{CsI}} = 2\sum_{i=1}^{9}\sum_{j=1}^{11}\left[\sum_{z=1}^{4}(1+\eta_z)N_{ij}^{z} - N_{ij}^{\mathrm{exp}} + N_{ij}^{\mathrm{exp}}\ln\left(\frac{N_{ij}^{\mathrm{exp}}}{\sum_{z=1}^{4}(1+\eta_z)N_{ij}^{z}}\right)\right] + \sum_{z=1}^{4}\left(\frac{\eta_z}{\sigma_z}\right)^2, \qquad (10)$$

where the indices i, j represent the nuclear-recoil energy and arrival time bin, respectively, while the indices $z = 1, 2, 3, 4$ for N_{ij}^{z} stand, respectively, for CEνNS, ($N_{ij}^{1} = N_{ij}^{\mathrm{CE}\nu\mathrm{NS}}$), beam-related neutron ($N_{ij}^{2} = N_{ij}^{\mathrm{BRN}}$), neutrino-induced neutron ($N_{ij}^{3} = N_{ij}^{\mathrm{NIN}}$) and steady-state ($N_{ij}^{4} = N_{ij}^{\mathrm{SS}}$) backgrounds obtained from the anti-coincidence data. In our notation, N_{ij}^{exp} is the experimental event number obtained from coincidence data and $N_{ij}^{\mathrm{CE}\nu\mathrm{NS}}$ is the predicted number of CEνNS events that depends on the physics model under consideration, according to the cross-section in Eq. (1), as well as on the neutrino flux, energy resolution, detector efficiency, number of target atoms and the CsI quenching factor [16]. We take into account the systematic uncertainties with the nuisance parameters η_z and the corresponding uncertainties $\sigma_{\mathrm{CE}\nu\mathrm{NS}} = 0.12$, $\sigma_{\mathrm{BRN}} = 0.25$, $\sigma_{\mathrm{NIN}} = 0.35$ and $\sigma_{\mathrm{SS}} = 0.021$ as explained in Refs. [6, 16].

Neutrino charge radius

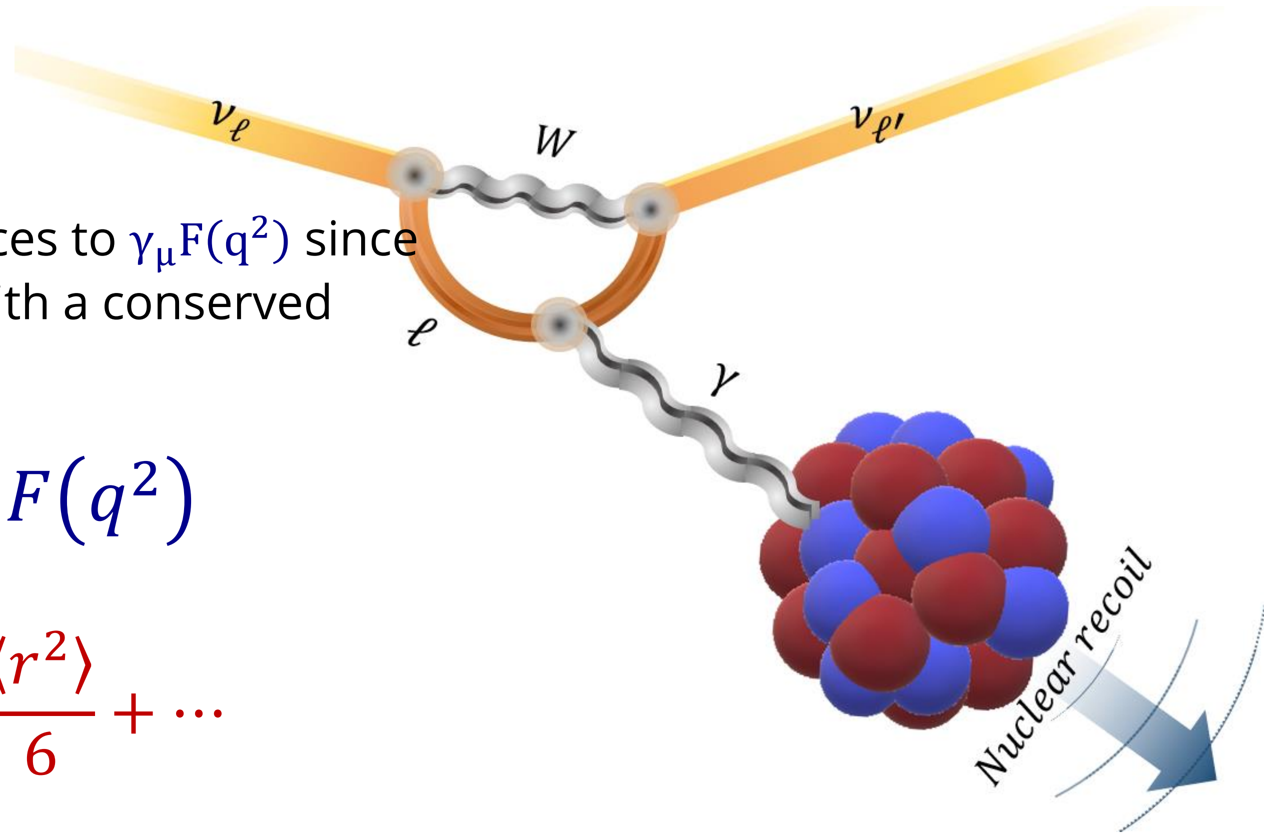

- In the Standard Model (SM) the effective vertex reduces to $\gamma_\mu F(q^2)$ since the contribution $q_\mu \gamma^\mu \, q_\mu/q^2$ vanishes in the coupling with a conserved current

$$\Lambda_\mu(q) = \left(\gamma_\mu - q_\mu \gamma^\mu \, q_\mu/q^2\right) F(q^2) \cong \gamma_\mu F\left(q^2\right)$$

$$F(q^2) = \cancel{F(0)} + q^2 \left.\frac{\mathrm{d}F(q^2)}{\mathrm{d}q^2}\right|_{q^2=0} + \cdots = q^2 \frac{\langle r^2 \rangle}{6} + \cdots$$

- In the Standard Model $\langle r^2_{\nu_\ell} \rangle_{SM} = -\frac{G_F}{2\sqrt{2}\pi^2}\left[3 - 2\log\left(\frac{m_\ell^2}{m_W^2}\right)\right]$

$$\langle r^2_{\nu_e} \rangle_{SM} = -8.2 \times 10^{-33}\ cm^2$$
$$\langle r^2_{\nu_\mu} \rangle_{SM} = -4.8 \times 10^{-33}\ cm^2$$
$$\langle r^2_{\nu_\tau} \rangle_{SM} = -3.0 \times 10^{-33}\ cm^2$$

"A charge radius that is gauge-independent, finite is achieved by including additional diagrams in the calculation of $F(q^2)$"

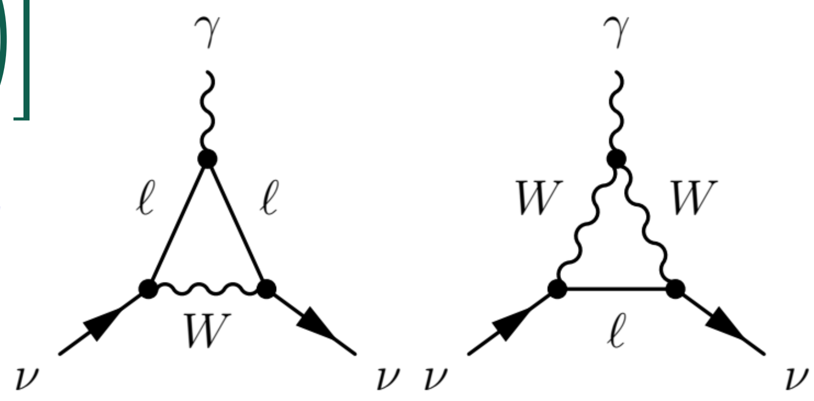

[Bernabeu et al, PRD 62 (2000) 113012, NPB 680 (2004) 450]

Dresden-II weak mixing angle results

+ Insensitive to $R_n(\mathrm{Ge})$
+ Insensitive to the antineutrino flux parametrization

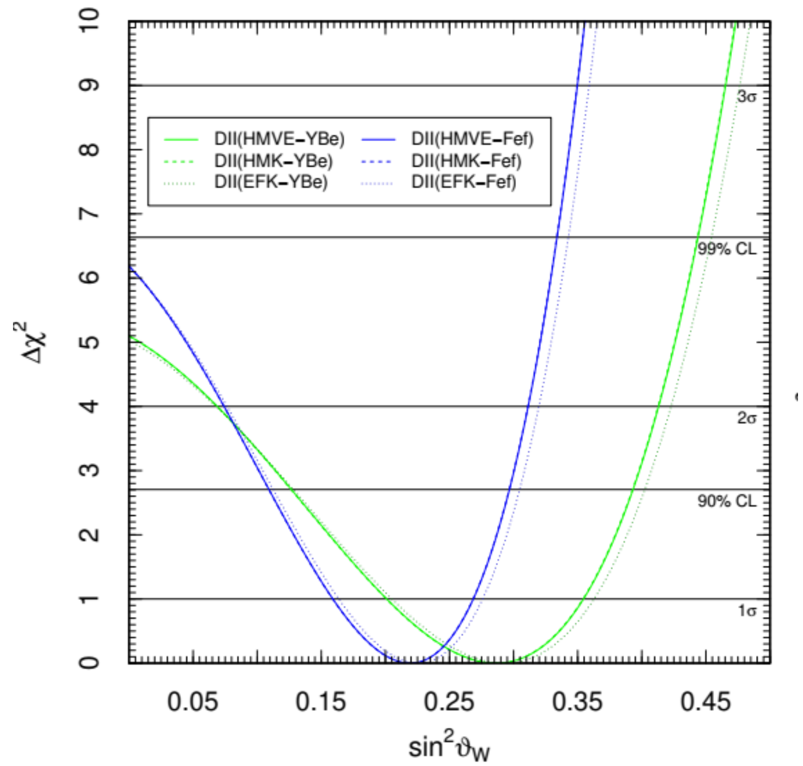

M. Atzori Corona et al., JHEP **09**, 164 (2022), arXiv:2205.09484

+ Very sensitive to the Ge quenching factor parametrization

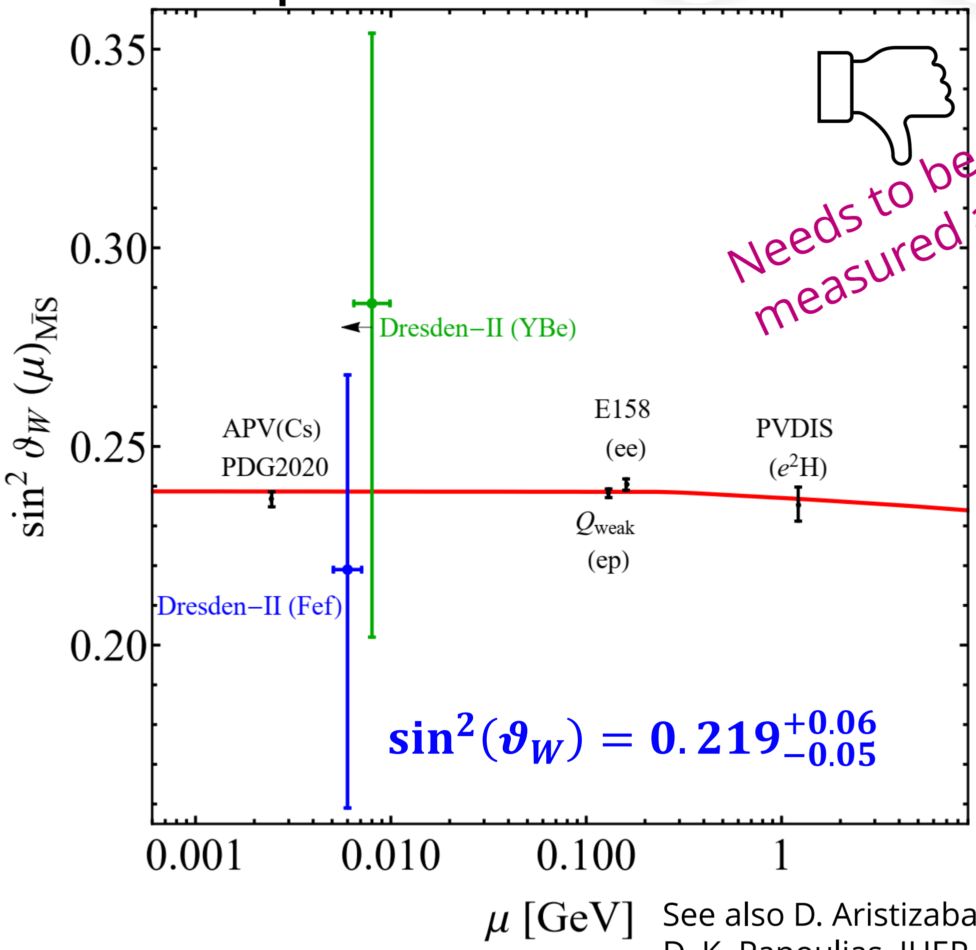

Needs to be accurately measured at low energies

See also D. Aristizabal Sierra, V. De Romeri, and D. K. Papoulias, JHEP **09**, 076 (2022)

THE NUCLEAR FORM FACTOR

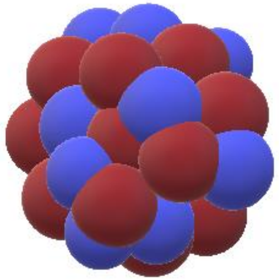

- The nuclear form factor, F(q), is taken to be the **Fourier transform** of a spherically symmetric ground state **mass distribution (both proton and neutrons)** normalized so that F(0) = 1:

For a weak interaction like for CEvNS you deal with the **weak form factor**: the Fourier transform of the weak charge distribution (neutron + proton distribution weighted by the weak mixing angle)

$$\frac{d\sigma}{dE_r} \cong \frac{G_F^2\, m_N}{4\pi}\left(1-\frac{m_N E_r}{2E_\nu^2}\right) Q_w^2 \times |F_{weak}(E_r)|^2$$

Weak charge × weak form factor

$$\left[g_V^p Z F_Z(E_r, R_p) + g_V^n N F_N(E_r, R_n)\right]^2$$

Proton + Neutron from factor

Extensively studied
Huge bibliography

Poorly known…

Helm R. Phys. Rev. **104**, 1466 (1956)

It is convenient to have an analytic expression like the **Helm form factor**

$$\boxed{F_N^{\mathrm{Helm}}(q^2) = 3\,\frac{j_1(qR_0)}{qR_0}\,e^{-q^2 s^2/2}}$$

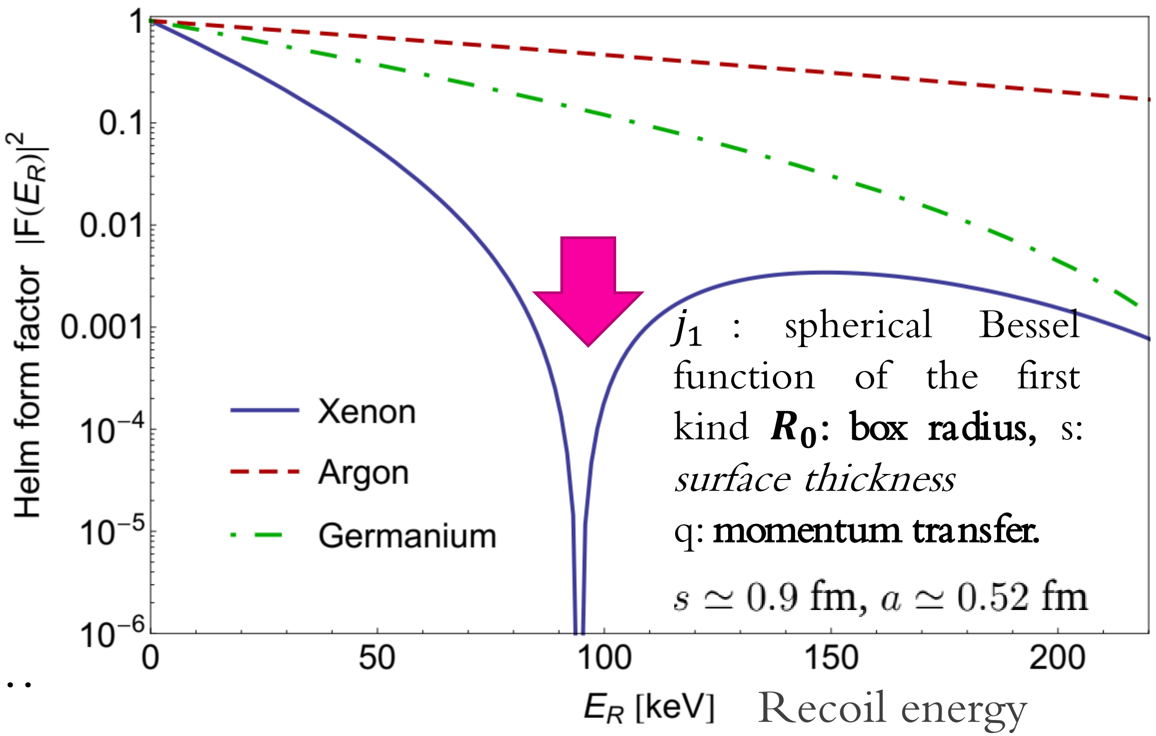

j_1 : spherical Bessel function of the first kind $\boldsymbol{R_0}$**: box radius,** s: *surface thickness*

q: **momentum transfer.**

$s \simeq 0.9$ fm, $a \simeq 0.52$ fm

Recoil energy

FITTING THE COHERENT CsI DATA FOR THE NEUTRON RADIUS

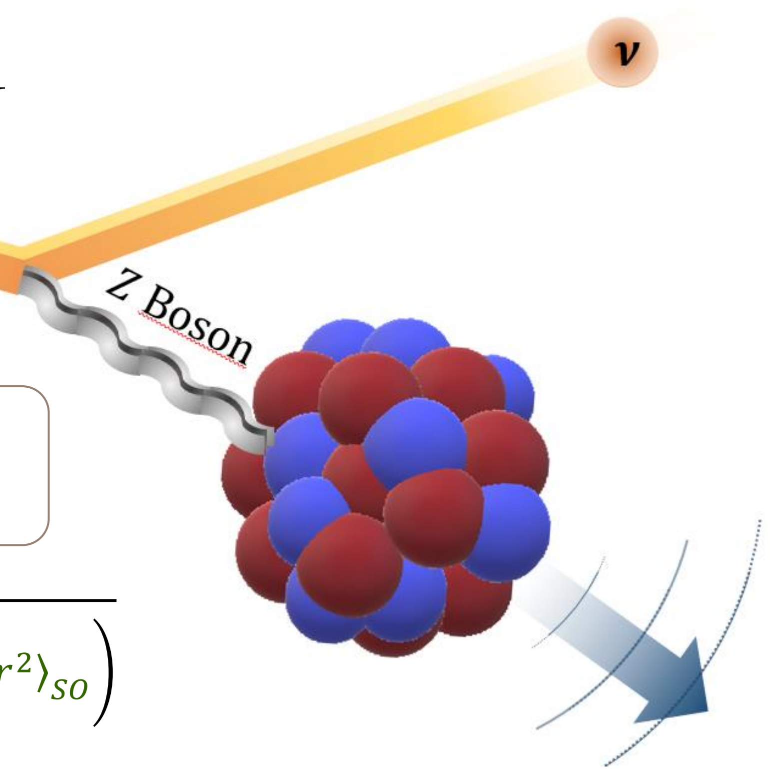

G. Fricke et al., Atom. Data Nucl. Data Tabl. **60**, 177 (1995)

- ✓ From muonic X-rays data we have

(For fixed $t = 2.3$ fm)

$R_{ch}^{Cs} = 4.804$ fm (Cesium charge rms radius)
$R_{ch}^{I} = 4.749$ fm (Iodine charge rms radius)

$$R_p^{\mathrm{rms}} = \sqrt{R_{\mathrm{ch}}^2 - \left(\frac{N}{Z}\langle r_{\mathrm{n}}^2\rangle + \frac{3}{4M^2} + \langle r^2\rangle_{SO}\right)}$$

$R_p^{Cs} = 4.821 \pm 0.005$ fm (Cesium rms proton radius)
$R_p^{I} = 4.766 \pm 0.008$ fm (Iodine rms-proton radius)

$$\frac{d\sigma}{dE_r} \cong \frac{G_F^2 m_N}{4\pi}\left(1 - \frac{m_N E_r}{2E_\nu^2}\right)\left[g_V^p Z F_Z\left(E_r, R_p^{Cs/I}\right) + g_V^n N F_N\left(E_r, R_n^{CsI}\right)\right]^2$$

R_n^{Cs} & R_n^{I} very well known so we fitted COHERENT CsI data looking for R_n^{CsI} …

FROM THE CHARGE TO THE PROTON RADIUS

One need to take into account finite size of both protons and neutrons plus other corrections

$$R_{ch}^2 = R_{\mathrm{point}}^2 + \langle r_{\mathrm{p}}^2 \rangle + \frac{N}{Z}\langle r_{\mathrm{n}}^2 \rangle + \frac{3}{4M^2} + \langle r^2 \rangle_{SO}$$

Charge radius

Point-proton radius

Mean squared charge radius of a single proton
$\langle r_{\mathrm{p}}^2 \rangle = 0.7071\ \mathrm{fm}^2$

Mean squared charge radius of a single neutron
$\langle r_{\mathrm{n}}^2 \rangle = -0.1161\ \mathrm{fm}^2$

Relativistic Darwin-Foldy correction
$\sim 0.033\ \mathrm{fm}^2$

Spin-orbit correction
$\sim 0.09\ \mathrm{fm}^2$ for ^{48}Ca
$\sim 0.028\ \mathrm{fm}^2$ for ^{208}Pb

G. Hagen et al. *Nature Physics* **12**, 186–190 (2016), Arxiv: 1509.07169

M. Cadeddu et al. PRD 102, 015030 (2020), Arxiv: 2005.01645

$$R_p^{\mathrm{rms}} = \sqrt{R_{\mathrm{point}}^2 + \langle r_{\mathrm{p}}^2 \rangle} =$$

$$= \sqrt{R_{ch}^2 - \left(\frac{N}{Z}\langle r_{\mathrm{n}}^2 \rangle + \frac{3}{4M^2} + \langle r^2 \rangle_{SO}\right)}$$

RMS proton distribution radius

COHERENT+APV compared to PREX

$\Delta R_{np}(^{133}\mathrm{Cs}) = 0.45^{+0.33}_{-0.33}$ fm

@fixed $\sin^2\hat{\theta}_W$

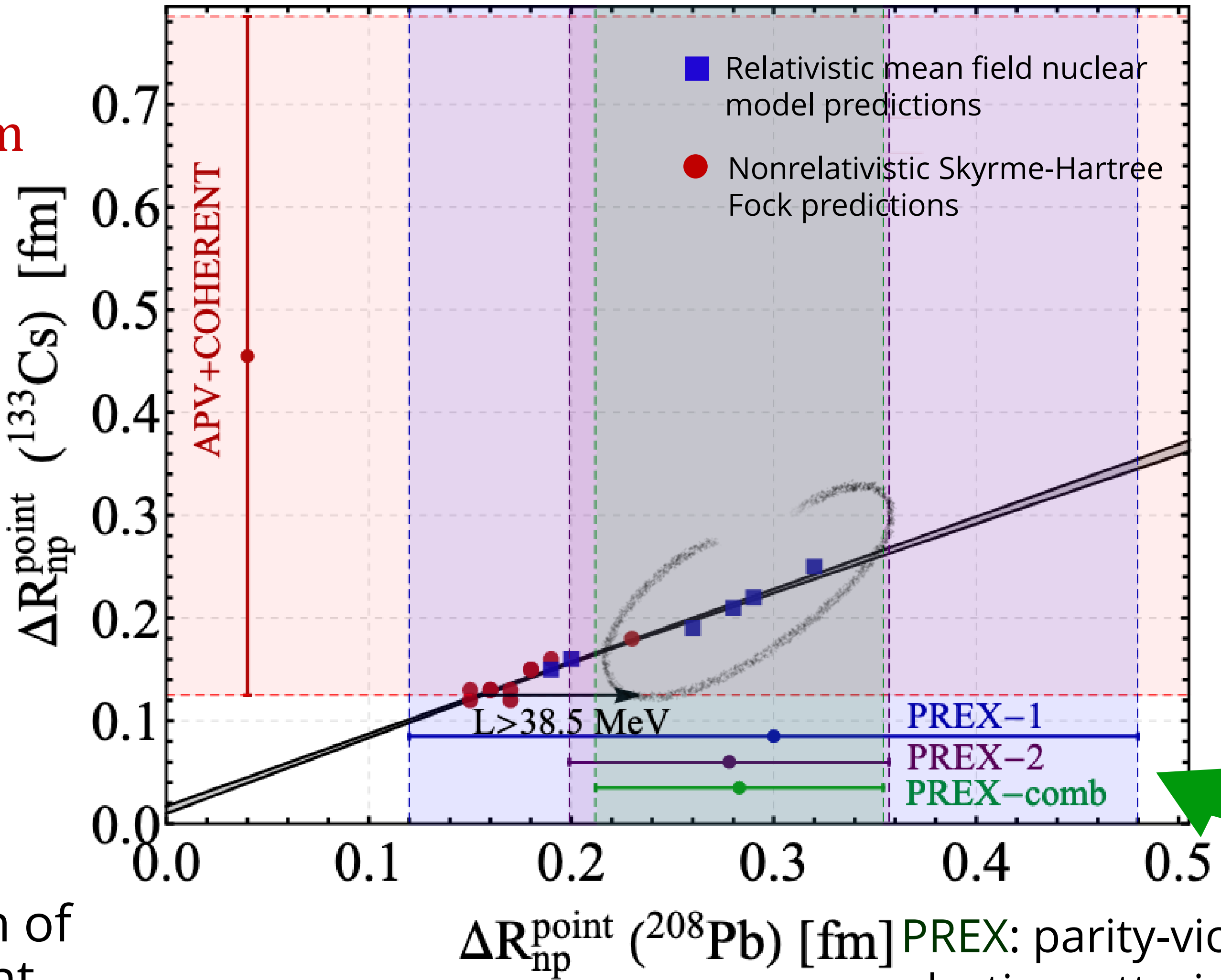

Cadeddu et al., PRC 104, 065502
arXiv:2102.06153

@fixed $\sin^2\hat{\theta}_W$

+ Strong linear correlation between the neutron skin of Cs and Pb among different nuclear model predictions

PREX: parity-violating asymmetry in the elastic scattering of longitudinally polarized electrons on ^{208}Pb

$$A_{\mathrm{PV}} = \frac{\sigma_R - \sigma_L}{\sigma_R + \sigma_L} \approx \frac{G_F Q^2 |Q_W|}{4\sqrt{2}\pi\alpha Z} \frac{F_{\mathrm{W}}(Q^2)}{F_{\mathrm{ch}}(Q^2)}$$

PREX, PRL 126, 172502 (2021)

The proton form factor

$$\frac{d\sigma_{\nu-CsI}}{dT} = \frac{G_F^2 M}{4\pi}\left(1-\frac{MT}{2E_\nu^2}\right)[N\,\boldsymbol{F_N(T,R_n)} - \varepsilon Z\,\boldsymbol{F_Z(T,R_p)}]^{\,2}$$

The proton structures of ${}^{133}_{55}Cs$ $(N=78)$ and ${}^{127}_{53}I$ $(N=74)$ have been studied with muonic spectroscopy and the data were fitted with **two-parameter Fermi density distributions** of the form

$$\boxed{\rho_F(r) = \frac{\rho_0}{1+e^{(r-c)/a}}}$$

Where, the **half-density radius *c*** is related to the **rms radius** and the *a* parameter quantifies the **surface thickness** $t = 4\,a\,\ln 3$ (in the analysis fixed to 2.30 fm).

- Fitting the data they obtained

$R_{ch}^{Cs} = 4.804$ fm (Caesium proton rms radius)

$R_{ch}^{I} = 4.749$ fm (Iodine proton rms radius)

[G. Fricke et al., Atom. Data Nucl. Data Tabl. **60**, 177 (1995)]

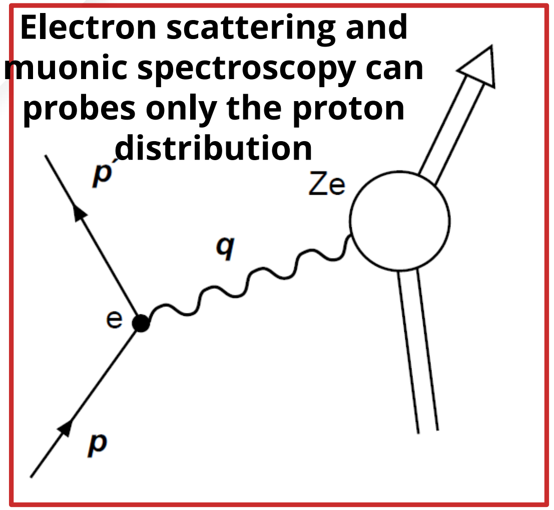

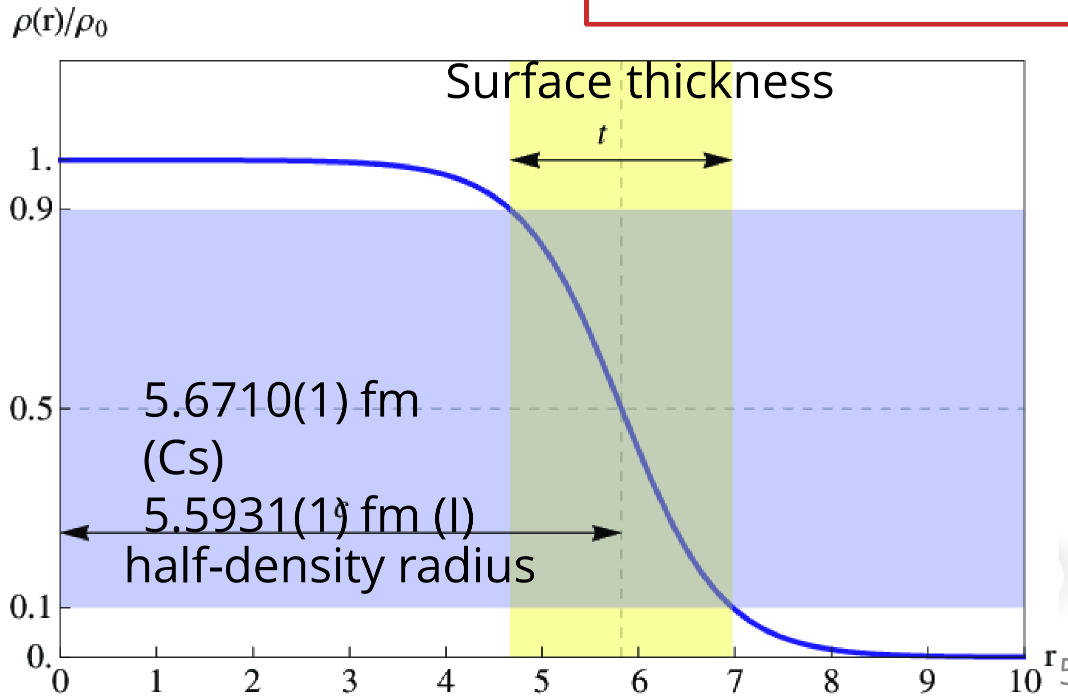

Weak mixing angle (WMA)

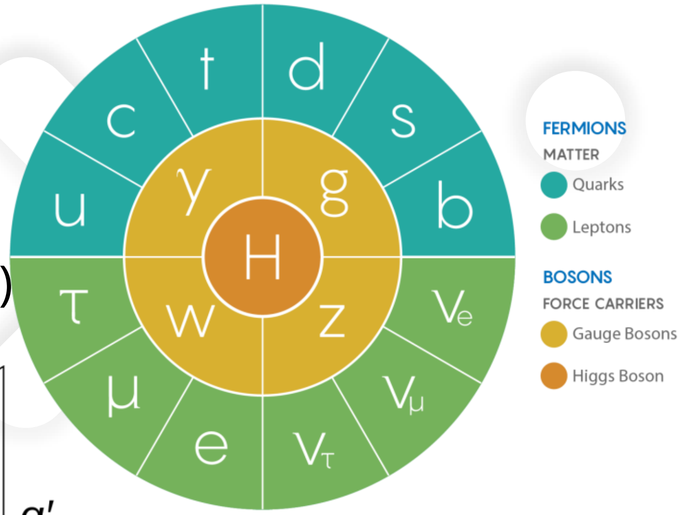

+ The Weinberg angle, θ_W is a fundamental parameter of the **electroweak** (EW) theory of the Standard Model (SM), usually expressed as $\sin^2\theta_W$
+ WMA determines the relative strength of the weak neutral current (NC) vs. electromagnetic interaction

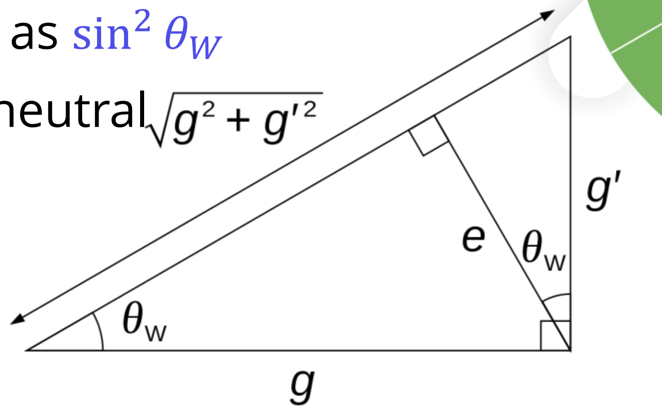

$$e = g\sin\theta_W$$
$$e = g'\cos\theta_W$$

➢ **Tree-level** $\sin^2\theta_W = 1 - \frac{M_W^2}{M_Z^2} = \frac{g'^2}{g^2+g'^2}$

+ The **on-shell scheme** promotes the tree-level formula to a definition of the renormalized $\sin^2\theta_W$ to all orders in perturbation theory (quite sensitive to the top mass)

➢ $\sin^2\theta_W \to s_W^2 \equiv 1 - \frac{M_W^2}{M_Z^2} = 0.22343 \pm 0.00007$ (on−shell)

+ **Minimal subtraction scheme** ($\overline{\mathrm{MS}}$) $\sin^2\hat{\theta}_W(\mu) = \frac{\hat{g}'^2(\mu)}{\hat{g}^2(\mu)+\hat{g}'^2(\mu)}$ where the couplings are defined in the $\overline{\mathrm{MS}}$ and the energy scale μ is conveniently chosen to be M_Z for many EW processes (less sensitive to the top mass)

➢ $\sin^2\hat{\theta}_W(M_Z) \equiv \hat{s}_Z^2 = 0.23122 \pm 0.00003$ ($\overline{\mathrm{MS}}$)

Scale dependent→ running of WMA

+ The value of $\sin^2\hat{\theta}_W$ varies as a function of the momentum transfer or energy scale («running»).
+ Working in the $\overline{\text{MS}}$, the main idea is to relate the case of the WMA to that of the electromagnetic coupling $\hat{\alpha}$
+ The vacuum polarization contributions are crucial

Allows precision tests of the Standard Model!

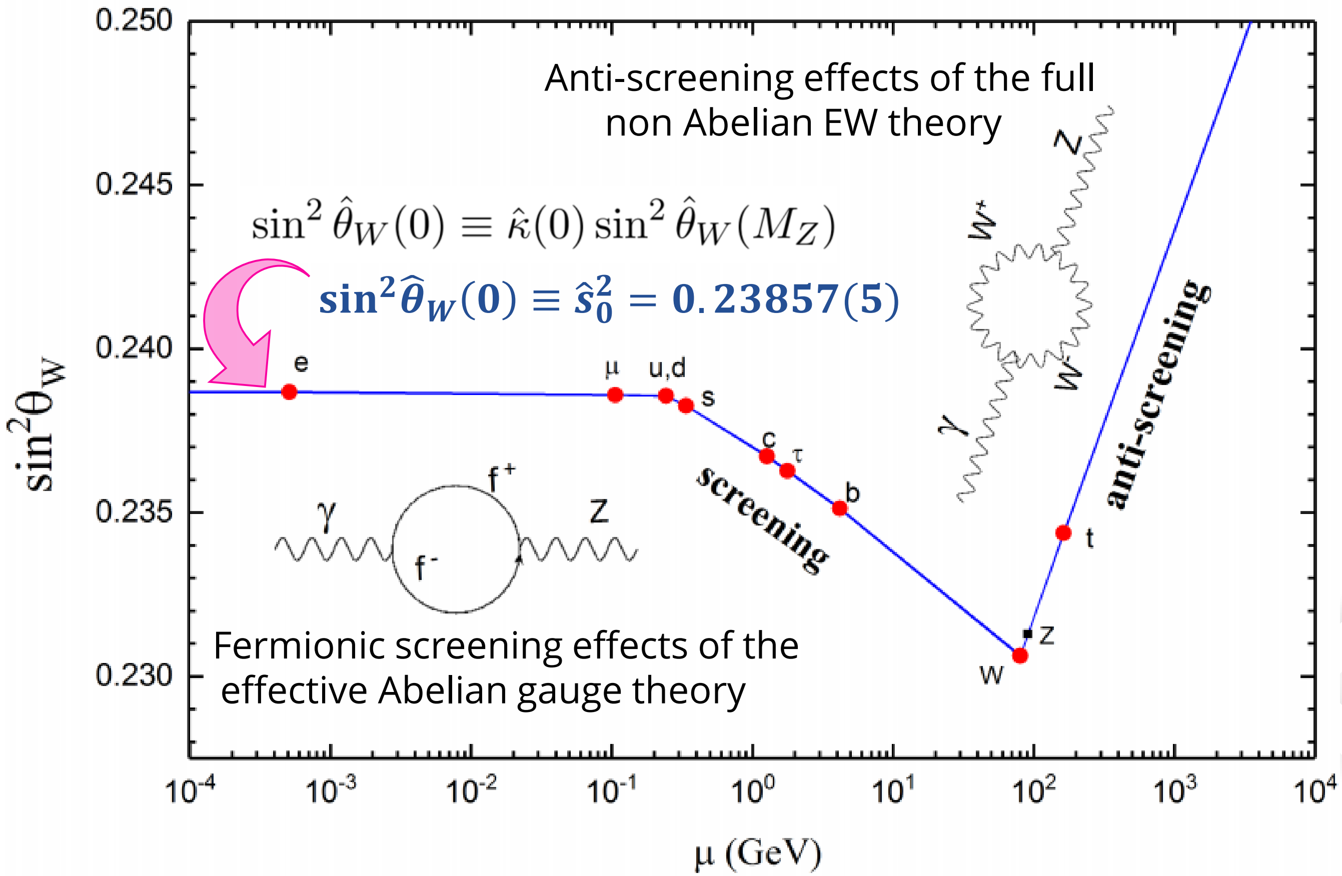

[Erler et al. JHEP 03 (2018) 196, ArXiv:1712.09146]

The «running» function changes sign at $\mu = M_W$ where the fermionic screening effects are overcompensated by the anti-screening effects

Dresden-II result

+ 3 kg ultra-low noise germanium detector 10 m away from a reactor
+ the background comes from the elastic scattering of epithermal neutrons and the electron capture in ^{71}Ge.
+ The Quenching Factor describes the suppression of the ionization yield produced by a nuclear recoil compared to an electron recoil.

Electron-equivalent energy:

$$T_e = f_Q(T_{nr})\, T_{nr}$$

- Dresden-II Ge quenching factor models

- Fef: iron filtered neutron beam
- YBe: photo-neutron source

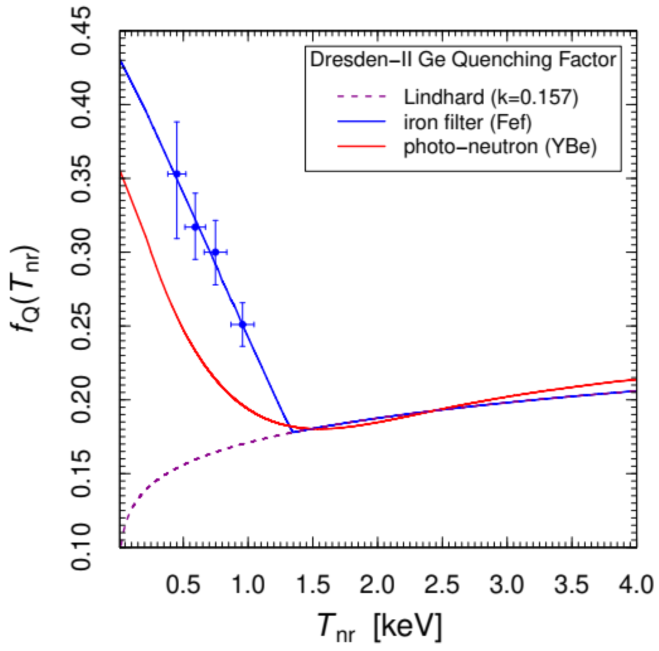

Colaresi et al. arXiv:2202.09672v1

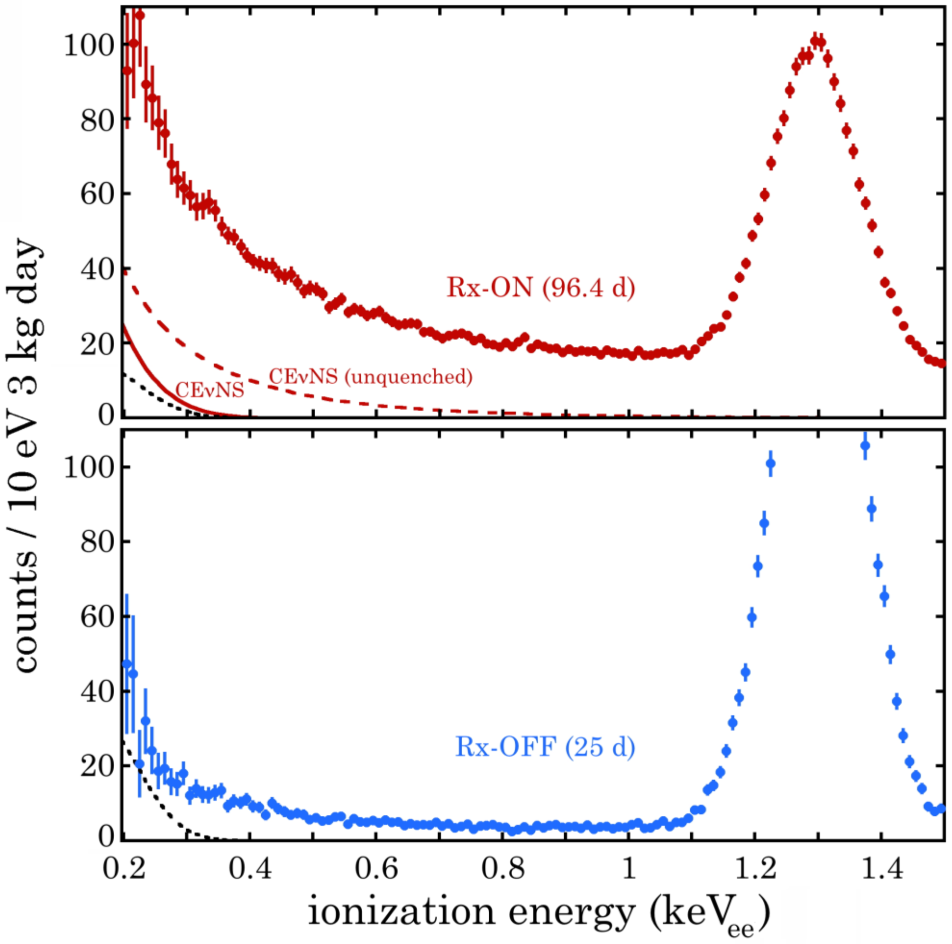

+ Ultra-low energy threshold

$$\boxed{0.2 < T_e < 1.5\ \mathrm{keV_{ee}}}$$

- This feature makes reactor neutrinos very sensitive to possible ν electromagnetic properties (millicharge, magnetic moment) since the related cross section goes like 1/T

Neutrino electromagnetic properties

For ν the electric charge is zero and there are no electromagnetic interactions at tree level. However, such interactions can arise at the quantum level from loop diagrams at higher order of the perturbative expansion of the interaction.

- In the SM the ν charge radius is

$$\langle r^2_{\nu_\ell}\rangle_{SM} = -\frac{G_F}{2\sqrt{2}\pi^2}\left[3 - 2\log\left(\frac{m_\ell^2}{m_W^2}\right)\right]$$

$$\langle r^2_{\nu_e}\rangle_{SM} = -8.2\times10^{-33}\ \mathrm{cm}^2$$
$$\langle r^2_{\nu_\mu}\rangle_{SM} = -4.8\times10^{-33}\ \mathrm{cm}^2$$
$$\langle r^2_{\nu_\tau}\rangle_{SM} = -3.0\times10^{-33}\ \mathrm{cm}^2$$

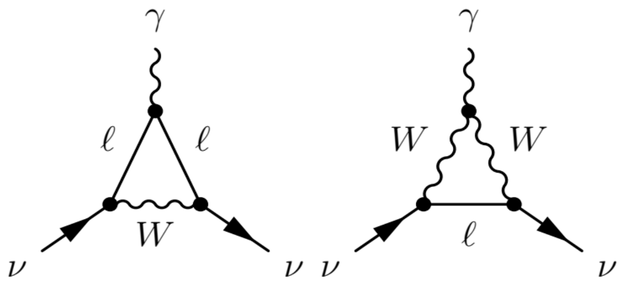

- The charge radius contributes as a correction to the neutrino-proton coupling

- In the minimally extended SM the ν magnetic moment

$$\mu_\nu = \frac{3eG_F}{8\sqrt{2}\pi^2}m_\nu \simeq 3.2\times10^{-19}\left(\frac{m_\nu}{\mathrm{eV}}\right)\mu_B$$

- In CEνNS $\displaystyle \frac{d\sigma_{\nu_\alpha\text{-}\mathcal{N}}}{dT}(E_\nu,T) = \frac{G_F^2 M}{\pi}\left(1-\frac{MT}{2E_\nu^2}\right)\left[g_V^n N F_N(|\vec{q}|) + g_V^p Z F_Z(|\vec{q}|)\right]^2 + \frac{\pi\alpha^2}{m_e^2}\left(\frac{1}{T}-\frac{1}{E_\nu}\right)Z^2F_Z^2(|\vec{q}|)\frac{\mu^2_{\nu_\alpha}}{\mu_B^2}$

- Neutrino-electron scattering in the SM is negligible

$$\frac{d\sigma^{\mathrm{ES}}_{\nu_\alpha-\mathcal{A}}}{dT_e}(E,T_e) = Z^{\mathcal{A}}_{\mathrm{eff}}(T_e)\frac{G_F^2 m_e}{2\pi}\left[\left(g_V^{\nu_\alpha}+g_A^{\nu_\alpha}\right)^2 + \left(g_V^{\nu_\alpha}-g_A^{\nu_\alpha}\right)^2\left(1-\frac{T_e}{E}\right)^2 - \left((g_V^{\nu_\alpha})^2-(g_A^{\nu_\alpha})^2\right)\frac{m_e T_e}{E^2}\right]$$

- Significant neutrino magnetic moment contribution for small T_e:

$$\frac{d\sigma^{\mathrm{ES,\,MM}}_{\nu_\alpha\text{-}\mathcal{A}}}{dT_e}(E,T_e) = Z^{\mathcal{A}}_{\mathrm{eff}}(T_e)\frac{\pi\alpha^2}{m_e^2}\left(\frac{1}{T_e}-\frac{1}{E}\right)\left|\frac{\mu_{\nu_\alpha}}{\mu_B}\right|^2$$

Neutrino charge radius limits

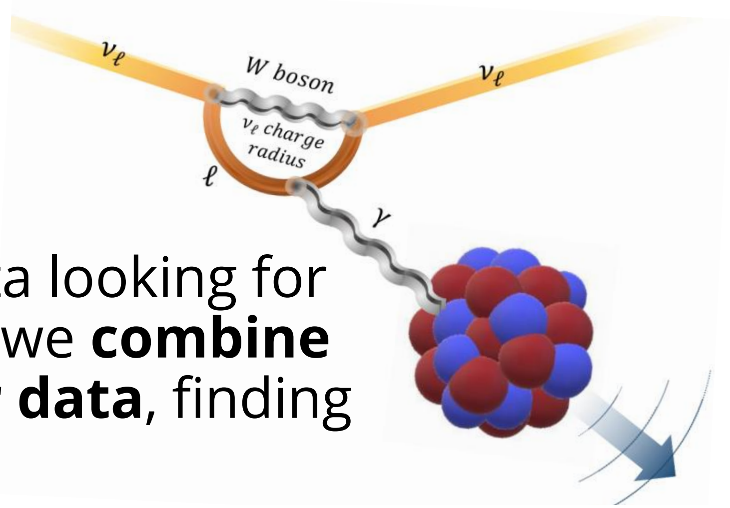

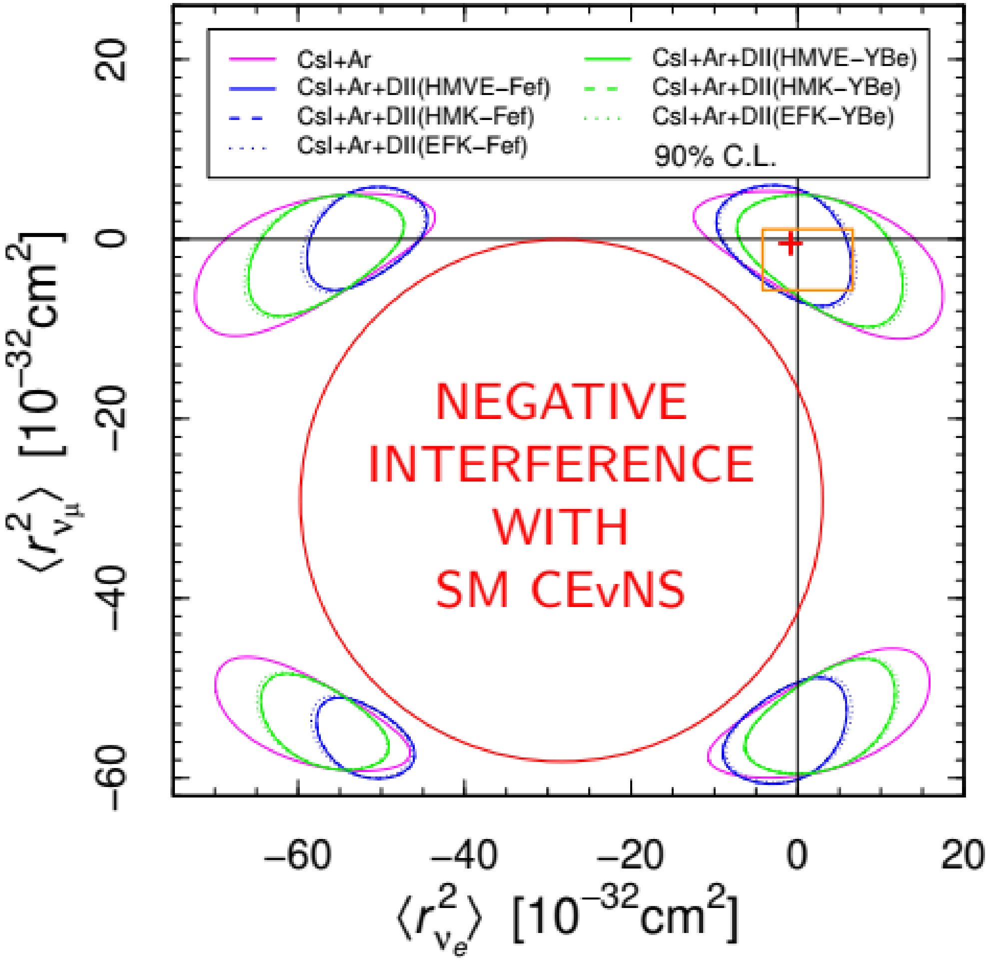

+ We fitted the **Dresden-II** data looking for neutrino EM properties and we **combine with COHERENT CsI and Ar data**, finding very interesting results.

Method	Experiment	Limit [10^{-32} cm^2]	C.L.	Year
Reactor $\bar{\nu}_e e^-$	Krasnoyarsk	$\lvert\langle r^2_{\bar{\nu}_e} \rangle\rvert < 7.3$	90%	1992
	TEXONO	$-4.2 < \langle r^2_{\nu_e} \rangle < 6.6^a$	90%	2009
Accelerator $\nu_e e^-$	LAMPF	$-7.12 < \langle r^2_{\nu_e} \rangle < 10.88^a$	90%	1992
	LSND	$-5.94 < \langle r^2_{\nu_e} \rangle < 8.28^a$	90%	2001
Accelerator $\nu_\mu e^-$	BNL-E734	$-5.7 < \langle r^2_{\nu_\mu} \rangle < 1.1^{a,b}$	90%	1990
	CHARM-II	$\lvert\langle r^2_{\nu_\mu} \rangle\rvert < 1.2^a$	90%	1994
CEvNS [arXiv:2205.09484]	COHERENT + Dresden-II	$-7.1 < \langle r^2_{\nu_e} \rangle < 11.2$ $-8.1 < \langle r^2_{\nu_\mu} \rangle < 4.3$	90%	2022

a Corrected by a factor of two due to a different convention.
b Corrected in Hirsch, Nardi, Restrepo, hep-ph/0210137.

M. Atzori Corona et al, arXiv:2205.09484

Most stringent upper limit on the electron neutrino charge radius when using the Fef quenching factor for germanium data

Neutrino magnetic moment limits

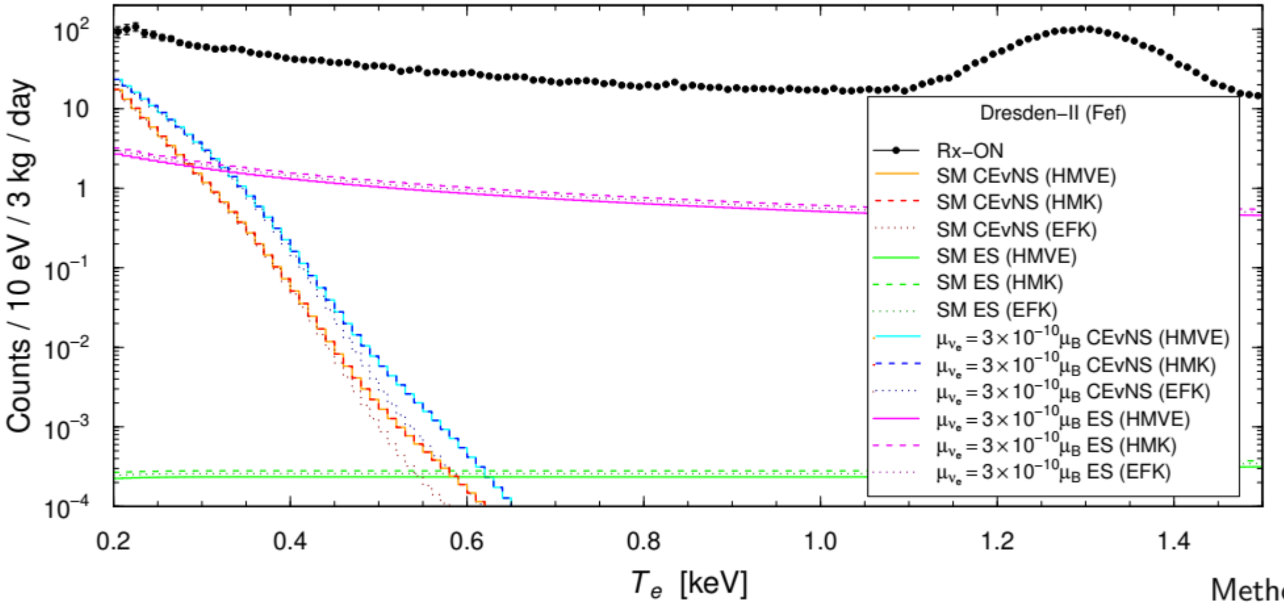

- SM ES are practically negligible
- The ES with magnetic moment are not negligible.
- Moreover ES is sensitive to the low energy antineutrino reactor flux:
  - **HMVE**: Huber-Mueller (2011) + Vogel-Engel (1989) ($E_\nu < 2$ MeV)
  - **HMK**: Huber-Mueller + Kopeikin (2012) ($E_\nu < 2$ MeV)
  - **EFK**: Estienne-Fallot (2019) + Kopeikin (2012) ($E_\nu < 0.44$ MeV)

Limits on ν magnetic moment @ 90% CL

$$|\mu_{\nu_e}| < 2.13 \times 10^{-10}\,\mu_B \quad \text{Dresden} - \text{II}\,(\text{CE}\nu\text{NS} + \text{ES}),$$
$$|\mu_{\nu_\mu}| < 18 \times 10^{-10}\,\mu_B \quad \text{CsI}\,(\text{CE}\nu\text{NS} + \text{ES}) + \text{Ar}\,(\text{CE}\nu\text{NS}),$$

Using the Fef quenching factor for germanium data

M. Atzori Corona et al, arXiv:2205.09484

These limits are still less stringent than the bounds obtained in other reactor and accelerator neutrino experiments, but the strategy looks promising.

Method	Experiment	Limit [μ_B]	CL	Year
Reactor ES ($\bar{\nu}_e\, e^-$)	Krasnoyarsk	$\lvert\mu_{\nu_e}\rvert < 2.4 \times 10^{-10}$	90%	1992
	Rovno	$\lvert\mu_{\nu_e}\rvert < 1.9 \times 10^{-10}$	95%	1993
	MUNU	$\lvert\mu_{\nu_e}\rvert < 9 \times 10^{-11}$	90%	2005
	TEXONO	$\lvert\mu_{\nu_e}\rvert < 7.4 \times 10^{-11}$	90%	2006
	GEMMA	$\lvert\mu_{\nu_e}\rvert < 2.9 \times 10^{-11}$	90%	2012
Reactor CEvNS+ES	Dresden-II [Coloma et al, arXiv:2202.10829] [Atzori Corona et al, arXiv:2205.09484]	$\lvert\mu_{\nu_e}\rvert < 3.3 \times 10^{-10}$	90%	2022
Accelerator ES ($\nu_\mu\, e^-$)	BNL-E734	$\lvert\mu_{\nu_\mu}\rvert < 8.5 \times 10^{-10}$	90%	1990
	LAMPF	$\lvert\mu_{\nu_\mu}\rvert < 7.4 \times 10^{-10}$	90%	1992
	LSND	$\lvert\mu_{\nu_\mu}\rvert < 6.8 \times 10^{-10}$	90%	2001
Accelerator CEvNS+ES	COHERENT [Coloma et al, arXiv:2202.10829] [Atzori Corona et al, arXiv:2205.09484]	$\lvert\mu_{\nu_\mu}\rvert < 2 \times 10^{-9}$	90%	2022

New constraint on neutrino magnetic moment from LZ dark matter search results

M. Atzori Corona,[1,2,a] W. Bonivento,[2,b] M. Cadeddu,[2,c] N. Cargioli,[1,2,d] and F. Dordei[2,e]

J. Aalbers et al., First Dark Matter Search Results from the LUX-ZEPLIN (LZ) Experiment (2022), arXiv:2207.03764

- LZ @the Sanford Underground Research Facility in South Dakota.
- Dual-phase TPC filled with about 10 t of LXe, of which 7 (5.5) t of the active (fiducial) region.

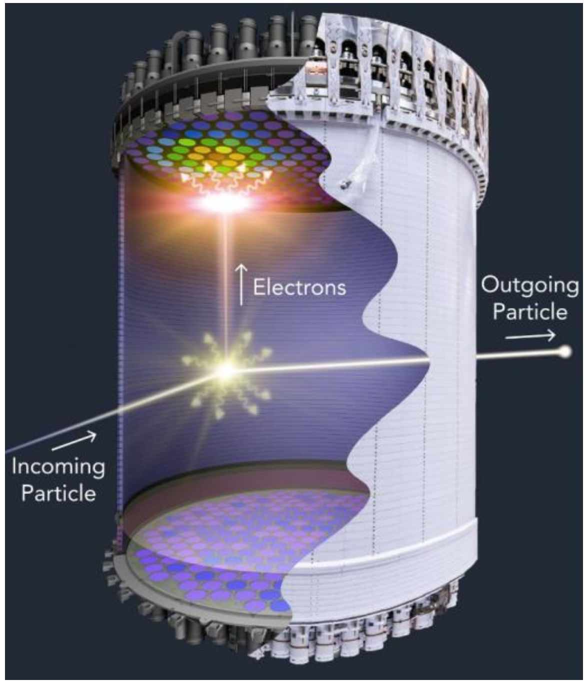

- The new LZ data allows us to set the **most stringent limit on the ν magnetic moment**
- It supersedes the previous best limit set by Borexino by almost a factor of 5
- It rejects by more than 5σ the hint of a possible ν magnetic moment found by the XENON1T Collaboration

M. Atzori Corona et al. arXiv:2207.05036v2 (2022)

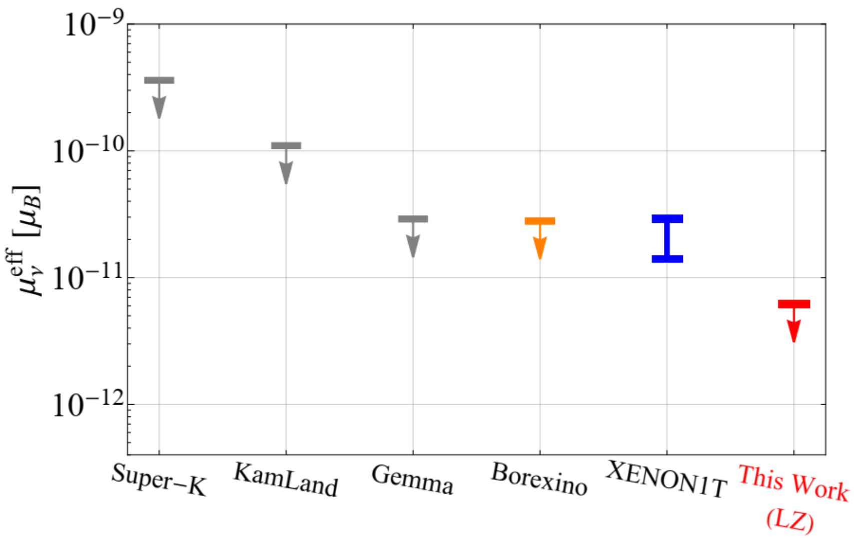

$\mu_\nu^{\rm eff} < 6.2 \times 10^{-12} \mu_B$ @ 90% CL $\quad \chi^2_{\rm min} = 106.2$

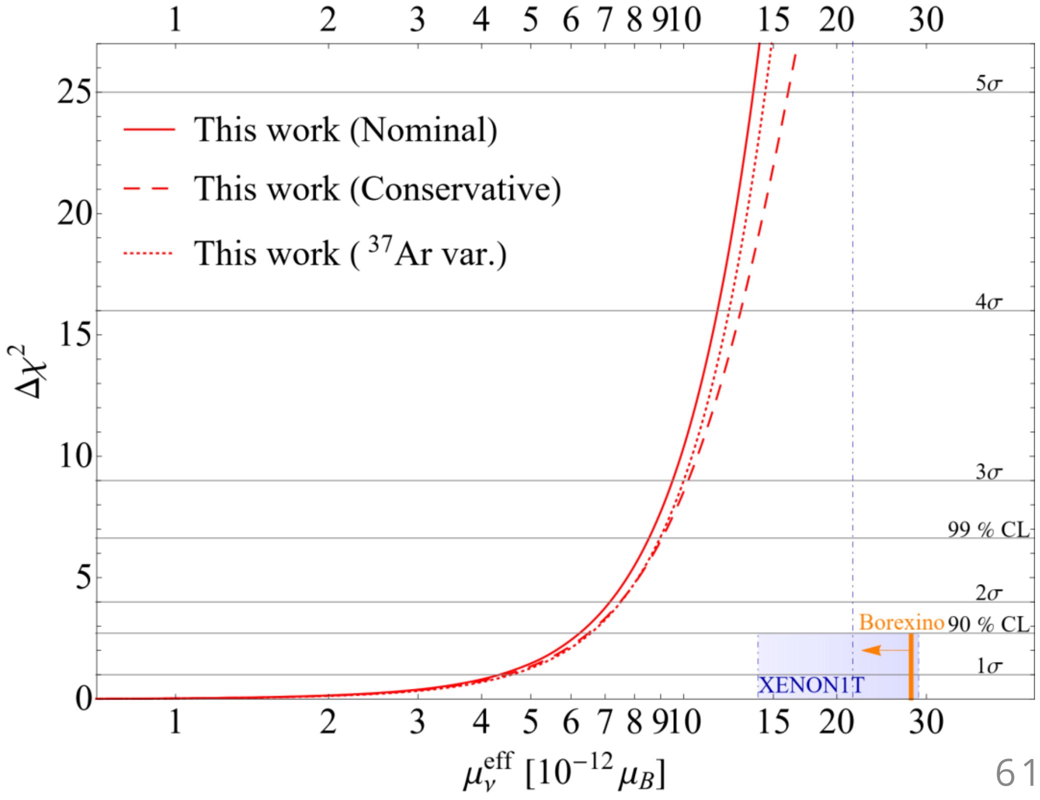

Heavy vs light mediators

$$\mathcal{L}_{\rm NSI}^{\rm NC} = -2\sqrt{2}G_{\rm F} \sum_{\alpha,\beta=e,\mu,\tau} (\overline{\nu_{\alpha L}}\gamma^\rho \nu_{\beta L}) \sum_{f=u,d} \varepsilon_{\alpha\beta}^{fV} (\bar{f}\gamma_\rho f)$$

$$\frac{d\sigma_{\nu_\alpha\text{-}\mathcal{N}}}{dT}(E,T) = \frac{G_{\rm F}^2 M}{\pi}\left(1 - \frac{MT}{2E^2}\right) Q_\alpha^2,$$

$$Q_\alpha^2 = [(g_V^p + 2\varepsilon_{\alpha\alpha}^{uV} + \varepsilon_{\alpha\alpha}^{dV}) Z F_Z(|\vec{q}|^2) + (g_V^n + \varepsilon_{\alpha\alpha}^{uV} + 2\varepsilon_{\alpha\alpha}^{dV}) N F_N(|\vec{q}|^2)]^2 + \sum_{\beta\neq\alpha} |(2\varepsilon_{\alpha\beta}^{uV} + \varepsilon_{\alpha\beta}^{dV}) Z F_Z(|\vec{q}|^2) + (\varepsilon_{\alpha\beta}^{uV} + 2\varepsilon_{\alpha\beta}^{dV}) N F_N(|\vec{q}|^2)|^2,$$

«Heavy» mediator

$$q^2 \ll M_{Z'}$$

Effective four fermion interaction Lagrangian. The parameters ε describe the size of NSI relative to standard neutral-current weak interactions.

$$\epsilon_{\ell\ell}^{fV} = \frac{g_{Z'}^2 Q'_\ell Q'_f}{\sqrt{2}G_F\,(|\vec{q}|^2 + M_{Z'}^2)}$$

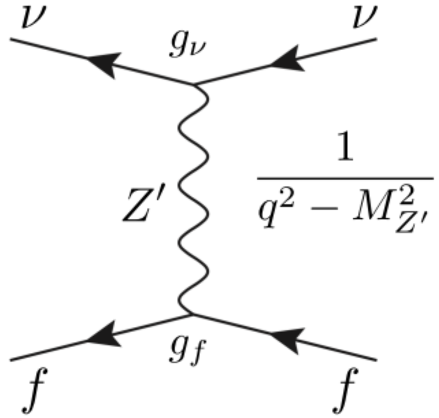

«Light» mediator

$$q^2 \gg M_{Z'}$$

One can assume the existence of U'(1) with an additional vector Z' or a scalar ϕ. One has also an explicit dependence on momentum transfer and Q charges.

arXiv:2008.05022v2

Constraints on light vector mediators through coherent elastic neutrino nucleus scattering data from COHERENT

M. Cadeddu,[a,b] and N. Cargioli,[b] F. Dordei,[a] C. Giunti,[c] Y.F. Li,[d,e] E. Picciau,[a,b] and Y.Y. Zhang[d,e]

«light» mediator scenario

✓ Limits on three different light mediator models combining CsI and argon COHERENT data

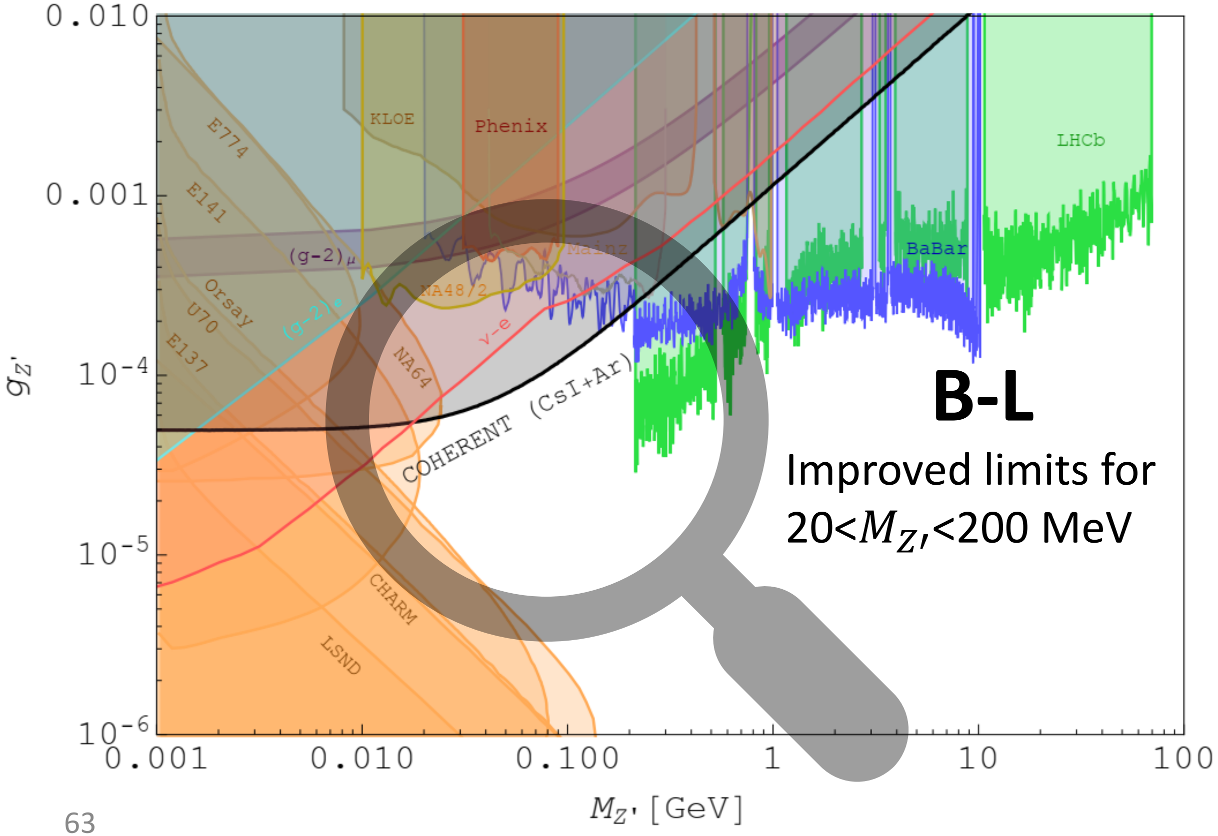

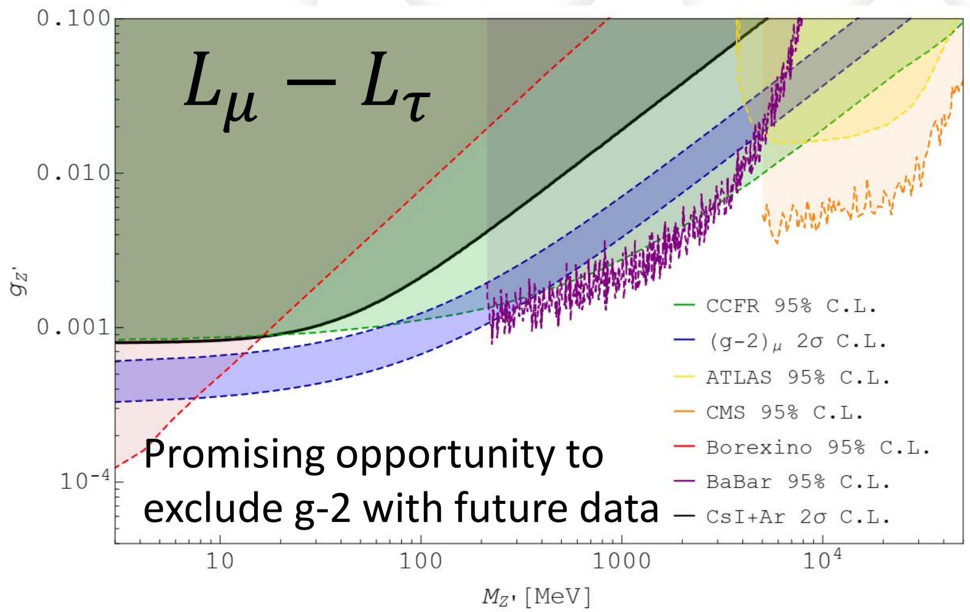

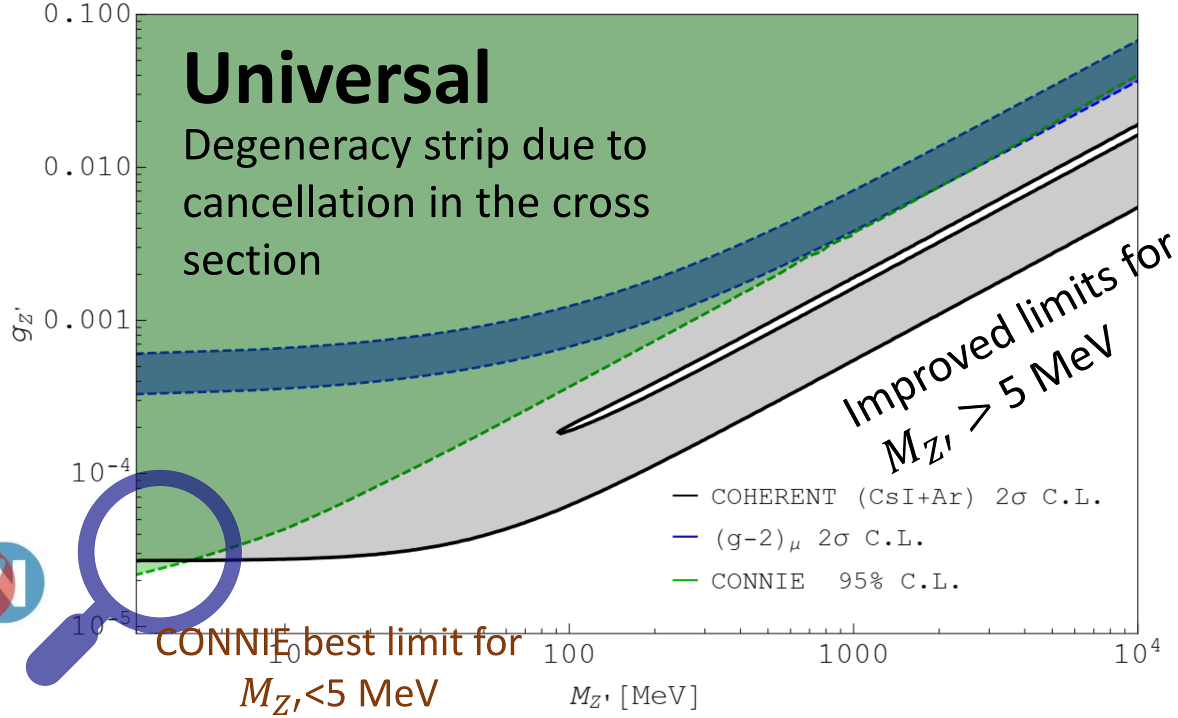

Light mediators (update)

- Non-standard interactions mediated by a vector boson Z' with mass $M_{Z'} \lesssim 100$ GeV, associated with a new $U(1)'$ gauge symmetry.
- Generic lepton flavor conserving Lagrangian:

$$\mathcal{L}_{Z'}^{V} = -g_{Z'}\, Z'_{\mu} \left[\sum_{\alpha=e,\mu,\tau} Q'_{\alpha}\, \overline{\nu_{\alpha L}} \gamma^{\mu} \nu_{\alpha L} + \sum_{q=u,d} Q'_{q}\, \overline{q} \gamma^{\mu} q \right]$$

- CEvNS:

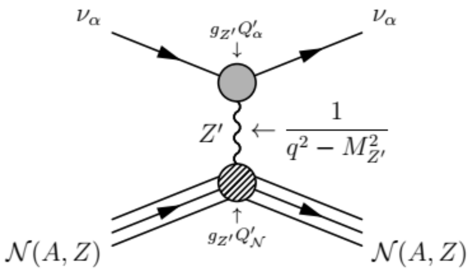

- Many models, that can be divided in
  - Anomaly-free models generated by appropriate combinations of

$$B,\ L_e,\ L_\mu,\ L_\tau$$

  - Anomalous models, assuming that the anomalies are canceled by the contributions of non-standard fermions an extended theory.

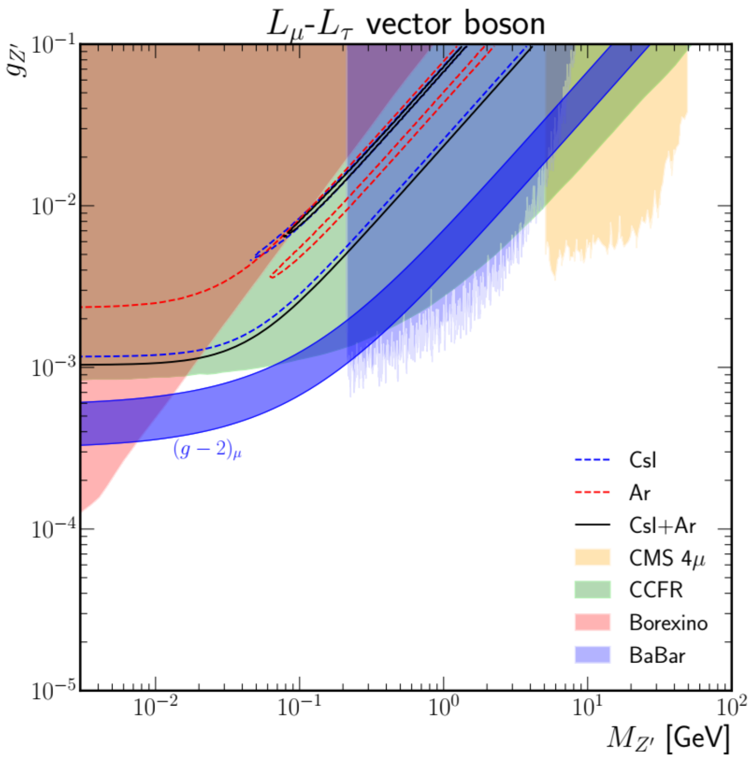

$$Q_W = Q_W^{SM} + \frac{3 g_{Z'}^2}{\sqrt{2} G_F} \left(\frac{Z F_Z(|\vec{q}|) + N F_N(|\vec{q}|)}{|\vec{q}|^2 + M_{Z'}^2} \right)$$

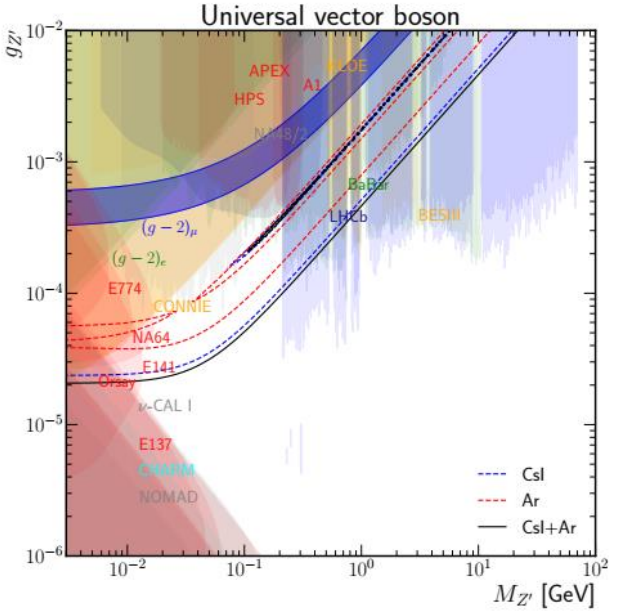

$$Q_W = Q_W^{SM} - \frac{g_{Z'}^2}{\sqrt{2} G_F} \left(\frac{Z F_Z(|\vec{q}|) + N F_N(|\vec{q}|)}{|\vec{q}|^2 + M_{Z'}^2} \right)$$

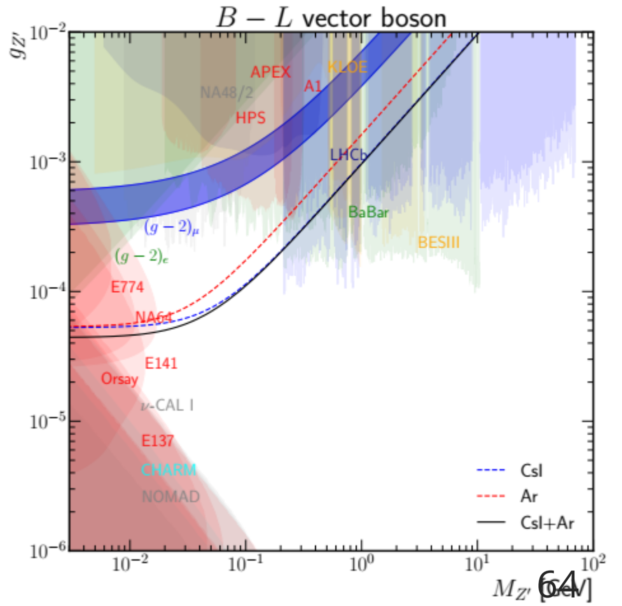

M. Atzori Corona et al. arXiv:2202.11002

New constraint on neutrino magnetic moment from LZ dark matter search results

M. Atzori Corona,[1,2,a] W. Bonivento,[2,b] M. Cadeddu,[2,c] N. Cargioli,[1,2,d] and F. Dordei[2,e]

[1] *Dipartimento di Fisica, Università degli Studi di Cagliari, Complesso Universitario di Monserrato - S.P. per Sestu Km 0.700, 09042 Monserrato (Cagliari), Italy*

[2] *Istituto Nazionale di Fisica Nucleare (INFN), Sezione di Cagliari, Complesso Universitario di Monserrato - S.P. per Sestu Km 0.700, 09042 Monserrato (Cagliari), Italy*

Elastic neutrino-electron scattering represents a powerful tool to investigate key neutrino properties. In view of the recent results released by the LUX-ZEPLIN Collaboration, we provide a first determination of the limits achievable on the neutrino magnetic moment, whose effect becomes non-negligible in some beyond the Standard Model theories. Interestingly, we are able to show that the new LUX-ZEPLIN data allows us to set the most stringent limit on the neutrino magnetic moment when compared to the other laboratory bounds, namely $\mu_\nu^{\rm eff} < 6.2 \times 10^{-12}\,\mu_B$ at 90% C.L.. This limit supersedes the previous best one set by the Borexino Collaboration by almost a factor of 5 and it rejects by more than 5σ the hint of a possible neutrino magnetic moment found by the XENON1T Collaboration.

arXiv:2207.05036v2